NTNU – Trondheim
Norwegian University of
Science and Technology

Study of the parameters to generate different sizes of micro-droplets

Antonio Jose Vera Palazon

Natural Gas Technology
Submission date: July 2013
Supervisor: Carlos Alberto Dorao, EPT

Norwegian University of Science and Technology
Department of Energy and Process Engineering

NTNU

Norwegian University
Science and Technology

Department of Energy of
and Process Engineering

EPT-M-2013-128

MASTER THESIS

for

Stud.techn Antonio J. Vera
Spring 2013

Study of the parameters to generate different sizes of micro-droplets

Studie av parameterne for å generere ulike størrelser av mikro-dråper

Background and objective

Oil-water separators are an integral part of oil processing facilities and in many industrial processes. Water entrained in oil and other hydrocarbon products can affect quality specifications. Vessels used for bulk separation operations in offshore activities to produce oil are of considerable size and weight. A critical parameter for the sizing of separators is related to the dynamics of the droplet interacting with the liquid-liquid interface. However in order to study the dynamic of such systems it is critical to generate micro-droplets.

In this work the main goal will be to generate different sizes of micro-droplets from 20 to 180 μm. As part of the work the parameters controlling the repeatability of the experiment will be studied. In addition a calibration of the droplet generated will be done using different visualization techniques.

The following tasks are to be considered:

1 Literature review on micro-droplet generation
2 Design and evaluation of the unit
3 Evaluation of the parameters controlling the repeatability of the generation

-- ” --

Within 14 days of receiving the written text on the master thesis, the candidate shall submit a research plan for his project to the department.

When the thesis is evaluated, emphasis is put on processing of the results, and that they are presented in tabular and/or graphic form in a clear manner, and that they are analyzed carefully.

The thesis should be formulated as a research report with summary both in English and Norwegian, conclusion, literature references, table of contents etc. During the preparation of the text, the candidate should make an effort to produce a well-structured and easily readable report. In order to ease the evaluation of the thesis, it is important that the cross-references are correct. In the making of the report, strong emphasis should be placed on both a thorough discussion of the results and an orderly presentation.

The candidate is requested to initiate and keep close contact with his/her academic supervisor(s) throughout the working period. The candidate must follow the rules and regulations of NTNU as well as passive directions given by the Department of Energy and Process Engineering.

Risk assessment of the candidate's work shall be carried out according to the department's procedures. The risk assessment must be documented and included as part of the final report. Events related to the candidate's work adversely affecting the health, safety or security, must be documented and included as part of the final report. If the documentation on risk assessment represents a large number of pages, the full version is to be submitted electronically to the supervisor and an excerpt is included in the report.

Pursuant to "Regulations concerning the supplementary provisions to the technology study program/Master of Science" at NTNU §20, the Department reserves the permission to utilize all the results and data for teaching and research purposes as well as in future publications.

The final report is to be submitted digitally in DAIM. An executive summary of the thesis including title, student's name, supervisor's name, year, department name, and NTNU's logo and name, shall be submitted to the department as a separate pdf file. Based on an agreement with the supervisor, the final report and other material and documents may be given to the supervisor in digital format.

X Work to be done in lab (Water power lab, Fluids engineering lab, Thermal engineering lab)
☐ Field work

Department of Energy and Process Engineering, 16. January 2013

Olav Bolland
Department Head

Carlos A. Dorao
Academic Supervisor

Research Advisors: Nicolas La forgia

Aknowledgements

I would like to thank to my supervisor, Prof. Carlos A. Dorao for his help and giving me the opportunity to perform this Master Thesis in the department of Energy and Process Engineering at NTNU.

I would also like to thank to Nicolas La Forgia who even being busy with his own project, he always found time to help me. Moreover I do not want forget the support received in the beginning of this work by Majed D. Malla and Jenny V. Bjerknes.

Abstract

Separators are regarded as an integral part of oil and gas processing equipment. Because of the sales specification of the finished products, a high level of separation is needed. The separators that are available today are of considerable weight and size which drives great desire to reduce both properties. Two major factors are of great importance regarding the effect on downsizing the separators, these factors are the settling velocity of droplets and the time needed for coalescence. To study these factors is critical generate micro-droplets; however the generation of micro-droplets is still a challenge.

This thesis was focused on the study of the parameters to generate micro-droplet in a wide range. Experiments were conducted using Exxsol D80 oil. Droplets in the range of 26 µm and 170 µm were created by electrohydrodynamic (EHD) application. It was found that the droplets size increased by the increasing of voltage pulse amplitude and pulse width, which corresponds to the existing literature. However the meniscus size is the key point to generated droplets over a wide range, so the approach was put on the generation of different droplet sizes for different menisci. Moreover a study of the relation between the needle shape and the drop size was performed without EHD application. Additionally a literature review of the different techniques to generate droplets was previously discussed in the theoretical part of this thesis.

Further work is recommended, as the study of the variation height of the electrode and its relation with the drop size. Moreover, measuring the pressure applied into the syringe and controlling it is a key point for the meniscus size, which was not completely achieved in this work.

Contents

1 Introduction

1.1 Background

Oil-water separators are an integral part of oil processing facilities in many industrial processes. Water entrained in oil and other hydrocarbon products can affect quality specifications. Vessels used for bulk separation operations in offshore activities to produce oil are of considerable size and weight. A critical parameter for the sizing of separators is related to the dynamics of the droplet interacting with the liquid-liquid interface. To study the dynamic of such systems it is critical to generate micro-droplet, however generation of micro droplets is still a challenge.

There are different techniques to generate droplet and they can be classified in two big groups, droplet based on continuous streaming (CS) and droplet generated on demand (DoD). Within each group it can be find numerous systems to generate drops. Some of them are T-junction, Piezoelectric actuation, Electrostatic actuation etc. These systems are applied for several types of industries as biomedicine, fuel injection, chemistry, pharmaceuticals, ink-jet printhead.

In particular to generate micro-droplet on demand there is a technique called electrohydrodynamic (EHD), which has a promising potential in this area.

1.2 Goal of the work

The main objective of this work will be to set an experiment for generating different droplet sizes in the order of sub millimeters. In particular the focus will be on the meniscus shape and its influence in the droplet size.

A literature review will be performed in order to construct the set up more appropriate for controlling the meniscus shape and generate micro-droplets.

1.3 Scope of the work

In this work drop sizes within the range between 25 μm and 180 μm will be generated. To perform this experiments it will be applied EHD. Parameters like voltage, pulse width and meniscus shape will be studied. It will be also studied influence of the needle shape and

infuse rate without applying EHD. In this case two types of needles will be used with blunt point and bevel tip, both for the diameters of 0.4 mm and 0.8 mm.

The oil-water system consist on Exxsol D80 oil and tap water, not water from the well and petroleum oil. The experiments will be performed at atmospheric conditions and ambient temperature.

1.4 Report structure

The structure of this report is explained in this section with a short description of the content of each chapter.

Chapter 2 consists of the theoretical part of the thesis, containing theory about gravity separation, literature review of droplet generators, meniscus influence and EHD application. In chapter 3 the experimental work with facilities and equipment are described with an explanation of the experimental method and procedure, including and error analysis. Results of the experiments performed in relation with this project thesis are found in chapter 4 along with a following discussion. In chapter 5 conclusions will be given, with recommendations for further work.

2 Theory

2.1 Oil-Water separation overview

Although the study of oil separator processes is outside of this thesis, it is important to understand some factors governing its operation since the improved efficiency and size reduction in the separators would be given by the control the parameters such as settling velocity and coalescence time of the droplets within the separators. So for this reason the generation of droplets is a key step for this study.

Separating water from continuous flows of oil is commonly required in oil production applications, oil refineries and chemical plants as well as some places where it is essential that the hydrocarbons not be contaminated with water. The possible problems with water contamination were first emphasized during the last part of World War II when it was found that airplanes could fly high enough to cause the water to freeze in the fuel lines. The pilots found this unreasonably inconvenient because it caused the engines to stop, so equipment was designed to ensure that only tiny amounts of water were allowed to remain in the aviation fuel. It was also found that refinery processes operated easier and better and corrosion problems were avoided by removing the water from the hydrocarbons. [Kirby, Mohr 2001]

In oil industries the most common separators for removing water from oil acting by gravity. This processes in generally accomplished in three stages. Firstly, the mixed-phase stream goes in the vessels through an inlet diverter to cause the largest drops to impact by momentum and then fall by gravity, this is the primary separation. Secondary separation is the second step, and consists of gravity separation of smaller droplets (in the order of sub mm). This takes place when the vapor flows through the disengagement area of the vessel. The use of baffles can aid this part of separation by creating an even velocity distribution in the fluid. The third and last stage is mist elimination; here the smallest droplets coalesce on an impingement device, forming larger droplets which will settle by gravity.

Gravity separators often classified by their geometrical configuration (vertical/horizontal) and by their function (two-phase/three-phase separator). In other words, gravity separators are classified as “two-phase” if they separate gas from the total liquid stream and “three-phase” if they also separate the liquid stream in its crude oil and water-rich phases. [Saeid, William et al. 2006].

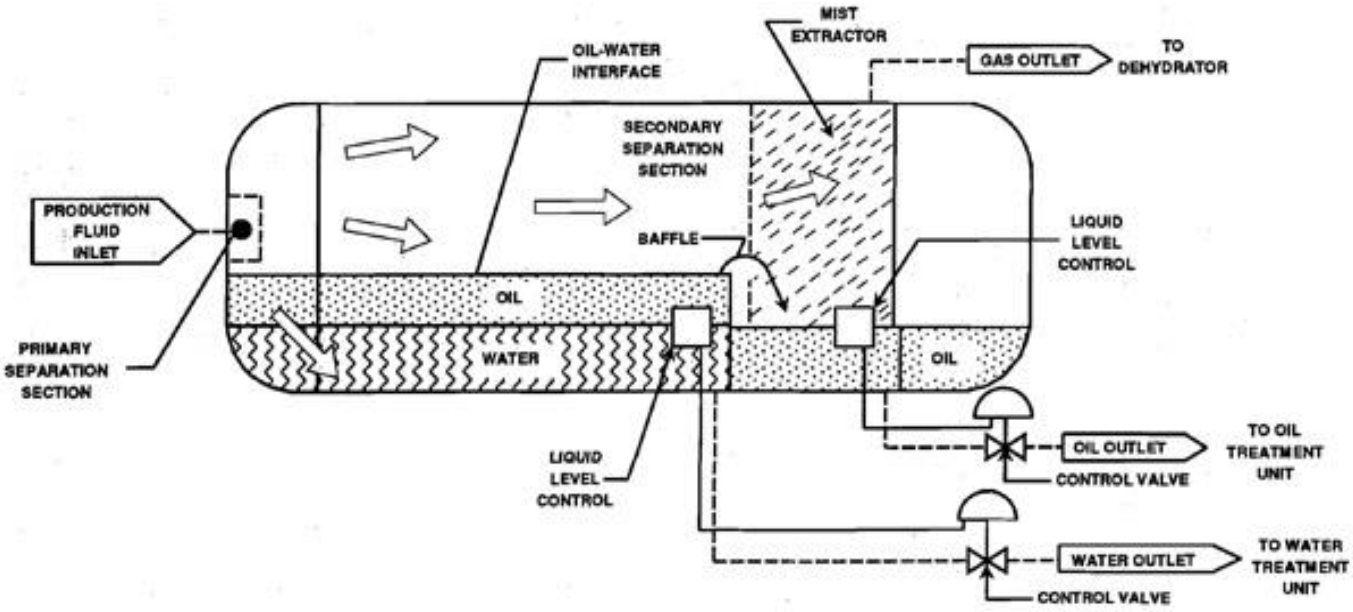

Figure 2.1 Horizontal three-phase separator (US environmental protection agency)

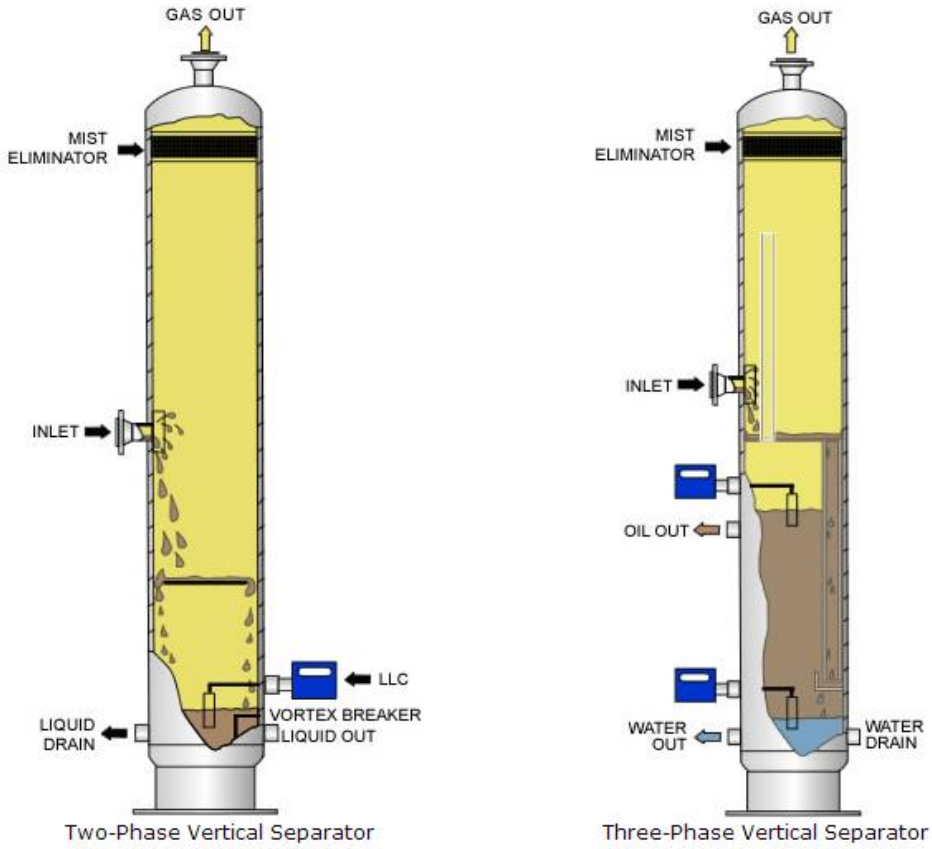

Figure 1.2 Two/Three-phase vertical separator (KW international)

2.2 Literature review of drops generation

As was previously mentioned, the generation of drops is a key step in the study of the efficiency improvement of oil separators. In this section it will review the available drops generation and manipulation techniques. The main focus of this review is not to be comprehensive and explain all techniques in great detail but to identify and shed light on similarities and channels are crucial factors for droplet generation.

Droplet generators can be classified in two groups depending on their operating, droplet based in continuous streaming (CS) or drops on-demand (DoD). The first one is based in liquid-liquid systems, through the action of hydrodynamic shear forces exerted by a flowing continuous phase or carrier fluid on a "monodisperse phase". In DoD generators, a single or a finite quantity of drop release is targeted. Either way, it results from the application of an external stimulus to a liquid meniscus, directly at its surface (e.g. EHD and focused ultrasound actuation [Amemiya et al., 1999]) or indirectly through bulk transmission (e.g. piezoelectric actuation).

Continuous streaming remains widely used in applications where high throughput is required, e.g. emulsification [Yobas et al., 2006], as it can achieve production rates on the order of a few MHz, that is two order of magnitudes greater than the best drop-on-demand generators. However, when the injection of only a discrete number of drops is required, as in our experiment, DoD techniques are almost always preferred.

2.2.1 Droplet based in continuous streaming (CS)

Droplet based microfluidics is a rapidly growing interdisciplinary field of research combining soft matter physics, biochemistry and microsystems engineering. Precise control of droplet volumes and reliable manipulation of individual droplets such as coalescence, mixing of their contents, and sorting in combination with fast analysis tools allow us to perform chemical reactions inside the droplets under defined conditions.

Although methods which were originally developed in bulk could successfully be transferred into a microfluidic devices they are rather optimized for high yield than for the controlled production of monodisperse droplets, and most microfluidic 'lab chip application' relies on *in situ* drop by drop production techniques for the sake of droplet homogeneity, simplicity of device fabrication, and controllable operational parameters. The most frequently applied

techniques or geometries are ‘T-junctions’, ‘flow focusing’, and ‘step emulsification’ which will be explained in the subsequent subsections followed by a discussion of the underlying physical principles.

- ***T-junction***

The easily controllable production of a single stream of monodisperse droplets in a microfluidic channel was first demonstrated using a T-channel geometry. The breakup of a continuous stream of one fluid is caused by shear from the cross flow of a stream of a second immiscible fluid.

The generic geometry of a T-channel is shown in figure 2.3(a) as it is frequently employed to generate bubbles and droplets in microfluidic channels. The composition of the generated droplets can be varied by merging several streams of miscible liquid into one common channel before dispensing.

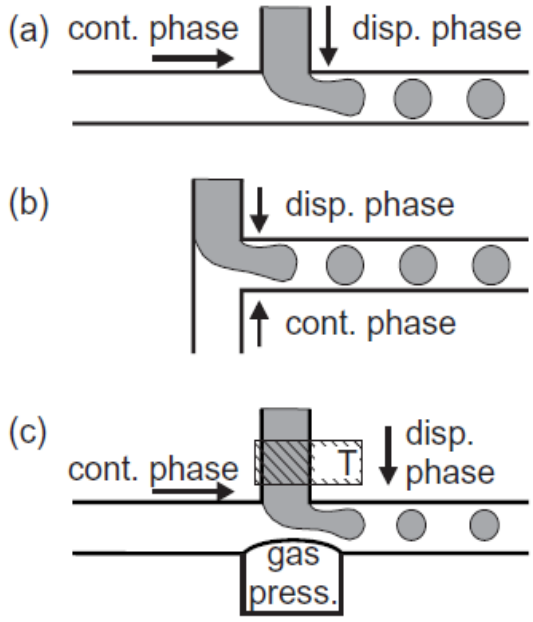

Figure 2.3 Schematic of various T-junction geometries

A variation of operation principle of T-junction is the so called head-on device which is displayed in figure 2.3(b). Here, also a T-channel or Y-channel geometry is employed but the two fluids are injected from the two straight channels facing each other having similar features as the droplet production by the other described T-junction geometry. Varying the physical properties of the fluids, the size of the produced droplets can be adjusted by heating

one of the connections of a T-junction by, e.g. Varying surface tension or viscosity of the injected liquid, figure 2.3(c).

- ***Flow focusing***

A second method to produce small droplets in microfluidic devices by viscous stress is so called ‘co-flow’ or ‘flow focusing’. In a ‘co-flow’ geometry two liquid streams are flowing together whereas the continuous fluid phase surrounds the dispersed liquid phase, which finally decays into droplets via Rayleigh-Plateau instability, figure 2.4(a).

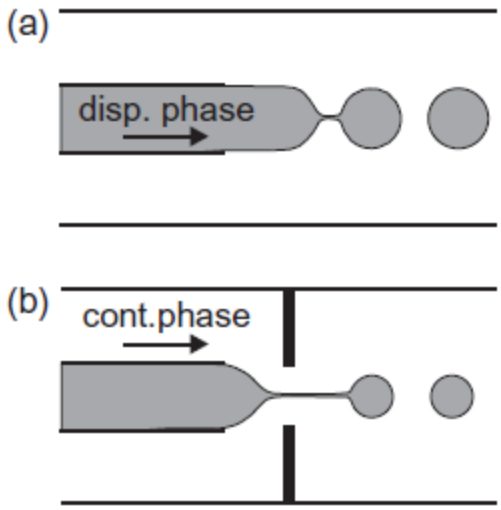

Figure 2.4 Schematic of co-flowing devices with flow focusing (b) and without flow focusing (a)

In a ‘flow-focusing’ geometry the streams of co-flowing liquids are additionally focused through an orifice, figure 2.4(b). In such a flow-focusing geometry the two immiscible liquid phases undergo large elongational flow as they pass the small orifice generating smaller droplets as in a flow-focusing device of similar geometry. Since a flow-focusing geometry can be considered as a special case of a co-flow geometry the distinction in the literature is not always unambiguous.

- ***Step emulsification***

A modified version of a co-flowing geometry is called ‘step emulsification’ and uses a geometric step to trigger droplet formation of a stream of a dispersed phase surrounded by a continuous phase. A typical realization is sketched in figure 2.5. The two liquids are brought

together at a T- or Y-junction into a high aspect ratio channel. It is of no significance whether the channel is very narrow or (as in the sketch) very flat, it is the difference between the width and the height which matters.

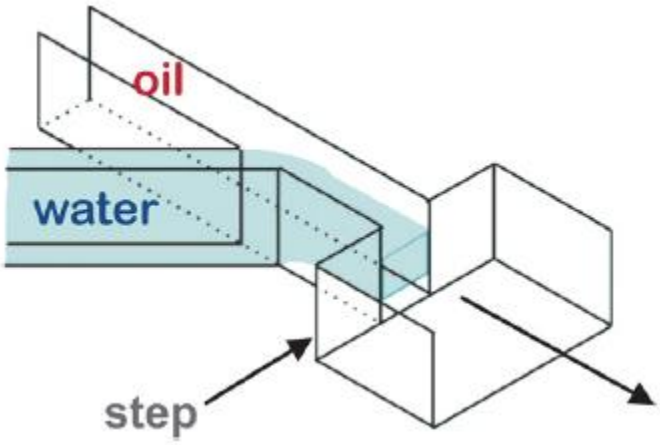

Figure 2.5 A step-emulsification device

The important feature of the step-emulsification technique is that the dispersed stream is stabilized between the two walls of a high aspect ratio channel suppressing interfacial induced instabilities.

2.2.2 Drop on demand (DoD)

Here microdroplet generators are defined as devices that generate microsized droplets in a controllable manner; that is, droplet size and number can be controlled and counted accurately.

Microdroplet generators usually employ mechanical actuation to generate high pressure that overcomes liquid surface tension and viscous force and permits droplet ejection. Depending on the droplet size, the applied pressure is usually higher than several atmospheres. The operation principles, structure/process designs, and materials often play key roles in the performance of droplet generators.

In addition to the well-known ink-jet printing, applications for microdroplet generators cover a wide spectrum in various fields such as direct writing, fuel injection, solid free form, solar cell fabrication, LEPD fabrication, packaging, micro optical components, particle sorting,

microdosage, plasma spraying, drug screening/delivery/dosage, micro propulsion, integrated circuit cooling, and chemical deposition. Many of these applications may become key technologies for integrated microsystems in the near future.

There have been many attempts to generate controllable micro droplets [Myers et al., 1984; Buehner et al., 1977; Twardeck et al., 1977; Carmichael et al., 1977; Ashley et al., 1977; Bugdayci et al., 1983; Darling et al., 1984; Lee et al., 1984; Nielsen et al., 1985; Bhaskar et al., 1985; Allen et al., 1985; Krause et al., 1995; Chen et al., 1995; Tseng et al., 1996; Hirata et al., 1996; Zhu et al., 1996].Most of these have followed the principle of creating pressure differences by either lowering the outer pressure of a nozzle or increasing the inner pressure to push or pull liquid out of the nozzle to form droplets. Typical techniques are pneumatic, piezoelectric, thermal bubble, thermal buckling, focused acoustic wave, and electrostatic actuations. The basic principles of those droplet generators are introduced below. Also included in the last section is an acceleration-based ejection method that employs inertial force for droplet generation.

- ***Piezoelectric Actuation***

Droplet ejection by piezoelectric actuation was invented by Sweet in 1964 and has been used in many applications including ink-jet printing, studies on droplet evaporation and combustion.

Two types of droplet ejection devices are based on piezoelectric technology. One is the continuous ink-jet [Buehner et al., 1977; Twardeck et al., 1977; Carmichael et al., 1977; Ashley et al., 1977]. Figure 2.6 (a) schematically shows the operational principle of this type of ink-jet. Conductive ink is forced out of the nozzles by pressure. The jet would break up continuously into droplets with random sizes and spacing, but uniform size and spacing of the droplets is controlled by applying an ultrasonic wave at a fixed frequency to the ink through a piezoelectric transducer. The continuously generated droplets pass through a charge plate, and only the desired droplets are charged by the electric field and deflected to print out, while the undesired droplets are collected by a gutter and recycled. One piezoelectric transducer can support multiple nozzles, so the nozzle spacing can be as small as desired for high-resolution arrays. The complexity of this device's droplet charging and collecting system is the major obstacle to its practical application.

The other device, the droplet-on-demand ink-jet, utilizes a piezoelectric tube or disc for droplet ejection only when printing a spot is desired [Bugdayci et al., 1983; Darling et al., 1984; Lee et al., 1984]. Figure 2.6 (b) shows a typical drop-on-demand drop generator. The operational principle is based on the generation of an acoustic wave in a fluid-filled chamber by a piezoelectric transducer through the application of a voltage pulse. The acoustic wave interacts with the free meniscus surface at the nozzle to eject a single drop. The major advantage of the drop-on-demand method is that it does not require a complex system for droplet deflection. Its main drawback is that the size of piezoelectric transducer tube or disc, in the order of sub mm to several mm, is too large for high-resolution applications. It was reported that the typical frequency for a stable operation of piezoelectric ink-jet would be tens of kHz [Chen et al., 1999].

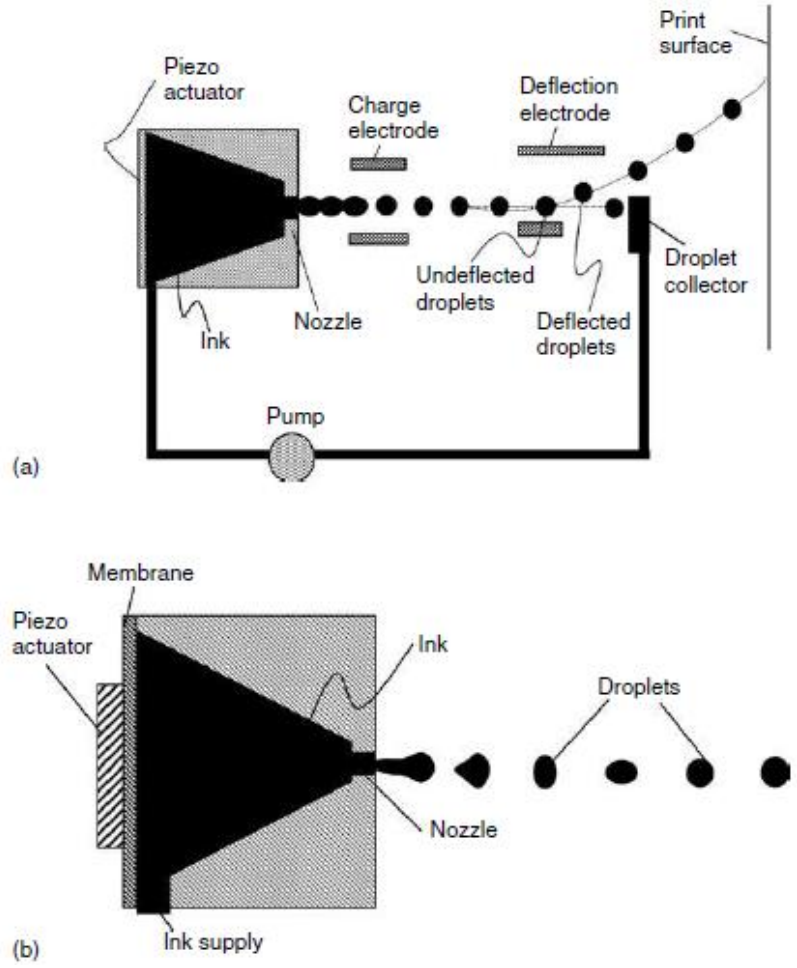

Figure 2.6 (a) Operation principle of a piezoelectric-actuated continuous droplet generator, after Buehner (1997). (b) Operation principle of a piezoelectric-actuated droplet-on-demand droplet generator, after Lee (1984)

- ***Pneumatic Actuation***

Spray nozzles are presently one of the most commonly used devices for generating droplets, as in airbrushes or sprayers. Two types of spray nozzles are shown in Figure 2.7. Figure 2.7 (a) shows an airbrush that lowers pressure at the outer area of the capillary tube by blowing air across the tube's end; this forces the liquid to move out of the tube and form droplets. The second device, a sprayer shown in Figure 2.7 (b), employs high pressure to push liquid through a small nozzle to form droplets. Typical sizes of the droplets generated by spray nozzles range from around tens to hundreds of μm in diameter. These devices can be fabricated in micro sizes by micromachining technology. However, controlling individual nozzles in an array format is difficult.

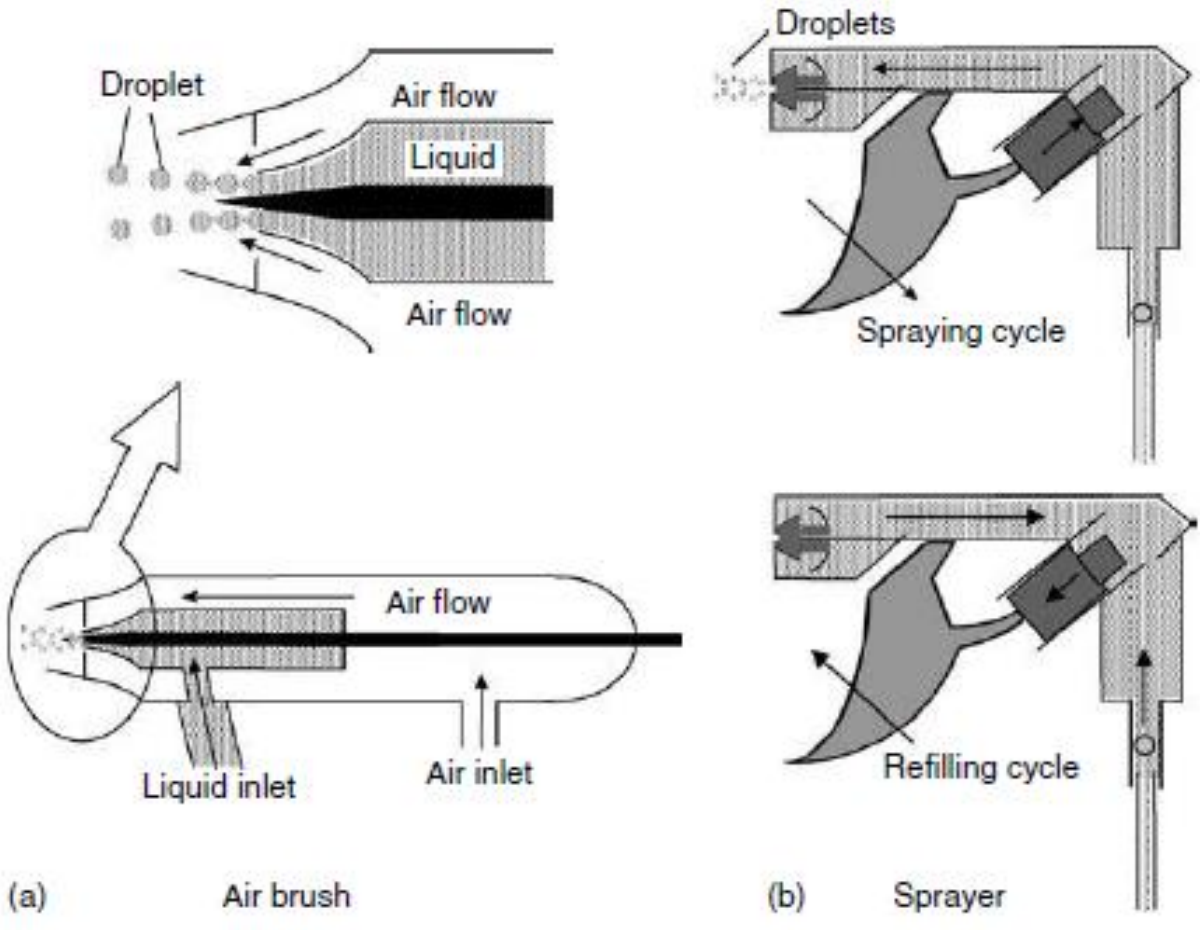

Figure 2.7 Operation principle of (a) airbrush and (b) sprayer, after Tseng (1998)

- ***Thermal-Bubble Actuation***

Thermal bubble jet technology has been studied by HP in the United States and by CANON in Japan since the early 1980s [Nielsen et al., 1985; Bhaskar et al., 1985; Allen et al., 1985]. Figure 2.8 shows the cross-section of a thermal bubble jet device. Liquid in the chamber is heated by applying a pulse current to the heater under the chamber. The temperature of the liquid covering the surface of the heater rises to around the liquid critical point in microseconds, and then a bubble grows on the surface of the heater, which serves as a pump. The bubble pump pushes liquid out of the nozzle to form a droplet. After the droplet is ejected, the heating pulse is turned off and the bubble starts to collapse.

Liquid refills the chamber when surface tension on the free surface of the meniscus returns it to the original position. A second pulse generates another droplet. The energy consumption for ejecting each droplet is around 0.04 mJ for an HP Think Jet printhead. Because bubbles can deform freely, the chamber size of the thermal bubble jet is smaller than that of other actuation means, which is important for highresolution applications. The resolution reported in the literature ranges from 150 to 600 dpi [Krause et al., 1995] and 1016 dpi [Chen et al., 1995]. The typical operational frequency for contemporary thermal bubble jets is around several to tens of kHz.

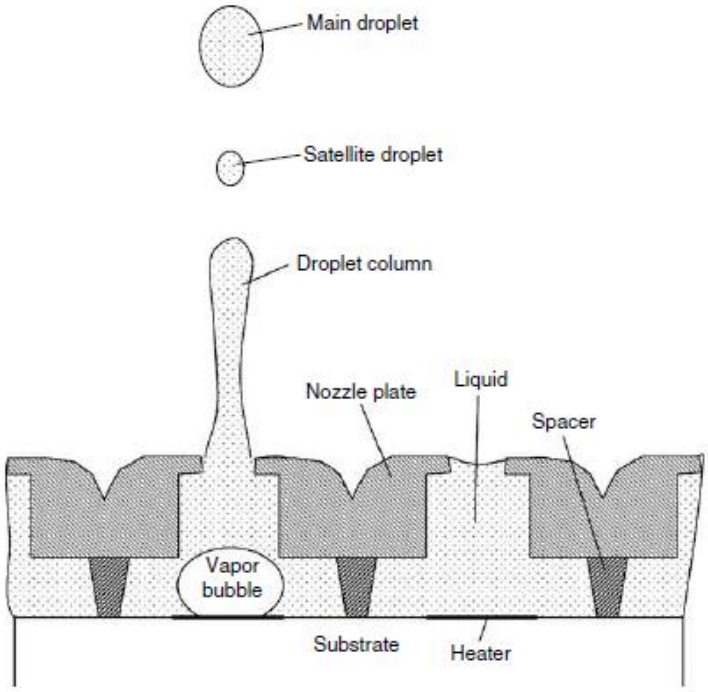

Figure 2.8 Operation principle of a thermal-bubble-actuated droplet generator, after Allen (1995)

- ***Thermal-Buckling Actuation***

Hirata et al. (1996) employed a buckling diaphragm for droplet generation. Figure 2.9 schematically shows the technique's basic operational principle. A composite circular membrane consisting of a silicon dioxide and nickel layer is fixed on the border and remains separated from the substrate by a small gap. A heater is placed at the center of the composite membrane and electrically isolated from it. Pulsed current is sent to the heater, and then the membrane is heated for several μs. When the thermally induced stress is greater than the critical stress, the diaphragm buckles abruptly and ejects a droplet out of the nozzle. The power required to generate a droplet at a speed of 10 m/s is around 0.1 mJ using a 300 μm diameter diaphragm. The power consumption and the size of the buckling membrane ink-jet device are much larger than those of the thermal bubble jet. The reported frequency response of a membrane buckling jet ranges from 1.8 to 5 kHz depending on the desired droplet velocity.

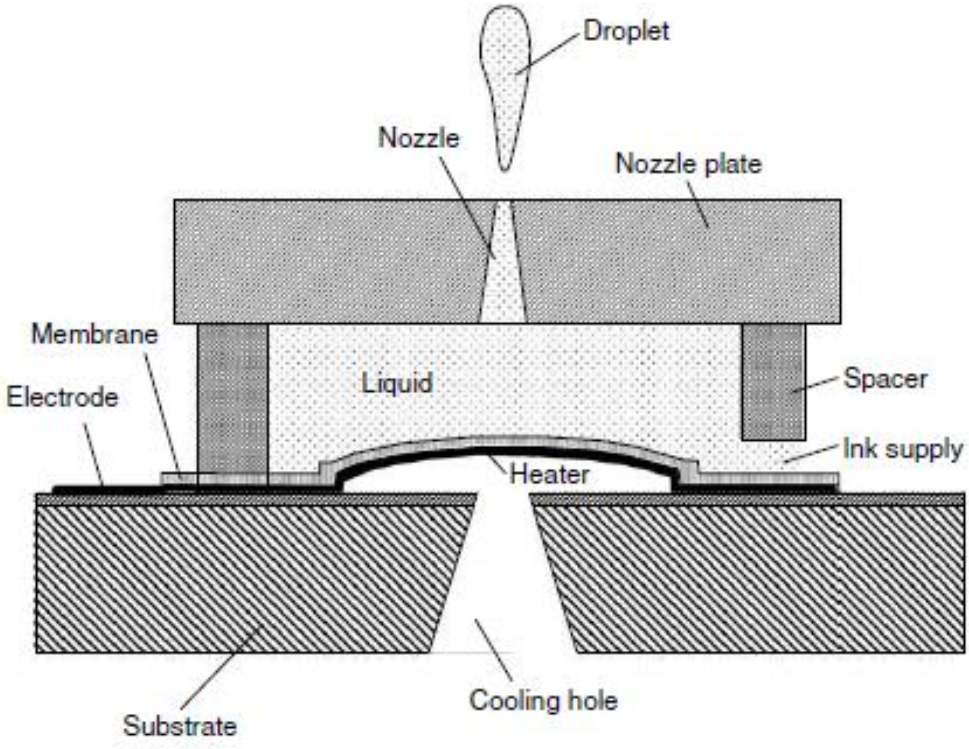

Figure 2.9 Operation principle of a thermal-buckling-actuated droplet generator, after Hirata (1996)

- ***Acoustic-Wave Actuation***

Figure 2.10 shows a lensless liquid ejector using constructive interference from acoustic waves to generate droplets [Zhu et al., 1996]. A PZT thin-film actuator with the help of an on-chip Fresnel lens was employed to generate and focus acoustic waves on the air–liquid interface for droplet formation. The actuation results from the excitation of a piezoelectric film under a burst of RF signal. The device does not need a nozzle to define droplets, reducing the clogging problems that trouble most droplet generators employing nozzles.

Droplet size also can be controlled by using acoustic waves with specific frequencies. However, due to the acoustic waves' vigorous agitation of the liquid, it is difficult to maintain a quiet interface for reliable and repeatable droplet generation. As a result, a "nozzle area" is still needed to maintain a stable interface.

The applied RF frequency ranges from 100 to 400 MHz, and the burst period is 100 μs. The power consumption for one droplet is around 1 mJ, which is high compared to other techniques. The droplet size ranges from 20 to 100 μm depending on the RF frequency. The reported size of the device is 1x1 mm^2, which is much larger than the droplet generators mentioned previously.

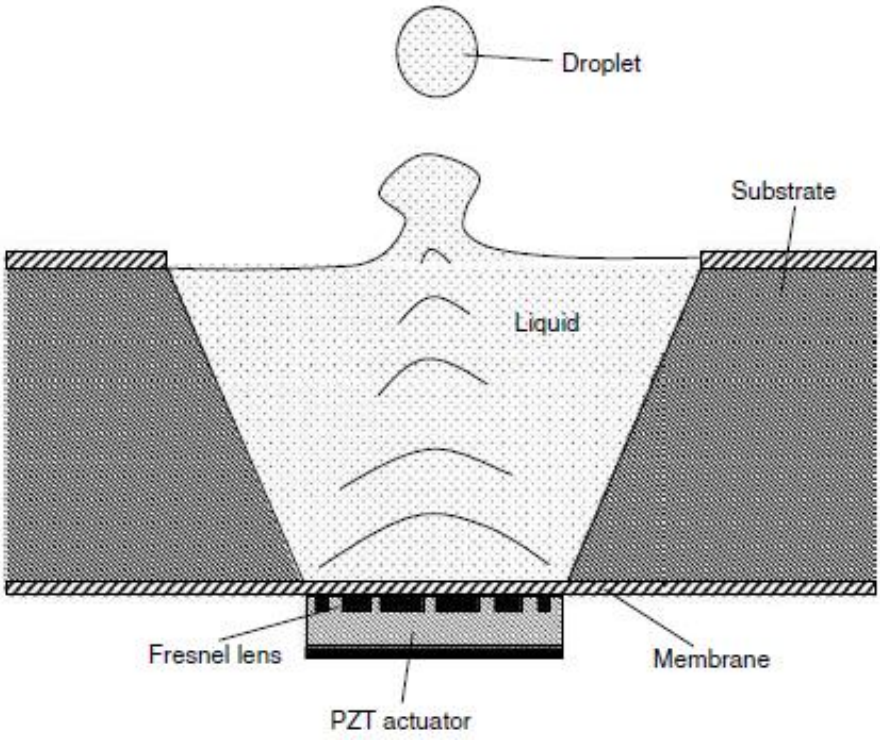

Figure 2.10 Operation principle of an acoustic-wave-actuated droplet generator, after Zhu (1996)

- ***Electrostatic Actuation***

The electrostatically driven ink-jet printhead was first introduced by the Seiko Epson Corporation [Kamisuki et al., 1998, 2000] for commercial printing. As shown in Figure 2.11, the actuation is initiated by applying a DC voltage between an electrode plate and a pressure plate; this deflects the pressure plate for ink filling. When the voltage stops, the pressure plate reflects back and pushes the droplet out of the nozzle. This device has been developed for use in electric calculators due to its low power consumption, less than 0.525 mW/ nozzle. The driving voltage for a SEAJet is 26.5 V, and the driving frequency can be up to 18 kHz with uniform ink ejection. A 128-nozzle chip with 360 dpi pitch resolution also has been demonstrated. This device was claimed to offer high printing quality (for bar code), high speed printing, low power consumption, and long lifetime (more than 4 billion ejections) under heavy-duty usage as well as low acoustic noise. However, the fabrication comprises a complex bonding process among three different micromachined pieces. Further, making the pressure plate requires a very precise etching process to control the accuracy and uniformity of its thickness. Due to the deformation limitation of solid materials and alignment accuracy in the bonding process, the nozzle pitch may not be easily reduced any further for higher resolution applications.

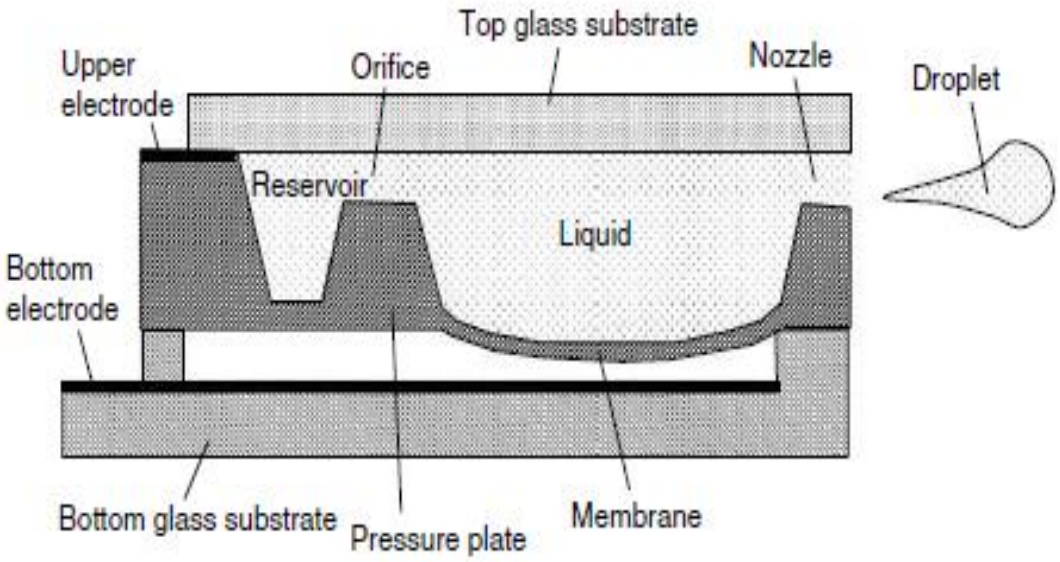

Figure 2.11 Operation principle of an electrostatic-actuated droplet generator, after Kamisuki (1998)

- ***Inertial Actuation***

Inertial droplet actuators apply a high acceleration to the nozzle chip to cause droplet ejection. This type of apparatus is shown in Figure 2.12. The print module consists of large reservoirs on the top plate, which is connected to nozzles on the bottom plate. The print module is mounted on a long cantilever beam with a piezo-bimorph-actuator for acceleration generation. Generating 1 nl droplets from 100 μm diameter nozzles requires 500 μs. Twenty-four liquid droplets of different solution types were demonstrated to be ejected simultaneously from the nozzles in a 500 μm pitch. The smallest droplet claimed to be generated is 100 pl from 50 μm diameter nozzles. This principle provides a gentle ejection process for bioreagent applications. However, the ejection of smaller droplets may encounter strong surface tension and flow-drag forces in micro scale that are much larger than the droplet inertial. That the droplets cannot be selectively and individually ejected from the desired nozzles also limits this technique's applications.

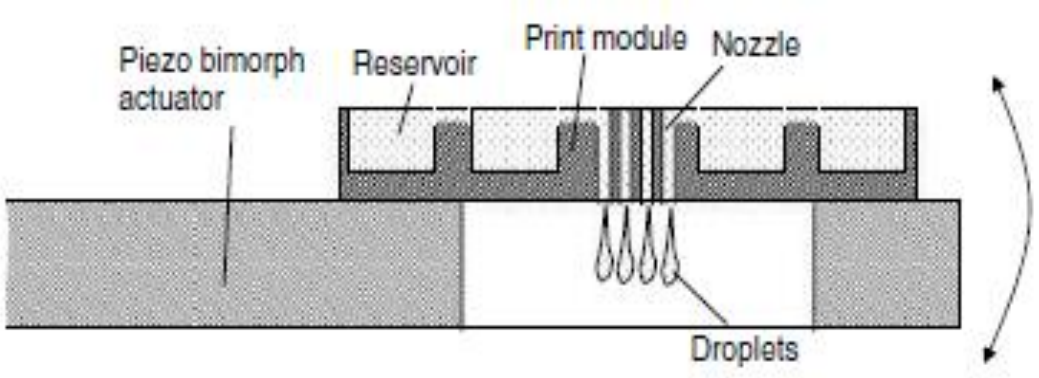

Figure 2.12 Operation principle of an inertia-actuated droplet generator, after Gruhler (1999)

Actuation Mechanism	Application	Drop diameter (µm)	Production rate (kHz)	Energy required (mJ)
T-junction	CS	5-1000	0.1-1000	-
Flow focusing	CS	10-1000	-	-
Step emulsification	CS	10-500	-	-
Piezoelectric	DoD	10-700	~10	-
Pneumatic	DoD	100-600	-	-
Thermal bubble	DoD	20-100	1-10	0.04
Thermal buckling	DoD	~100	1.8-5	0.1
Acoustic wave	DoD	20-100	100-400	~1
Electrostatic	DoD	10-100	~18	0.525
Inertial	DoD	50-500	1-10	-

Table 2.1 Summary of the characteristic features of drop generation techniques

2.3 Droplet generation by electrohydrodynamic (EHD) application

As shows previously several techniques are utilized to generate small droplets and are used to different applications ranging from printing industries to medical research. However a particular technique to generate drop on demand using a simple needle for getting smaller droplets is applying high voltage to deform the meniscus on the tip of the needle, this technique is called as electrohydrodynamics (EHD), also known as electro-fluid-dynamics (EFD) or electro kinetics which is the study of the dynamics of electrically charged fluids such as the motions of ionized particles or molecules and their interactions with electric fields and the surrounding fluid. This technique will be performed later in the experiments of this thesis.

For performing DOD through electrohydrodynamics, a voltage pulse (typically a square pulse) is generally applied between a metallic nozzle and a ground electrode. The applied voltage can deform the initial meniscus formed at the nozzle front due to the strong electrical forces acting at the interface, resulting in a jet of liquid that eventually detaches and forms droplets on the grounded substrate.

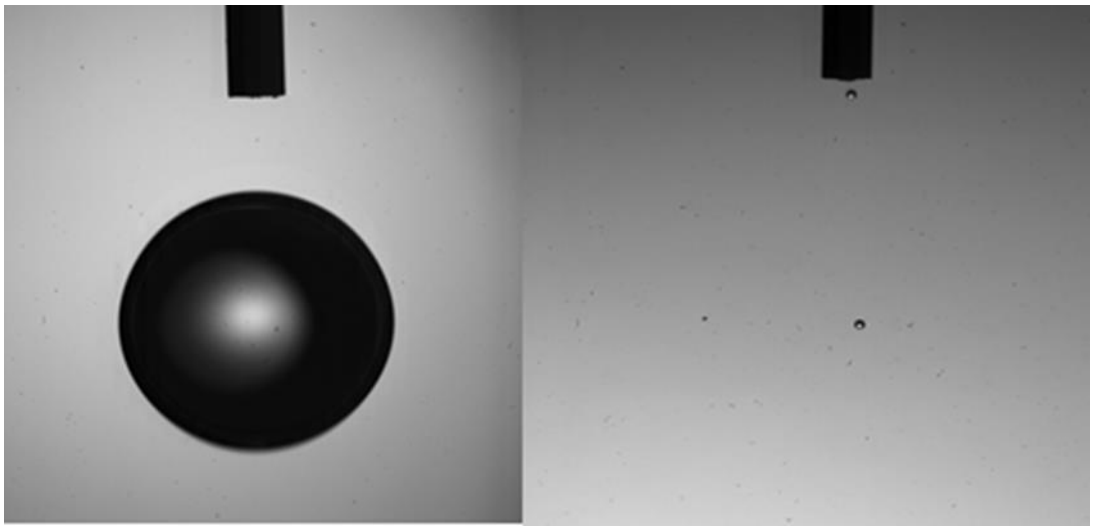

Figure 2.13 Drop size without applying EHD (left) and with applying EHD (right)

In principle, the electrostatic forces can act on the liquid surface instead of acting on the whole fluid as the pressure pulses method does. The EHD can be categorized into two parts:

- The cone-jet mode which produces a very fine spray of drops but not suited for the droplet generation. The most commonly used mode of EHD liquid atomization in

industrial applications such as spray coating or crop spraying and on the identification of the parameters leading to continuous generation of discrete charged drops.

- The drop periodic mode is whenever drops are produced one by one as in dripping.

The work done by [P. Atten] indicated that a single non-charged droplet of water in oil is obtained by applying a voltage pulse on a conductive liquid meniscus, this droplets deforms and makes a neck and breaks up. The behavior and generation of such a droplet are investigated further by [Raisin, 2011] which successfully produced and captured microdroplet generation. In these works were reported that for a given meniscus shape, the diameter of the extracted droplet depends on the voltage amplitude V and on the pulse duration Δt. Order of magnitude considerations on the meniscus deformation process suggest that the main parameter which determines the size of the generated droplet is the product $V^2\Delta t$. An image sequence taken from this work shows the deformation and ejection of a droplet from a meniscus, the diameter of the ejected drop is about 238 µm.

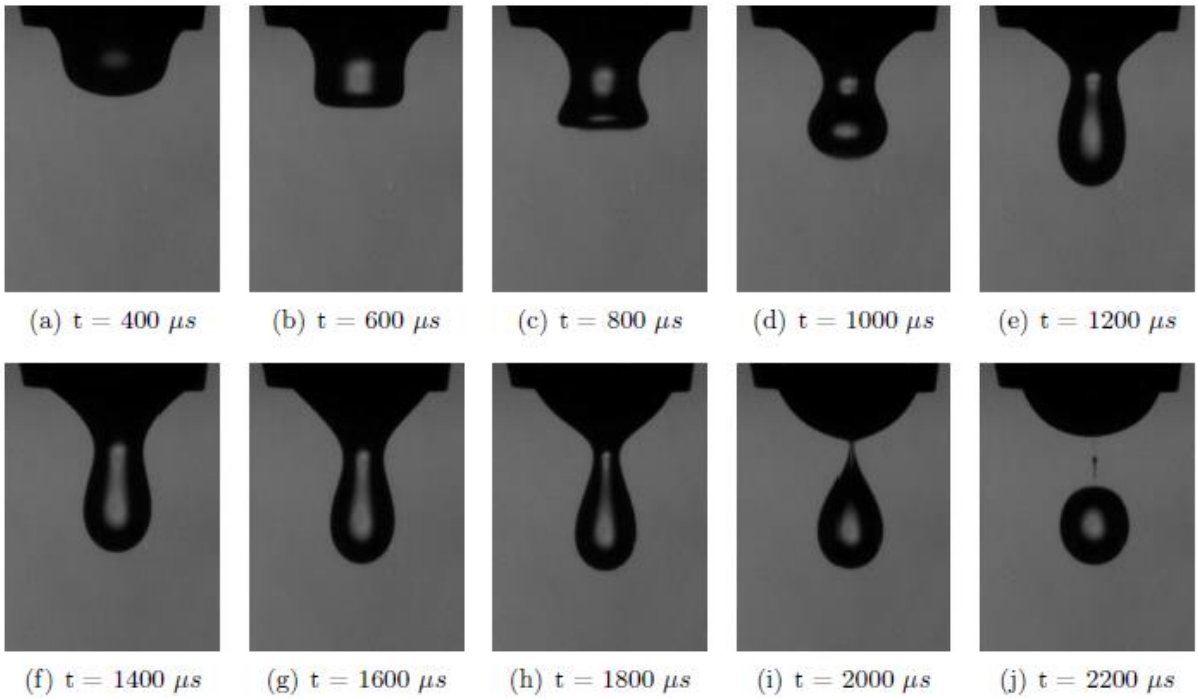

Figure 1.14 Deformation of meniscus and ejection of a droplet, [Raisisn, 2011]

As shows in the above figure by introducing a high voltage pulse to the needle that is submerged in oil, the meniscus starts to deform due to the action of the induced electrostatic pressure leading to the release of one or more drops. And in order to achieve the charge free

condition, the electric pulse has to be finished before the last stage of meniscus elongation. After the deformation of the neck, the meniscus splitting takes place a few hundred microseconds after the end of the pulse. The gravity force then works on separating the droplet from meniscus. The physics behind this is explained by showing the only pressure acting upon the meniscus in this case is the electrostatic pressure.

$$P_{es} = \frac{1}{2}\varepsilon E_n^2 \qquad (2.1)$$

Where E_n is the normal component of the electrical field ε is defined as the oil permittivity and P_{es} is the electrostatic pressure.

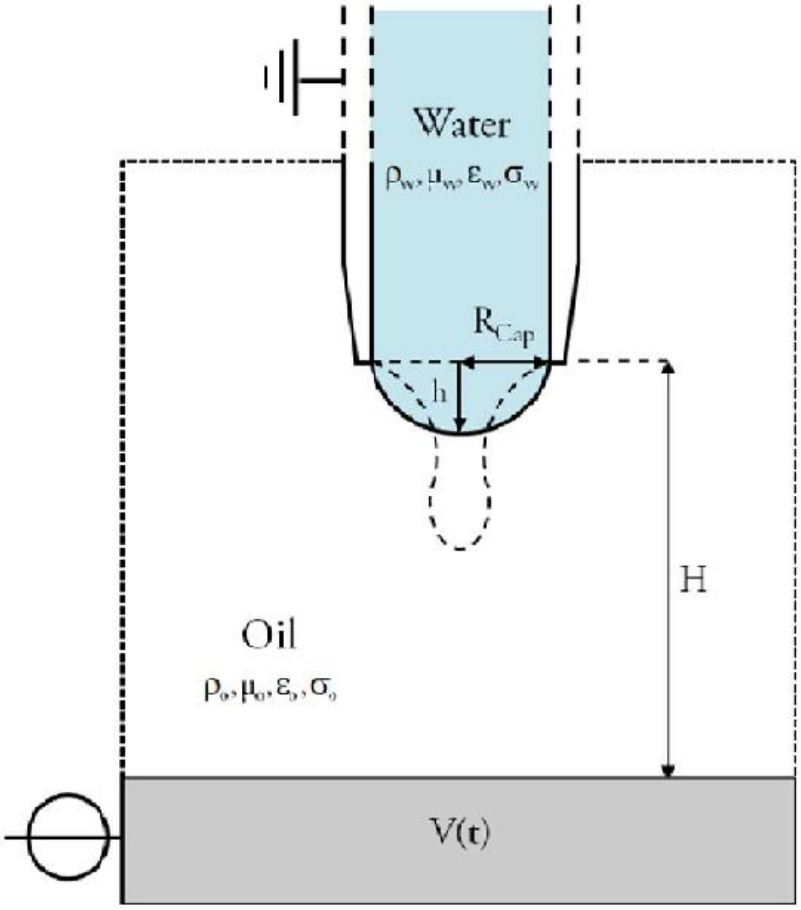

Figure 2.15 Main geometrical parameters

By referring to Figure 2.15, the distance between the electrode and the meniscus is given by H and the capillary radius by R_{cap}. With respect to the forces pulse amplitude V, balancing the capillary pressure P_{cap} and the electrostatic pressure P_{es} on the meniscus surface gives the minimum of deformation.

$$P_{es} = P_{cap} \tag{2.2}$$

$$\frac{1}{2}\varepsilon E_n^2 = 2T/R_{cap} \tag{2.3}$$

T is defined as the interfacial tension coefficient and R_{cap} is the radius of curvature. Break-up and instability happens in the region of the highest field. The maximum field intensity can be defined as:

$$E_{max} = \frac{2V}{R_{cap} \ln \frac{4H}{R_{cap}}} \tag{2.4}$$

The water meniscus must be faced with an electric field pulse based injection of a charge free drop which requires the supply of large amount of energy in a limited time. Having potential differences of V_{high} than V_{low} might be necessary regarding the pulse duration.

In order to get a neutral droplet, the electoral pulse must be finished before the drop break free which happens after estimating the pulse duration. This can be explained as the point of a liquid filament appearing between the drop and meniscus. However Δt (the difference in time) must be less than the characteristic capillary time t_{cap} to prevent producing a charged drop of the pulse duration.

$$t_{cap} = \sqrt{\frac{\rho R_{cap}^3}{T}} \tag{2.5}$$

where ρ is the density of the liquid flowing in the capillary (here water). Typically t_{cap} ~ 1.6 ms

[P. Atten] has modified a Weber number to compare the water injection using square voltage pulses having different amplitude and duration. This modified Weber number represents the work of the electrostatic forces acting on a non-deformable meniscus.

$$W_e^* = \int V(t)^2 \, dt \tag{2.6}$$

2.3.1 Importance to control meniscus size

In DOD, before the voltage pulse can be applied, it is important to form a suitable initial meniscus at the capillary front. The meniscus can be easily formed by adjusting the air pressure that continuously acts on the liquid surface. The shape and the size of the initial meniscus are important in DOD applications because an oversized hanging globule of liquid can adversely affect the performance.

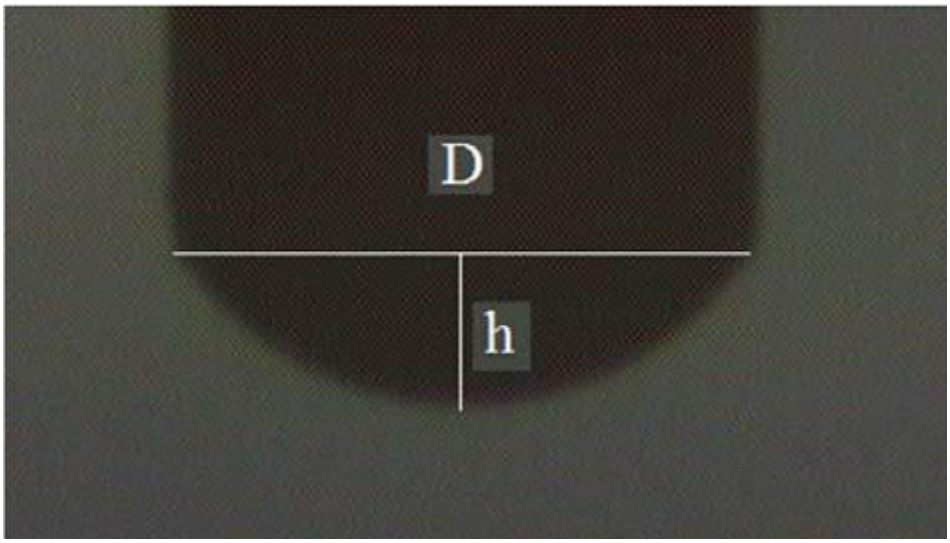

Figure 2.16 Meniscus geometrical dimensions

To control the meniscus, liquid properties such as the surface tension coefficient (σ), density (ρ) and dynamic viscosity (μ), are considered to be important variables.

Beside the liquid properties other important variables of the system are the shape and the outer diameter (D) of the nozzle (because for blunt edge and unmodified nozzles, the meniscus always attaches to the outer diameter of the nozzle (see Fig. 2.16)). One solution to control this phenomenon is given by other important parameter, the wettability on the front of the nozzle (the tip of the needle). In the work performed by [Stachewicz et al. 2008] reported the importance of anchoring the meniscus on the inner diameter. To achieve this, the tip of a glass capillary (front nozzle) was modified with an antiwetting coating based on a self-assembled monolayer (SAM) to restrict the meniscus to the inner diameter (ID) of the glass pipet. (See figure 2.17)

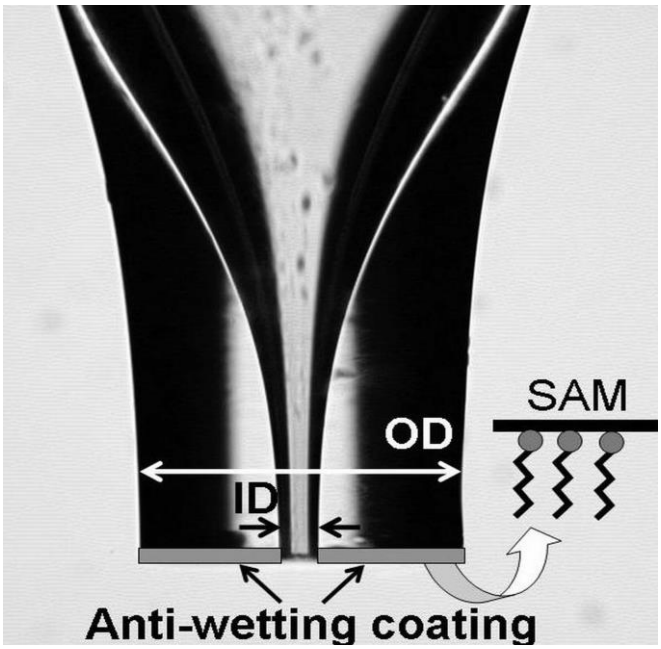

Figure 2.17 Antiwetting coating based on SAM

Without this modification, the meniscus attaches on the outer diameter (OD) of the nozzle therefore the droplets generated are larger as shows the figure below.

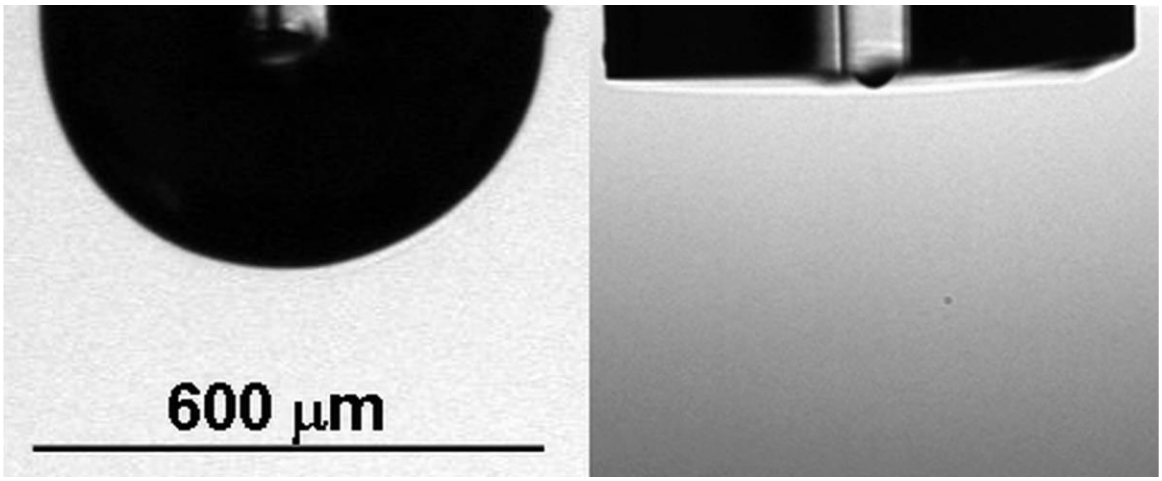

Figure 2.18 Effect of the antiwetting coating of the meniscus size [Stachewiczet al. 2008]

However one of parameters more important to achieve a meniscus and keeping with a constant size is the air pressure that acts on the system.

[Stachewicz et al. 2010] also reported that the equilibrium situation of the liquid inside the capillary is determined by three major pressures that are in balance. The first pressure is

related to the pressure of the meniscus inside the capillary far above the nozzle, $P_{mc} = 2cos\Theta \sigma /b$, where Θ is the contact angle between the liquid and the inside of the Teflon tube (in this case), and b is the radius of the Teflon tube. The second one is the static pressure of the liquid column, $P_{fc} = \rho gH$, where g is the acceleration due to gravity, H is the total liquid height in the capillary and the Teflon tube. Here, the meniscus height is neglected because it is very small in comparison with the liquid height in the capillary and the Teflon tube. The third pressure is caused by the meniscus hanging outside the nozzle, $Pm = 2\sigma_m/r_c$, where σ_m is the effective surface tension on the meniscus, which accounts for the surface charge and r_c is the meniscus curvature radius.

On the other hand, dimensional analysis performed by [Hyun et al. 2013] revealed that height of meniscus (h) actually depends on two important dimensionless numbers:

1) the S number defined as ($S = \sigma/\rho D2g$)

2) the P number defined as ($P = pabs/\rho Dg$).

The S number signifies the relative importance of the surface tension force and the gravity acting on the meniscus while the P number highlights the significance of the pressure force and the gravity. By observing these numbers, one can well understand that when the liquid properties and the diameter of the nozzle are fixed, the meniscus height h depends on the P number because under such circumstances the S number will remain fixed. On the other hand, the S number is varied by changing the diameter of the nozzle or the liquid properties.

Summarizing the work of [Hyun et al. 2013], the following main points can be taken from this study.

1) Small-diameter nozzles, a high viscosity and a high surface tension coefficient offer a wider range of working pressures.

2) The surface tension force and the pressure force remain higher than the gravitational force acting on the meniscus.

3) The non-dimensionless meniscus height h/D increases with increasing S and P numbers.

4) At a given value of the S number, the dimensionless meniscus height h/D increases linearly with increasing P number.

3 Experimental work

The experiments performed in this thesis can be separated in two parts. In the first part will be created drops only injecting water from the syringe pump, without high voltage application or EHD. In this case the effect of the needle diameter and shape on the drop size and time to generate it will be studied. The second part smaller drops will be generated applying high voltage (EHD) and parameters like meniscus shape and voltage pulse will be studied in comparison with drop size.

To perform these experiments the experimental setup composed of the following devices was used:

• 20ml syringe with 0.4-0.8 mm needle with/without bevel tip

• Photron FASTCAM SA3 high-speed camera

• THORLABS MCWHL2 Cold White Mounted High Power LED

• THORLABS M530L2 Green (530nm) Mounted High Power LED

• INFINITY K2-SC lens

• EX SIGMA DG MACRO 105mm 1:2.8D lens

• THORLABS High Power Led Driver LEDD1B

• Tektronix Arbitrary/Function Generator AFG 3021B

• TREK MODEL 5/80 power amplifier

• Test cell containing EXXSOL D80 oil and water

• HARVARD APPARATUS PHD 2000 pump

Properties of EXXSOL D80 [ExxonMobil]:

- Physical State: Liquid
- Form: Clear
- Color: Colorless
- Odor: Mild Petroleum/Solvent
- Density: 798 Kg/m^3
- Auto ignition Temperature: 251 °C
- Boiling Point Range: 200-250 °C
- Viscosity: $2.1610^{-6}\, m^2/sec$ at 25 °C

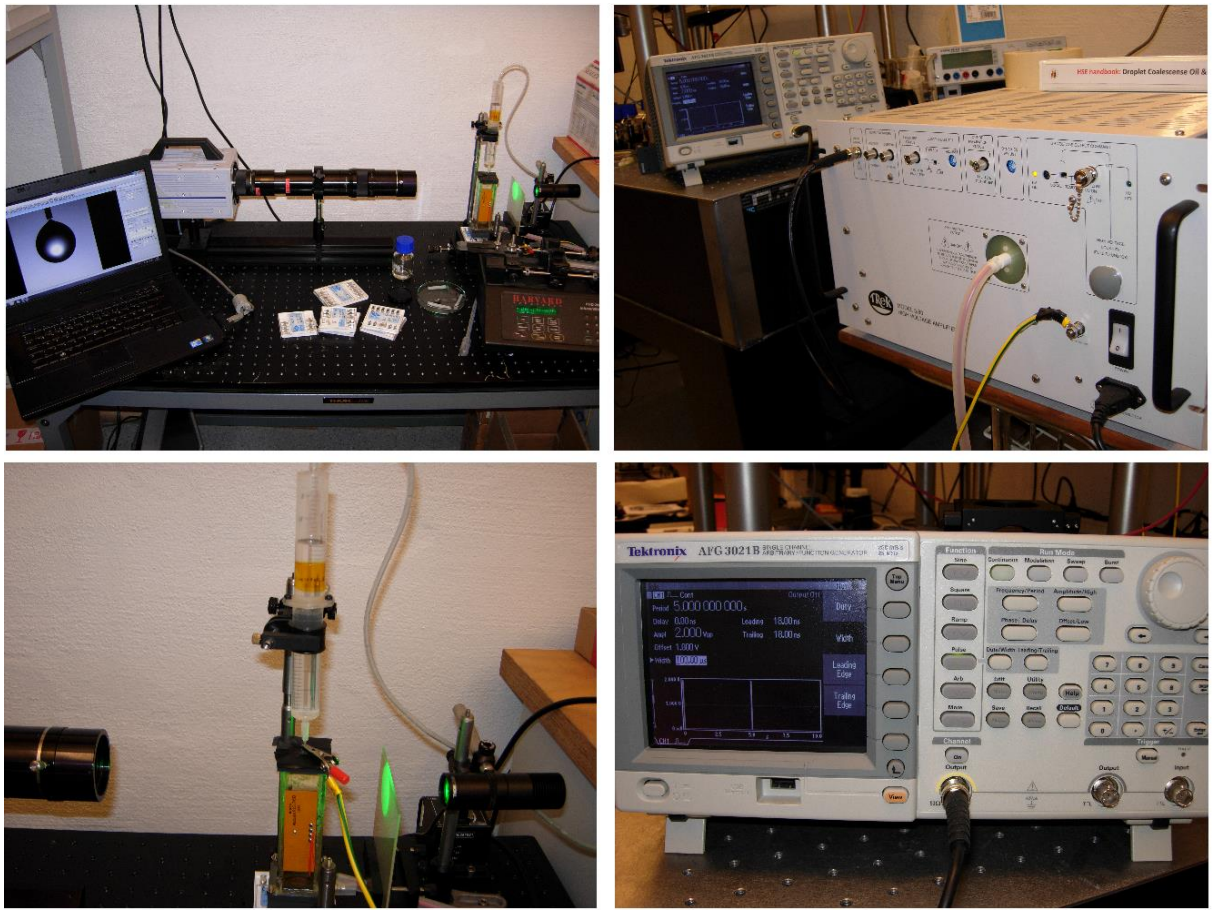

Figure 3.1 Experimental setup

3.1 Drops generation without EHD application

As previous study, it was studied the influence of the needle shape in the drop size and the time needed to generate a single drop, the voltage will be not applied. To perform this, a test cell containing Exxsol D80 oil is used. On the top of the cell there is a needle submerge in the oil and it is connected to a syringe with water that is installed at HARVARD APPARATUS PHD 2000 pump. A Photron FASTCAM SA3 high-speed camera is aimed with focus on the tip of the needle and the water meniscus. The Photron FASTCAM SA3 high-speed camera is connected to a computer and the recording is controlled from there, storing both in .avi and .tif format. A THORLABS M530L2 Green light with 530nm wavelength provides the backlight for the camera.

To generate drops a infuse rate between 7.5 µl/min and 120 µl/min is applied in the pump. Two diameters of needles are used, 0.4mm and 0.8 and both with two different tip, blunt point

and bevel tip. In the pump is the syringe of 20 ml with water and no air. In this experiment drops size varying from around 2,6 mm to 3,7 mm were created.

3.2 Droplets Generation applying EHD

3.2.1 Description of the unit

In this part of the experiments the main focus is generating droplets between 25 μm to 180 μm. To achieve these results EHD will be used and the next procedure is performed.

Tektronix Arbitrary/Function Generator AFG 3021B is connected to a TREK MODEL 5/80 power amplifier. The TREK MODEL 5/80 power amplifier is connected to the bottom plate of the test chamber by a cable, and to the needle with a grounded cable. A Photron FASTCAM SA3 high-speed camera is aimed with focus on the tip of the needle and the water meniscus. The Photron FASTCAM SA3 high-speed camera is connected to a computer and the recording is controlled from there, storing both in .avi and .tif format. A THORLABS M530L2 Green light with 530nm wavelength provides the backlight for the camera.

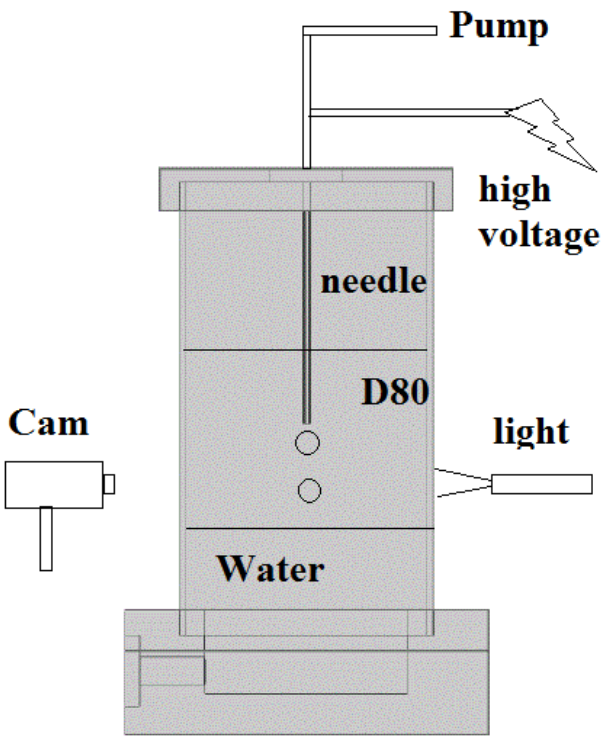

Figure 3.2 Visualization of the process

Applying high voltage pulses supplied by Tektronix Arbitrary/Function Generator AFG 3021B and amplified by the TREK MODEL 5/80 power amplifier enables the generation of drops. By changing the settings for on the Function Generator and controlling the voltage, drops from the water meniscus at the tip of the needle are released. Changes made to the interval, voltage and period of the pulse are performed to study the generated drop size. A Photron FASTCAM SA3 high-speed camera is aimed with focus on the tip of the needle and the water meniscus. This allows for the deformation of meniscus and eventually the release of drops to be studied. Variation in the syringe is performed and consists of two syringes of 20 ml connected by one end. This modification creates bigger water-to-air ratio and level and allows anchoring of the meniscus on the tip of the needle easier manner.

3.2.2 Procedure

In this case three tests types will be performed. The first test was performed with a constant voltage of 2kV and 130 μs pulse width were applied for a variable meniscus size. The second test, different values for the voltage was used, from 1.8 kV to 3.2 kV with a width of pulse constant of 130 μs. Last, the pulse width was varied ranging from 126 μs up to 138 μs for 2kV and constant meniscus.

An almost constant interval between each pulse was generated of 5 s, with the exception of one experimental run where the interval used was smaller. The type of pulse used was always a square pulse.

An air-to-water ratio in the modified syringe was utilized, varying from 5 ml to 17 ml air. The needle used in all of this experiment is 0.4 mm with blunt point. The height (H) of the electrode (from tip of the needle to bottom cell) was 10.36 cm but small variations could happen.

In these experiments drops of sizes varying from around 25 μm to 180 μm were created.

3.3 Data collection

Water drops of several sizes are generated by the droplet generation procedures mentioned in the previous section. The high speed camera record the trajectory of the droplet as it descends through the oil. For all experiments described previously is the below procedure.

The video sequences recorded using the described method need further processing enabling the gathering of data regarding drop size. Matlab scripts are used for this procedure. (See appendix 2)

First the video .avi files are transformed into .bmp picture files with Matlab script “avi2bmp”, which can be further processed. This process outputs the frame rate for the given video. The frame range where the drop is detected and descends through the oil is selected. As the pictures are in a grey color scheme, a conversion into black and white is performed, also removing small particles and disturbances in the picture.

3.3.1 Calibration of drop size and meniscus

After recording the videos and transformed to pictures the diameter of the drop can be calculated using the Matlab script “diameter”. Taking a snapshot of the tip of the needle submerged in the oil the millimeter to pixel ratio is determined. Measurements of the needle diameter in advance using a Cocraft Digital Caliper measures the diameter of the needle with a given error and supplies the calibration used for the videos. With a picture, the diameter of the drop can be determined using Matlab script. This script calculates two diameters, one on the *x* axis and another one on *y* axis. This is because the drops experimental a shape deformation to spherical to spheroid while they are going down through the fluid as shows the picture below. So taking two the minor and major radios Matlab calculates the average diameter and the dimensions of the drops are calculated.

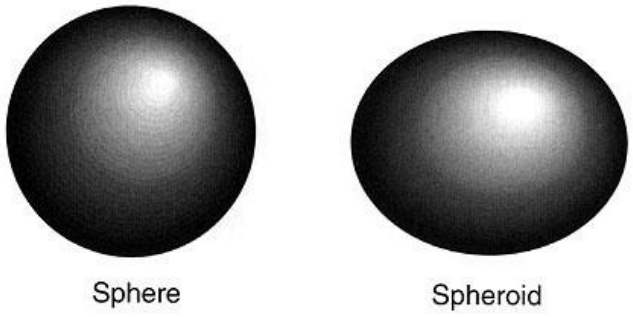

Figure 3.3 Sphere and spheroid drops

However to calculate the meniscus size the Matlab script is not used. The height (h) and diameter (D) of the meniscus is determined counting the number of pixel. This is possible

since the diameter of de needle is known; therefore the pixel to mm ratio is determined as it was commented previously.

3.3.2 Error Analysis

For the calibration a snapshot of the needle tip was taken with the Photron FASTCAM SA3 high-speed camera. A high level of magnification enabled the measurement of number of pixels corresponding to the needle. Two needle diameters were used, 0.4 mm and 0.8 mm and were measured using Cocraft Digital Caliper.

For the bigger needle was found to be d = 0.8 mm $\pm$ 0.01 mm. The error corresponds to 1.25%. The lens uses was EX SIGMA DG MACRO 105mm 1:2.8D lens and measurement was found to be d = 111 $pixels$ $\pm$ 1 $pixel$. The error corresponds to 0.9 %.

To the small needle was found to be d = 0.4 mm $\pm$ 0.01 mm. The error corresponds to 2.5 %. In this case INFINITY K2-SC lens was used and the measurement was d = 90 $pixels$ $\pm$ 1 $pixel$. The error corresponds to 1.11 %

These measurements of the needle in both mm and $pixels$ resulted in the ratio of pixels to millimeters used for the video and image processing.

As mentioned previously the measurement of the drops was performed with Matlab script "Diameter". The drops crated by the 0.8 needle was found an error of $\pm$ 1 $pixel = 7$ μm such us for a drops of 3.5 mm the error corresponds to ~ 0.2%.

The drops crated by the 0.4 needle was found an error of $\pm$ 1 $pixel = 4$ μm. In this case there is a bigger range of error. Such as for the diameter of the smallest droplet created (27 μm) corresponds a 14.8 % of error. For the biggest droplet generated in this case (169 μm) corresponds a 2.2% of error.

4 Results and discussion

4.1 Drops generation without EHD application

As mentioned previously, several cases were conducted and recorded to check and analyze the variety of results. Figure 4.1 shows how vary the diameter size as a function of the water injected into a syringe for needles of 0.4 mm and 0.8 mm with blunt point and bevel tip (chamfer).

	Diameter (mm)			
Volume (µl/min)	**0.4**	**0.4 chamfer**	**0.8**	**0.8 chamfer**
7,5	2,64	2,64	3,44	3,33
15	2,67	2,68	3,55	3,41
30	2,74	2,75	3,64	3,43
60	2,74	2,75	3,70	3,46
90	2,79	2,75	3,73	3,47
120	2,80	2,80	3,73	3,51

Table 4.1Volume and diameter

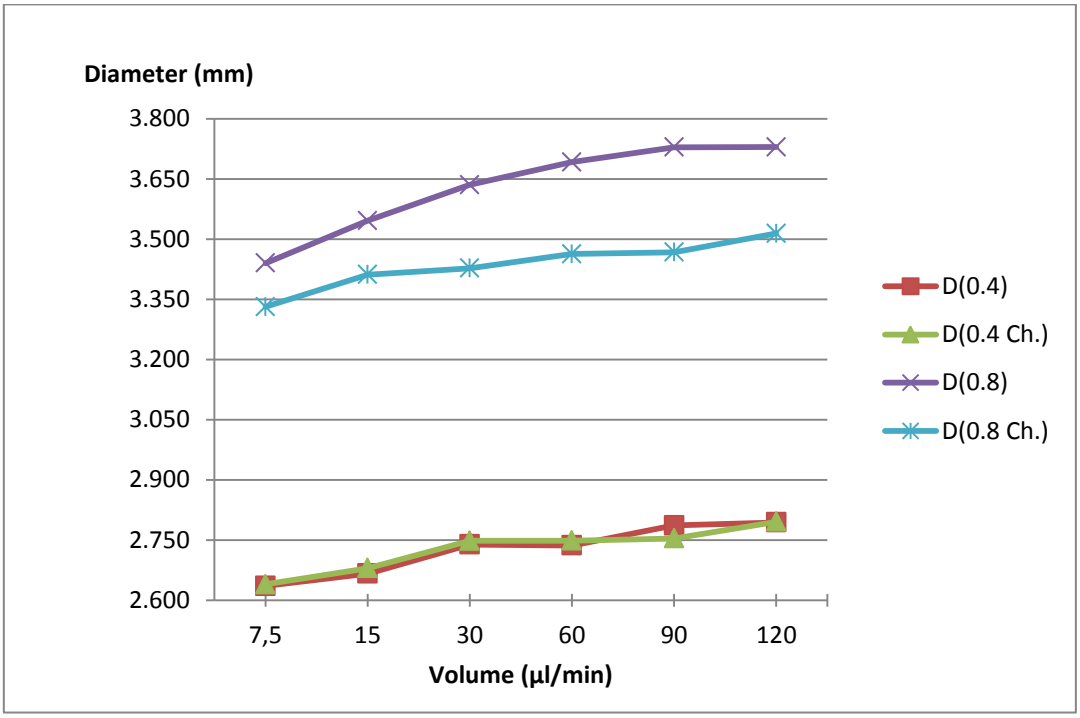

Figure 4.1 Variation of the diameter of injected droplet as a function infuse rate for different types of needles

Table 4.2 shows how vary the time for generating a single drop as a function of the water injected into a syringe for different types of needles.

	Time (s)			
Volume (µl/min)	**0.4**	**0.4 chamfer**	**0.8**	**0.8 chamfer**
7,5	76,66	77,02	170,55	154,86
15	39,70	40,30	93,38	83,16
30	21,51	21,73	50,31	42,17
60	10,73	10,87	26,35	21,74
90	7,55	7,29	18,10	14,55
120	5,71	5,72	13,58	11,36

Table 4.2 Volume and time

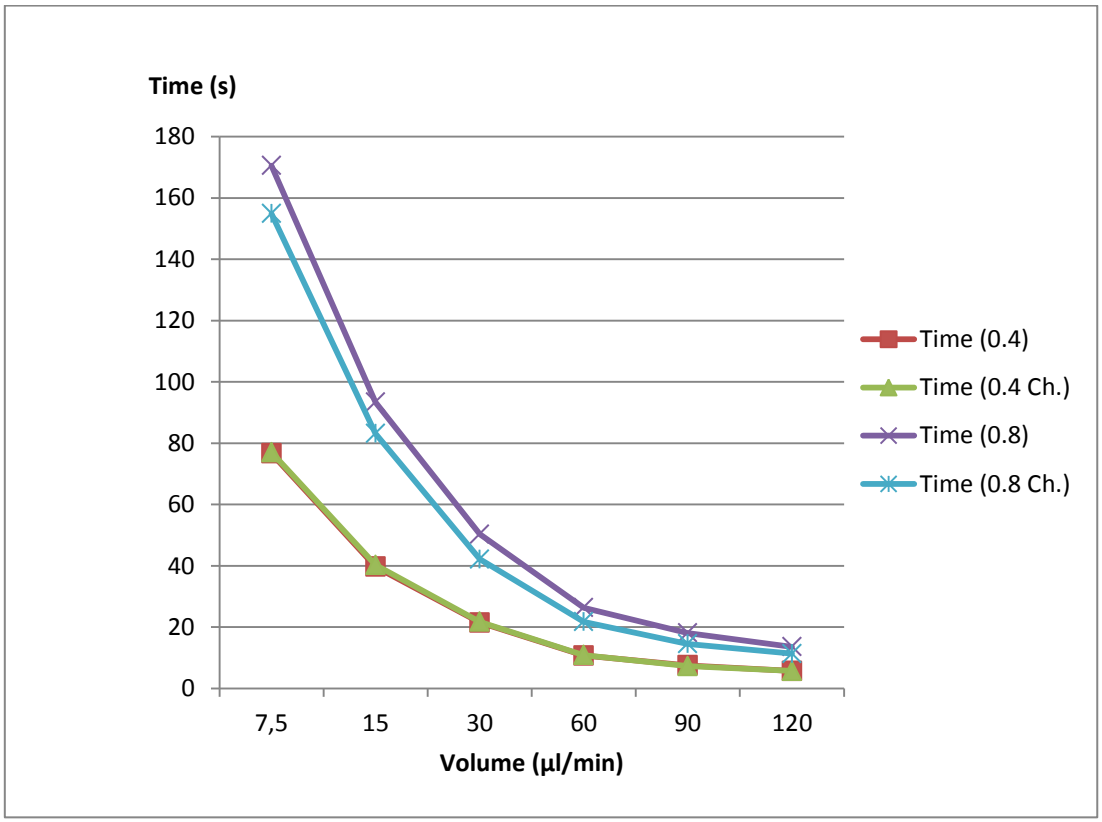

Figure 4.2 Variation of time generation of injected droplet as a function infuse rate for different types of needle

4.2 Droplets generations applying EHD

As aforementioned in this section was applied EHD, this is applying high voltage to generate smaller droplet than needle diameter (0.4mm). The droplet diameter will be compared with the shape of meniscus that is defined by the height (h) and width or meniscus diameter (D). The influence the other parameters as high and width of the voltage pulse applied will be studied as well.

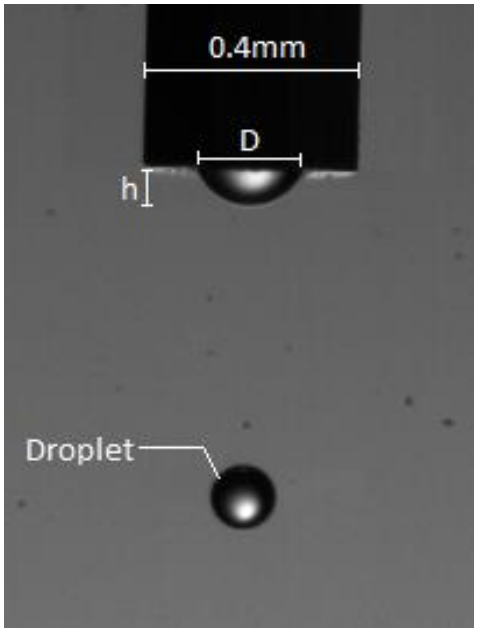

Figure 4.3 Geometrical parameters studied

4.2.1 Drop size as a function of meniscus shape

In this part of the experiment was studied the relation of droplet diameter for different meniscus sizes. A range of droplets from 26 to 180 µm were generated. To perform this, a constant voltage pulse of 2kV and 130 µs of width were applied. The pictures below show the comparison of droplet size with every parameter of meniscus, height (h) and width or diameter (D).

Droplet size (µm)	h (µm)	D(µm)	h/D
27	27	84	0,653
38	36	164	0,553
47	40	169	0,565
56	40	173	0,522
58	44	169	0,467
60	44	191	0,432
60	49	178	0,432
69	53	187	0,409
69	49	173	0,395
82	53	178	0,349
84	53	178	0,326
87	58	187	0,333
89	67	187	0,357
93	62	191	0,310
93	62	187	0,300
107	67	191	0,300
109	76	191	0,286
116	80	196	0,282
118	84	196	0,233
122	84	196	0,275
131	93	200	0,263
136	107	204	0,231
144	116	204	0,237
149	116	209	0,216
169	142	218	0,316

Table 4.3 Droplet size and meniscus shape

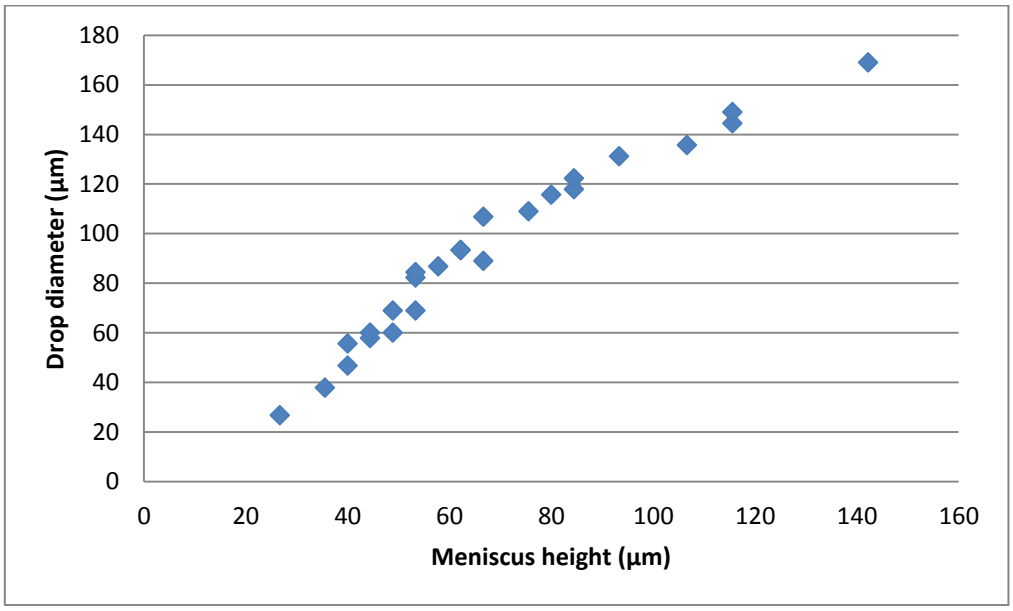

Figure 4.4 Relation of meniscus height (h) with the droplet diameter

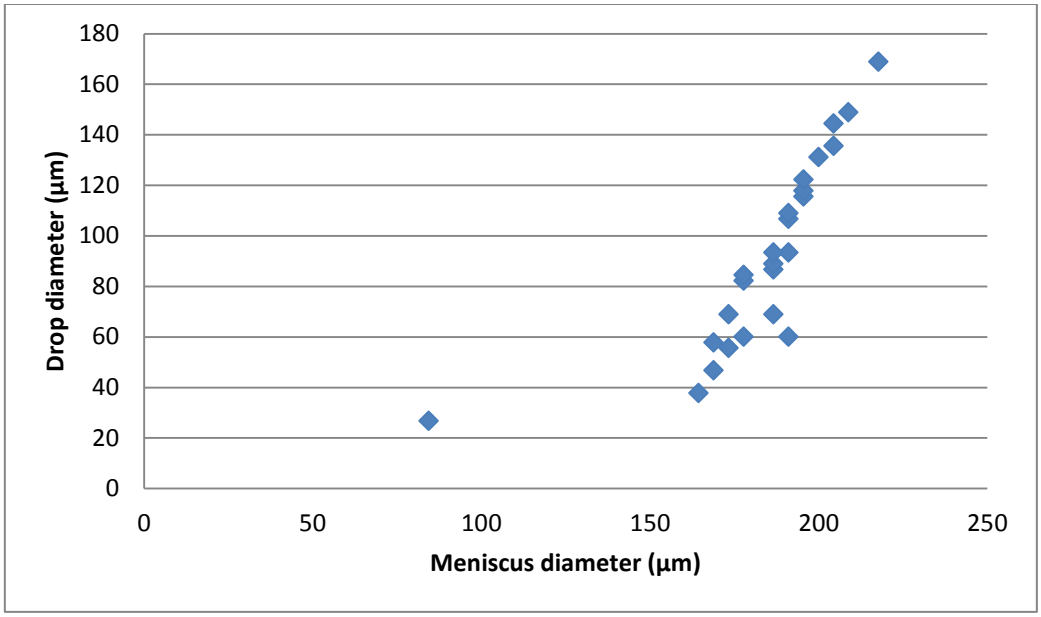

Figure 4.5 Relation of meniscus diameter (D) with the droplet diameter

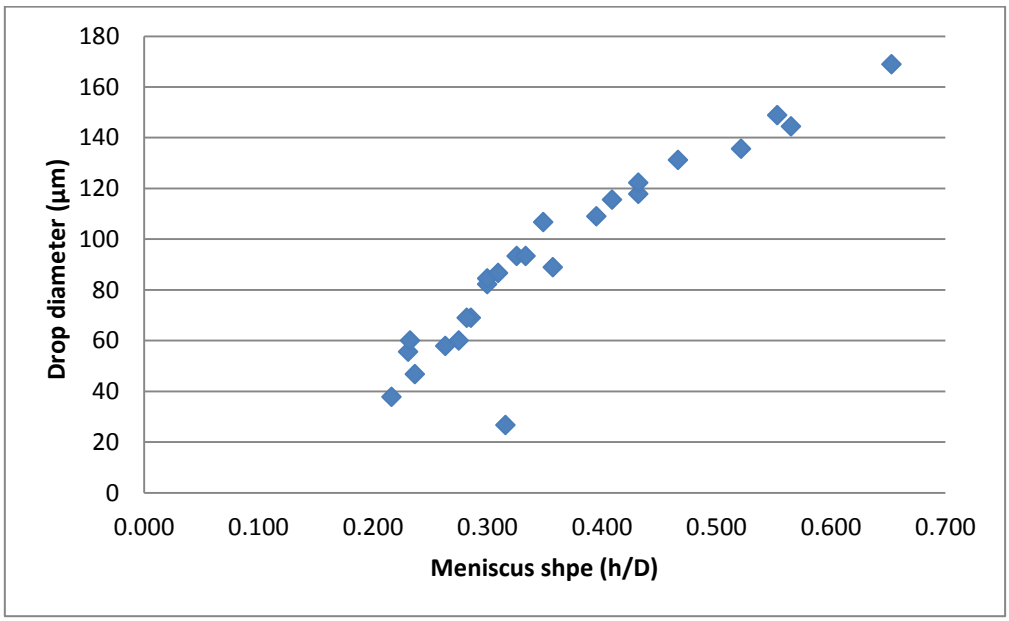

Figure 4.6 Relation of meniscus shape (h/D) with the droplet diameter

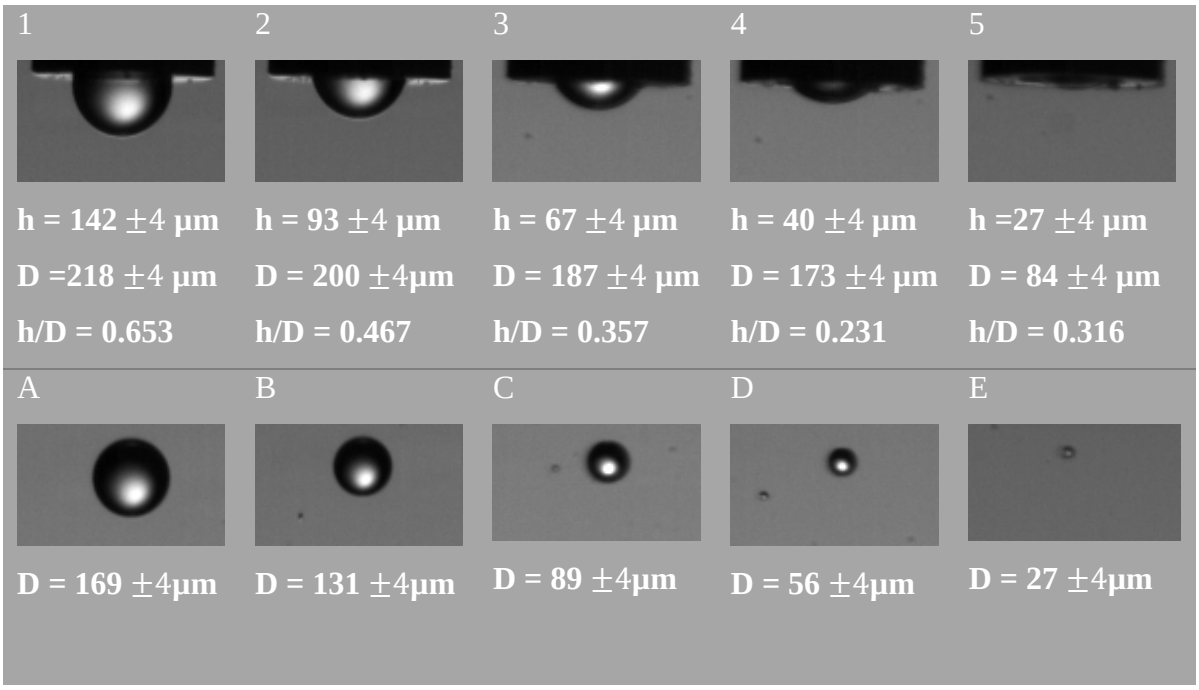

Figure 4.7 Different sizes of menisci with their corresponding drop diameters created from left to right respectively. For a needle of 0.4 mm, 2kV and 130 µs pulse width.

4.2.2 Drop size as a function of voltage pulse amplitude

Below is shown the influence of voltage pulse amplitude in the droplet size. To perform this, a pulse width of 130 µs was applied and trying to keep a meniscus shape (h/D) constant. In the next figures can be seen the comparison of diameter of the drop with the height (h) and diameter (D) of the water meniscus for an increasing of voltage.

Voltage (kV)	Droplet size (µm)	h (µm)	D (µm)	h/D
1,8	35	31	163	0,189
1,9	53	33	163	0,203
2,0	62	33	165	0,200
2,1	66	35	163	0,216
2,2	77	40	167	0,237
2,3	77	33	167	0,197

2,4	84	35	167	0,211
2,5	88	33	163	0,203
2,6	90	35	163	0,216
2,7	92	33	165	0,200
2,8	92	33	163	0,203
2,9	92	33	163	0,203
3,0	90	33	165	0,200
3,1	92	33	163	0,203
3,2	97	42	171	0,244

Table 4.4 Voltage, droplet size and meniscus

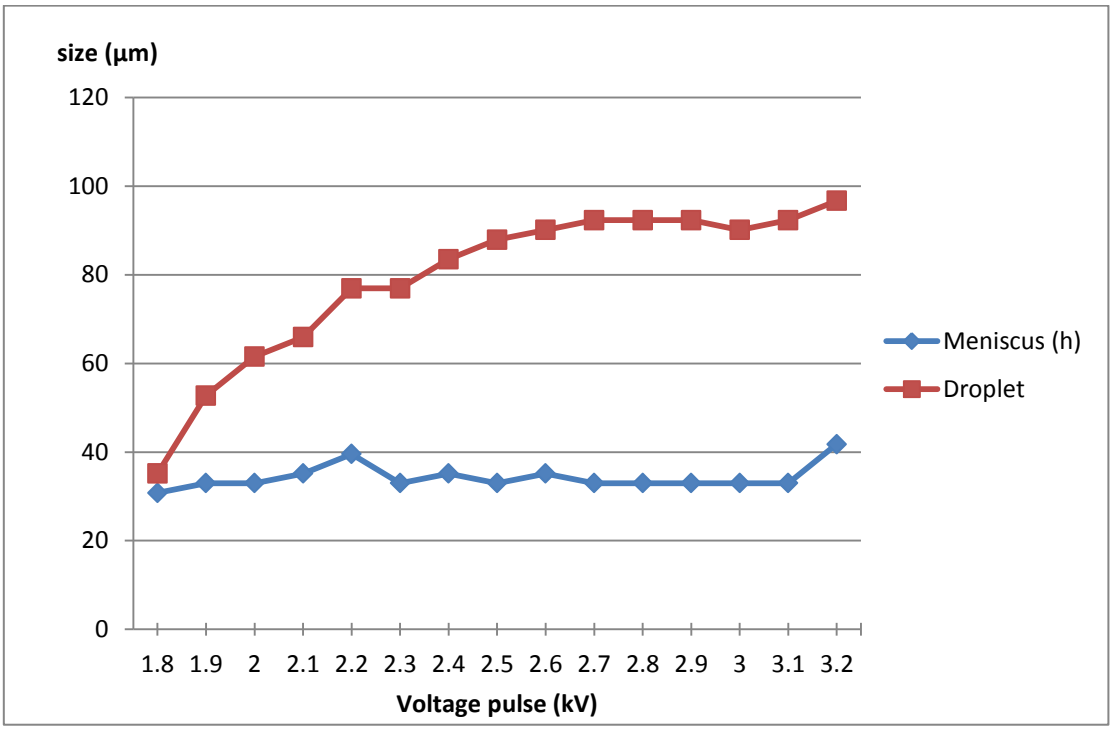

Figure 4.8 Variation of the meniscus high and droplet diameter as a function of voltage pulse

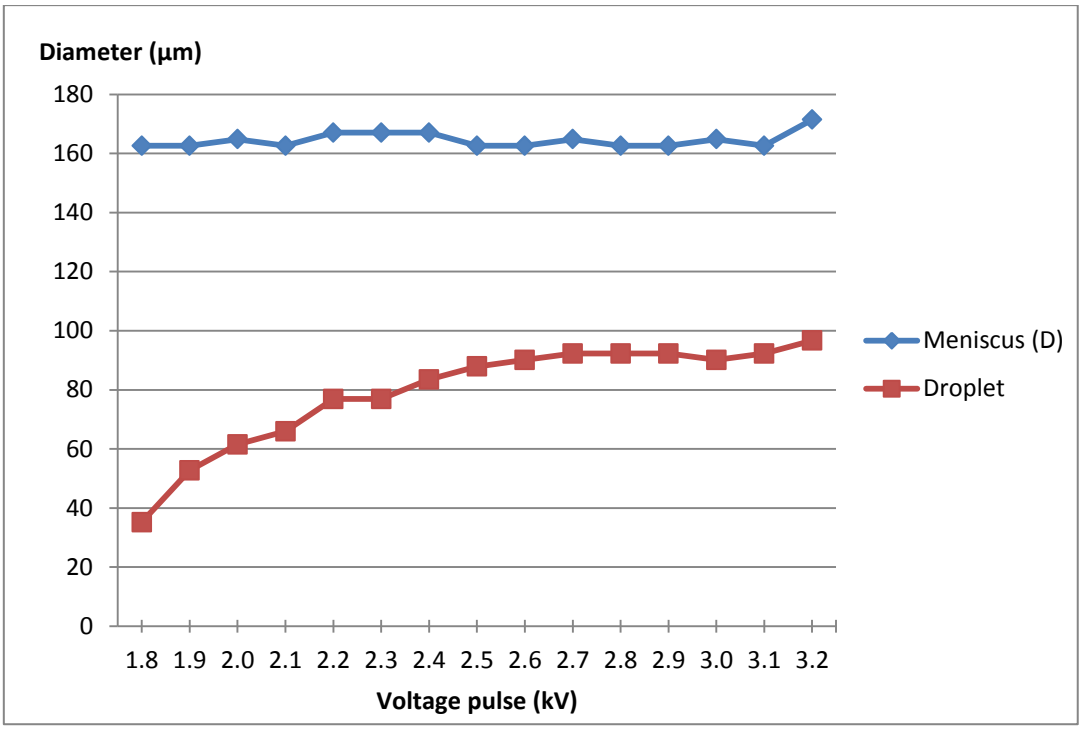

Figure 4.9 Variation of the meniscus diameter and droplet diameter as a function of voltage pulse

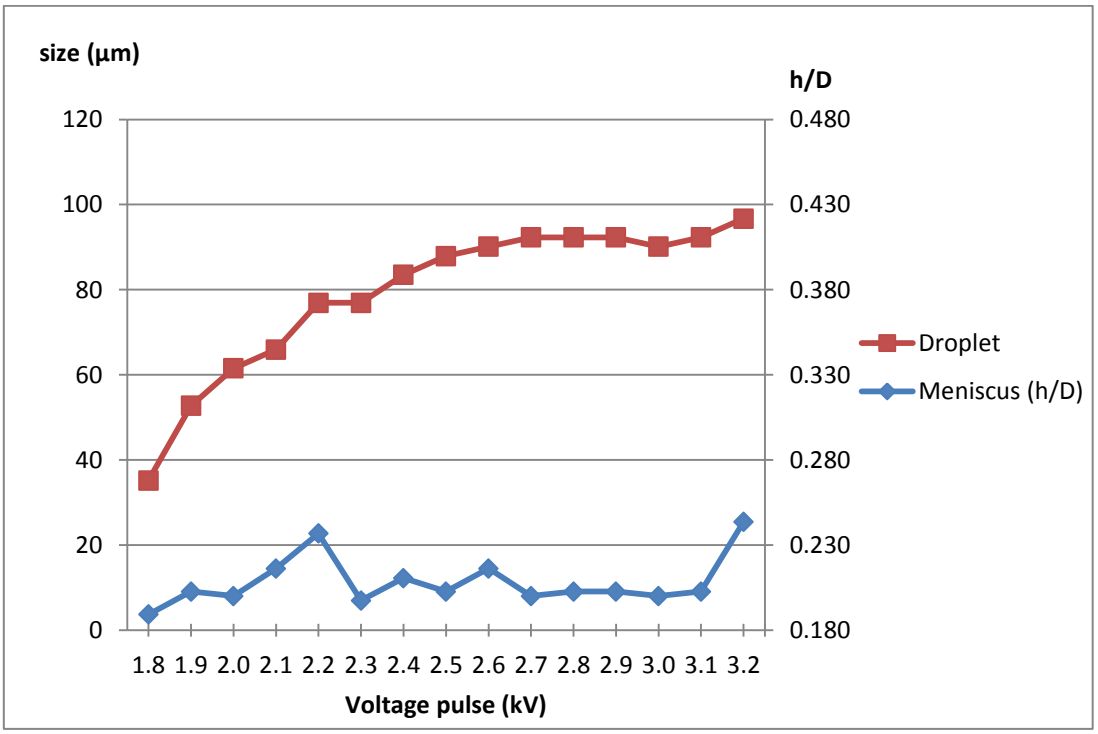

Figure 4.10 Variation of the meniscus parameter (h/D) and droplet diameter as a function of voltage pulse

4.2.3 Drop size as a function of pulse width

Below are shown the results for a variable pulse width and his influence with the diameter of the droplet. Here the meniscus shape (h/D) is kept constant with a width (D) of 226 µm and 39 µm high (h). The voltage applied was 2 kV.

Width (µs)	Droplet size (µm)	D (µm)	h (µm)	h/D
126	65	226	39	0,173
127	65	226	39	0,173
128	67	226	39	0,173
129	67	226	39	0,173
130	67	226	39	0,173
131	70	226	39	0,173
132	70	226	39	0,173
133	70	226	39	0,173
134	72	226	39	0,173
135	72	226	39	0,173
136	74	226	39	0,173
137	74	226	39	0,173
138	74	226	39	0,173

Table 4.5 Pulse width and droplet size for a constant meniscus and 2kV

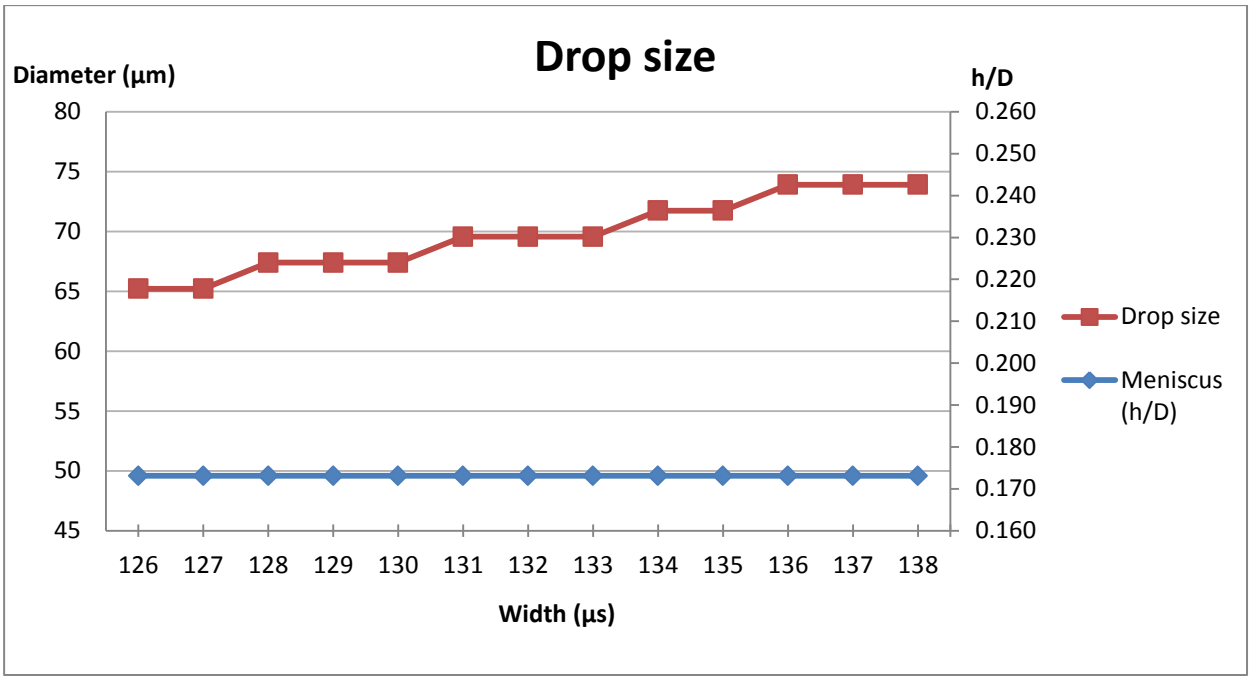

Figure 4.11 Droplet diameter variation as a function of width pulse for a shape of meniscus constant

4.3 Discussion

4.3.1 Drops generation without EHD application

The first part of the experiments in this thesis consists of generating large drops without high voltage application. During these experiments, the parameters like diameter of the needle and shape of the tip were studied and their effect on the time and diameter of the drop generated.

As can be seen in figure 4.1 bigger drops with a diameter around 3.5 mm were created by needles of 0.8 mm. The biggest drops were achieved by the needle with blunt tip, those results are logical since it is easier to anchor a bigger water meniscus in the tip of the needle thus can be created larger drops. On the other hand, smaller drops with a diameter around 2.7 mm were created by the needle of 0.4 mm. In this case the shape of the needle has minor influence in the size of the drops as can be seen in the figure 4.1. For both cases can be observed increasing the diameter of the drops for a bigger water infuse rate. This is because the low infuse rate takes more time for generating a drop (see figure 4.2) hence the meniscus remains more time anchored in the tip of the needle and any external perturbation can bring down before reaching its maximum size. See Appendix 1 for more details.

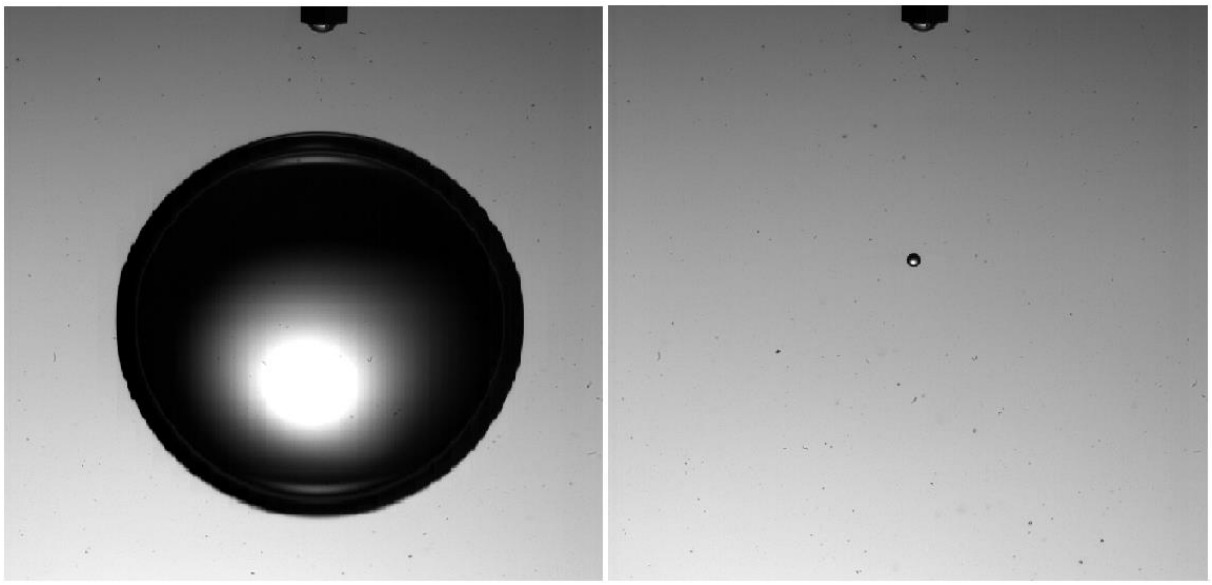

Figure 4.12 Difference of the size for a single droplet without applying EHD (left) and applying EHD (right)

4.3.2 Drops generation by EHD application

As shows the figure 4.12 for generating smaller droplets high voltage was applied. The results achieved with this technique, also called electrohydrodynamics (EHD) as was mentioned in the section 2.3, are described below.

Firstly, the influence of meniscus shape with the droplet size was studied. Analyzing the data achieved, droplets from 26 to 169 μm were generated for different menisci sizes. It is observed a direct trend of increases of droplet with a bigger meniscus. An example of which can be seen in the figure 4.7. The biggest droplet was created by a meniscus with the maximum height (142μm) and width (218μm).On the other hand, the smallest droplet was generated with the minor meniscus possible, almost nonexistent as can be seen in the figure 4.7 (5). The geometrical parameters that describing the meniscus size are the height (h) and width (D) and their relation with the droplet size are shown in the figures 4.4 and 4.5. The figure 4.6 shows the relation between both parameters and can be observed that the shape of the meniscus tends to form a spherical shape with the increasing of meniscus except for the smallest one. This is because there is less difference between the height and width of meniscus as shows the figure 5.7(1) (2).

Noteworthy that when the meniscus reached the maximum size for the inner diameter suddenly it grows up rapidly creating a huge drop. This is because when it touches the edge of the inner diameter grows up to outer diameter along with the needle thickness. This phenomenon could be avoided decreasing the thickness or using a tip with a hydrophobic layer (as was shown in the section 2.3.1). Also small variations of pressure have a big effect on the meniscus shape. For all of these reasons, it was always difficult to keep a meniscus with the same shape.

The droplet size was also studied as a function of the voltage pulse amplitude. Is attempted to keep the meniscus with the same shape in this case, but a small variation was observed. The range of voltage pulse applied was from 1.8 to 3.2 kV for a width pulse constant of 130 µs and a current of 1 mA. Below this range it was difficult to generate drops and above it, the satellite droplets begin to be considerable size. From 1.8 until 2.4 kV there is a more pronounced increase. After, the size tend to be constant up to reaching 3.2 where increases suddenly. This may be because it was observed the existence of a satellite droplet. See figures 4.8, 4.9 and 4.10.

Finally, the size of the drop was related with the pulse width for a constant voltage of 2 kV. Here the meniscus shape is keeping with the same shape. The range of pulse width applied is small, from 126 to 138 µs. Also the influence in the droplet size is small, around 10 µm (with an error of ±4 µm). It was difficult to generate droplet below of 126 µs and above 138 µs the satellite droplets increased. Also a long pulse could cause a large deformation to the meniscus causing it to break into a spray, however it was observed slightly increases of droplet size with the increases of pulse width as shows the figure 4.11.

After studied the results of the previous tests, the most important parameter in generating microdroplet is the meniscus size (as shows the figure 4.7). It is controlled mainly through pressure and shape and size of the needle. By the other side, it was observed an increases of the droplet size with the increasing the voltage and pulse width which corresponds to the existing literature. However although the voltage effect is bigger than the pulse width on the droplet size, it cannot be said that the droplet size meets the relationship $V^2\Delta t$ as was reported by Atten, Raisin et al. (See 2.3) Therefore the parameters like voltage and pulse width help to create the droplets but have less influence in the droplet size. So they are finer adjustments for varying the droplet size.

5 Conclusions and further recommendations

5.1 Conclusions

In this thesis droplets with a diameter between 26 µm to 170 µm have been generated by applying EHD. These experiments were performed in a test container with Exxsol D80 oil. On the top a 0.4 mm needle was connected to a syringe with water. The importance of the meniscus size was demonstrated since it has a direct relation with the droplet size. A relation of the different droplet sizes with their corresponding menisci was reported, and the difficulty for keeping the meniscus always with the same size was also reported.

Moreover other parameters like the voltage and pulse width were studied. However these are less helpful to form a specific droplet sizes because mainly they help to tear the droplet from the meniscus and determine whether they create satellite drops or not, which can be termed as fine adjustment.

On the other hand it was studied the influence of the needle size and shape in relation with droplet size a time required to generate it for different infuse ranges. In this case was not applied EHD. Here it is shown that the needle diameter is more relevant than the needle shape. Generated drops were in the range of 2.6 mm to 3.7 mm.

To perform these experiments took first a literature review of the different techniques to generate droplets explained in the theoretical part.

5.2 Further recommendations

Although the work and experiments performed for this project thesis has given a noticeable amount of data and results, there is still need for more testing and experiments to be performed.

The study of the variation height of the electrode (H) and its relation with the drop size it would be recommended. Moreover, measuring the pressure applied into the syringe and controlling it will be a key point for the meniscus size, which is not completely achieved in this work. Additionally the creation of the satellite droplets must be avoided for the measure of the results.

As contamination has been present in the performed experiments for this thesis, cleaner test cells and leak proof are recommended used. Work in an environment free from external disturbances such as vibration and noise is also highly recommended.

The oil used in the experiments for this thesis is an Exxsol D80 lamp oil, transparent oil with properties differing from that of crude oil. As real separators separate crude oil and water from the reservoir, this would be recommended to experiments further on. The water used is tap water, and ideally the water used should be from the same well as the oil. Experimenting with different fluids may also be experimented on, studying the difference in oil properties on meniscus size and drop diameter.

The effect of temperature on droplet and meniscus size has not been studied. The temperature was keeping constant during the experiment, varying the temperature would be a recommended experiment to see the effect on both.

References

Allen, R.R., Meyer, J.D., and Knight, W.R. (1985) “Thermodynamics and Hydrodynamics of Thermal Ink Jets,” Hewlett-Packard J., May, pp. 21–27.

American Petroleum Institute. 1990. "Design and Operation of Oil-Water Separators”, Publication 421, American Petroleum Institute, Washington, D.C.

Ashley, C.T., Edds, K.E., and Elbert, D.L. (1977) “Development and Characterization of Ink for an Electrostatic Ink Jet Printer,” *IBM J. Res. Dev.*, 21, pp. 69–74.

Atten, Pierre, et al. "Drop-on-demand extraction from a water meniscus by a high field pulse." Dielectric Liquids, 2008. ICDL 2008. *IEEE International Conference on.* IEEE, 2008.

Buehner,W.L., Hill, J.D.,Williams, T.H., and Woods, J.W. (1977) “Application of Ink Jet Technology to a Word Processing Output Printer,” *IBM J. Res. Dev.*, 21, pp. 2–9.

Bugdayci, N., Bogy. D.B., and Talke, F.E. (1983) “Axisymmetric Motion of Radially Polarized Piezoelectric Cylinders Used in Ink jet Printing,” *IBM J. Res. Dev.*, **27**, pp. 171–80.

Chen, P.-H., Peng, H.-Y., Liu, H.-Y., Chang, S.-L., Wu, T.-I., and Cheng C.-H. (1999) “Pressure Response and Droplet Ejection of a Piezoelectric Inkjet Printhead,” *Int. J. Mec. Sci*., 41, pp. 235–48.

Darling, R.H., Lee, C.-H., and Kuhn, L. (1984) “Multiple-Nozzle Ink Jet Printing Experiment,” *IBM J. Res. Dev*., 28, pp. 300–6.

De Almeida, Valmor F., Rodney D. Hunt, and Jack L. Collins. "Pneumatic drop-on-demand generation for production of metal oxide microspheres by internal gelation." *Journal of Nuclear Materials* 404.1 (2010): 44-49.

Deshpande, Kiran B., and William B. Zimmerman. "Simulation of interfacial mass transfer by droplet dynamics using the level set method." *Chemical engineering science* 61.19 (2006): 6486-6498.

Hida, H., et al. "Micromachined tube-type of Si droplet generator." *Solid-State Sensors, Actuators and Microsystems Conference, 2009. TRANSDUCERS 2009. International*. IEEE, 2009.

Hirata, S., Ishii, Y., Matoba, H., and Inui, T. (1996) “An Ink-Jet Head Using Diaphragm Microactuator,”*Proc. of the 9th IEEE Micro Electro Mechanical Systems Workshop*, pp. 418–23, February 11–15, San Diego.

Hyun, C. K., & Mehdi, S. M. (2013). Meniscus height as a function of dimensionless variables for drop-on-demand applications. *Journal of the Korean Physical Society*, *62*(9), 1247-1251.

Jaworek, A. "Micro-and nanoparticle production by electrospraying." *Powder technology* 176.1 (2007): 18-35.

Kirby S. Mohr. “How Oil-Water Separators Work and How to Use Them” P.E 2001-2013.

Lai, S. C. S. "Mimicking nature: Physical basis and artificial synthesis of the Lotus-effect." (0020370) Universiteit Leiden (2003).

Lee, Eric R. *Microdrop generation*. Vol. 5. CRC press, 2010.

Lindemann, Timo. "Droplet generation-from the nanoliter to the femtoliter range". *Diss. Universitätsbibliothek Freiburg*, 2006.

M. Saeid, A. P. William and G. S. James, "Handbook of Natural Gas Transmission and Processing*". Burlington, Gulf Professional publishing*.

Mikami, Masato, et al. "Microgravity experiments on flame spread along fuel-droplet arrays using a new droplet-generation technique." *Combustion and flame* 141.3 (2005): 241-252.

Myers, R.A., and Tamulis, J.C. (1984) "Introduction to Topical Issue on Non-Impact Printing Technologies," *IBM J. Res. Dev*., 28, pp. 234–40.

Nielsen, N.J. (1985) "History of ThinkJet Printhead Development," *Hewlett-Packard J.*, May, pp. 4–10.

Nilsson, J., Bergkvist, J., and Laurell, T. (2000) "Optimization of the Droplet Formation in a Piezo-Electric Flow-Through Microdispenser," *Proc.* µ*TAS '00*, pp. 75–78, May 14–18.

Rahman, Ahsan, et al. "Drop on Demand Non-contact Hydrophilic Electrostatic Deposition Head." *International Journal of Engineering & Technology* 10.1: 61-69.

Raisin, J (2011) "*Electrocoalescence in Water-in-Oil Emulsions: Toward an Efficiency Criterion"*. University of Grenoble, France.

Ristenpart, William D., et al. "Non-coalescence of oppositely charged drops." *Nature* 461.7262 (2009): 377-380.

Seemann, R., Brinkmann, M., Pfohl, T., & Herminghaus, S. (2012). Droplet based microfluidics. *Reports on Progress in Physics*, *75*(1), 016601.

Stachewicz, Urszula, et al. "Volume of liquid deposited per single event electrospraying controlled by nozzle front surface modification." *Microfluidics and nanofluidics* 9.4-5 (2010): 635-644.

Stokes, George Gabriel. 1845. Transactions, Cambridge Philosophical Society 8, no. 287.

Taylor, G. I.(1934). "The Formation of Emulsions in Definable Fields of Flow." Proceedings of the Royal Society of London. Series A 146(858): 501---523.

Tseng, F.-G., Linder, C., Kim, C.-J., and Ho, C.-M (1996) "Control of Mixing with Micro Injectors for Combustion Application," *Micro-Electro-Mechanical Systems (MEMS) DSC-ASME IMECE*, pp. 183–87, November 17–22, Atlanta.

Tseng, Fan-Gang. "Micro-droplet generators." *The MEMS Handbook* (2001): 30-1.

Verplanck, Nicolas, et al. "Wettability switching techniques on superhydrophobic surfaces." *Nanoscale Research Letters* 2.12 (2007): 577-596.

Wenzel, Robert N. "Resistance of solid surfaces to wetting by water." *Industrial & Engineering Chemistry* 28.8 (1936): 988-994.

Wright, G. S., P. T. Krein, and J. C. Chato. "Factors affecting dynamic electrical manipulation of menisci." *Industry Applications, IEEE Transactions on* 29.1 (1993): 103-112.

Zhu, X., Tran, E., Wang, W., Kim, E.S., and Lee, S.Y. (1996) "Micromachined Acoustic-Wave Liquid Ejector," *Solid-State Sensor and Actuator Workshop*, pp. 280–82, June 2–6, Hilton Head, South Carolina.

Appendix 1.

Part 1. Relation between needle shape and drop size. No EHD application

Case A. No voltage. Diamenter needle = 400 µm

- ***Volume: 7,5 µl/min***

Measurement	Time (mm:ss,00)	Time between drops
1	**01:14,43**	01:14,43
2	**02:21,91**	01:07,48
3	**03:42,43**	01:20,52
4	**05:00,64**	01:18,21
5	**06:16,06**	01:15,42
6	**07:32,65**	01:16,59
7	**08:49,92**	01:17,27
8	**10:08,40**	01:18,48
9	**11:27,01**	01:18,61
10	**12:46,62**	01:19,61

Average time: 76,66 s

Droplet Volume: 9,58 µl

Droplet Diameter: 2,635 mm

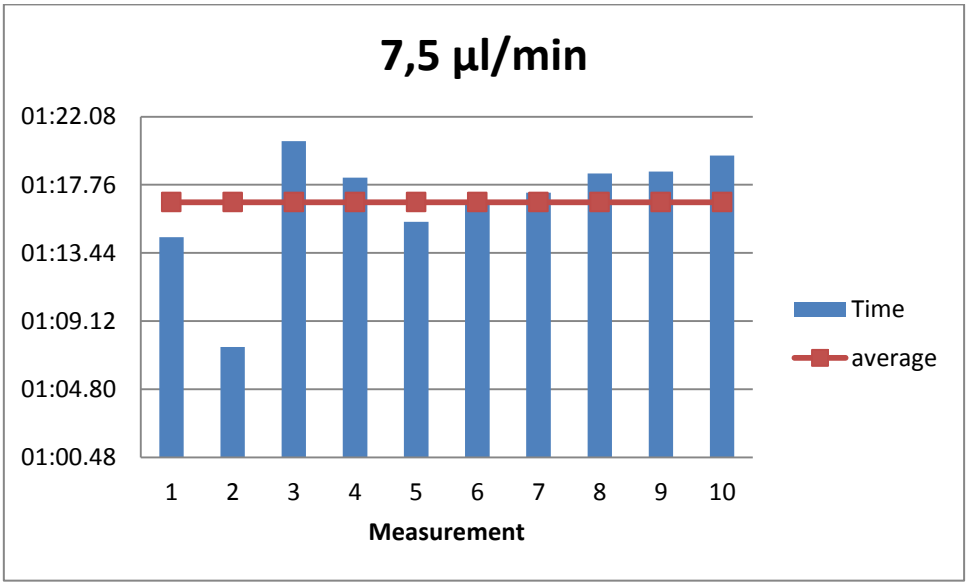

- ***Volume: 15 µl/min***

Measurement	Time (mm:ss,00)	Time between drops
1	**00:39,60**	00:39,60
2	**01:19,96**	00:40,36
3	**02:00,06**	00:40,10
4	**02:39,66**	00:39,60
5	**03:19,48**	00:39,82
6	**03:59,40**	00:39,92
7	**04:38,82**	00:39,42
8	**05:18,46**	00:39,64
9	**05:57,39**	00:38,93
10	**06:37,03**	00:39,64

Average time: 39,70 s

Droplet Volume: 9,93 µl

Droplet Diameter: 2,666 mm

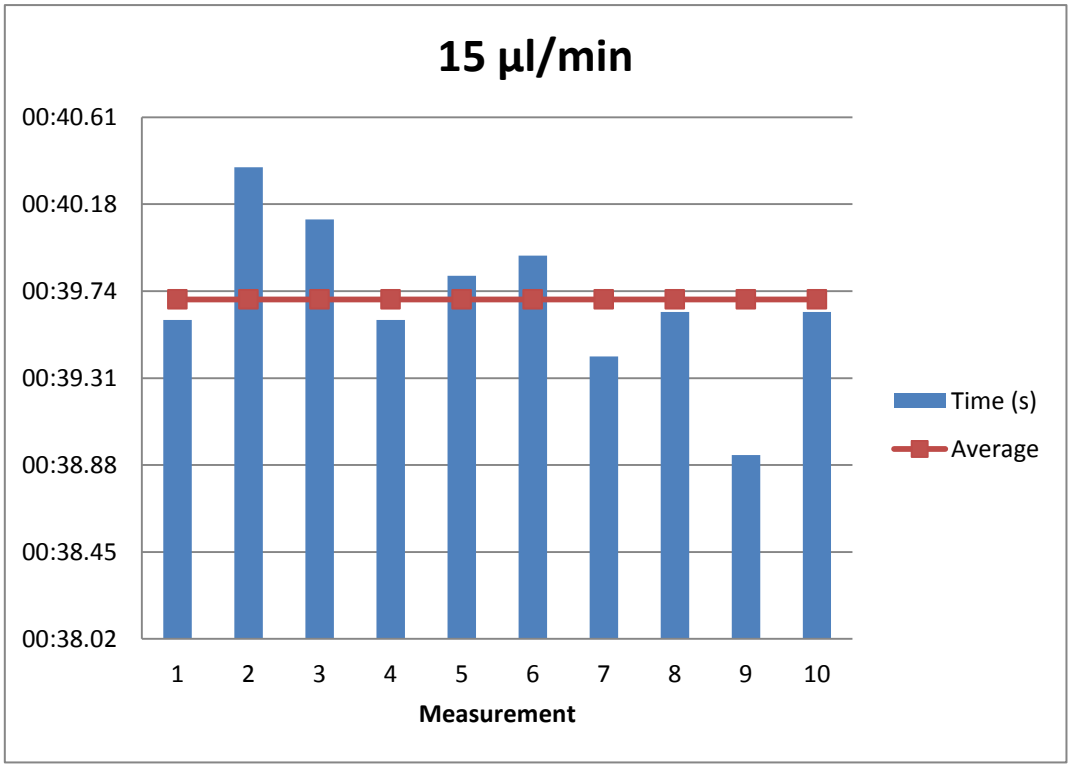

- ***Volume: 30 µl/min***

Measurement	Time (mm:ss,00)	Time between drops
1	**00:21,01**	00:21,01
2	**00:42,34**	00:21,33
3	**01:03,22**	00:20,88
4	**01:24,69**	00:21,47
5	**01:46,92**	00:22,23
6	**02:07,93**	00:21,01
7	**02:29,71**	00:21,78
8	**02:51,67**	00:21,96
9	**03:13,50**	00:21,83
10	**03:35,14**	00:21,64

Average time: 21,51 s

Droplet Volume: 10,76 µl

Droplet Diameter: 2,739 mm

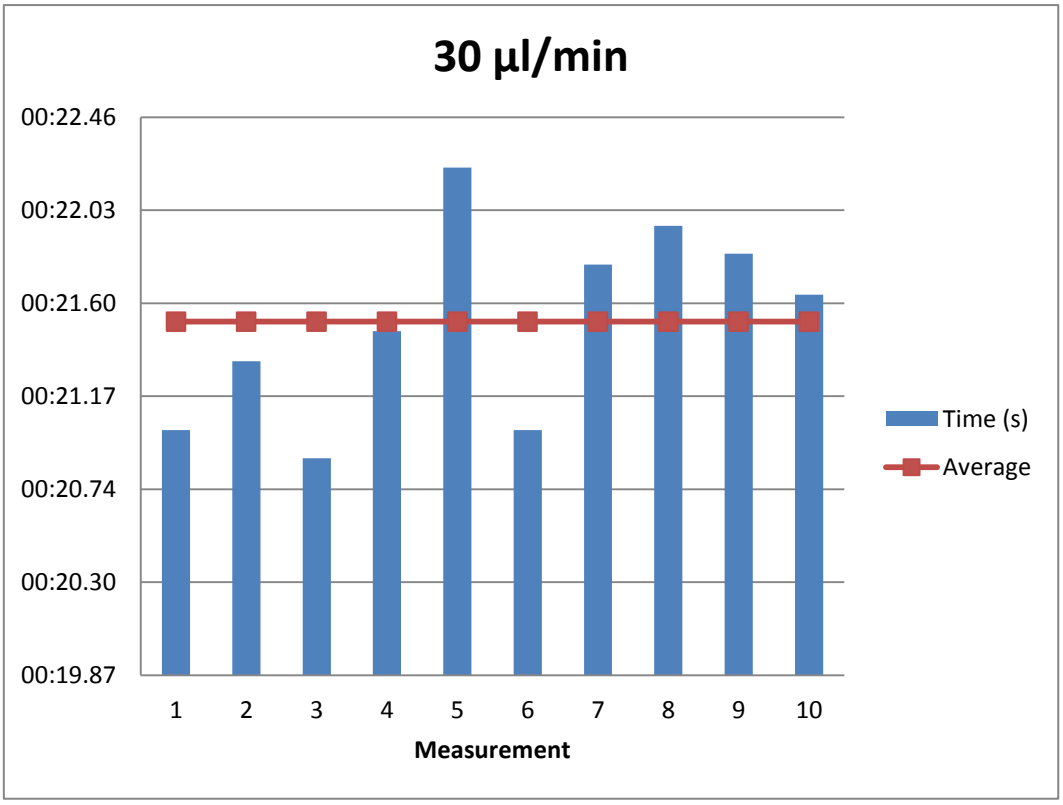

- ***Volume: 60 µl/min***

Measurement	Time (mm:ss,00)	Time between drops
1	**00:10,66**	00:10,66
2	**00:21,60**	00:10,94
3	**00:33,12**	00:11,52
4	**00:42,61**	00:09,49
5	**00:53,77**	00:11,16
6	**01:04,17**	00:10,40
7	**01:14,61**	00:10,44
8	**01:25,41**	00:10,80
9	**01:36,25**	00:10,84
10	**01:47,32**	00:11,07

Average time: 10,73 s

Droplet Volume: 10,73 µl

Droplet Diameter: 2,737 mm

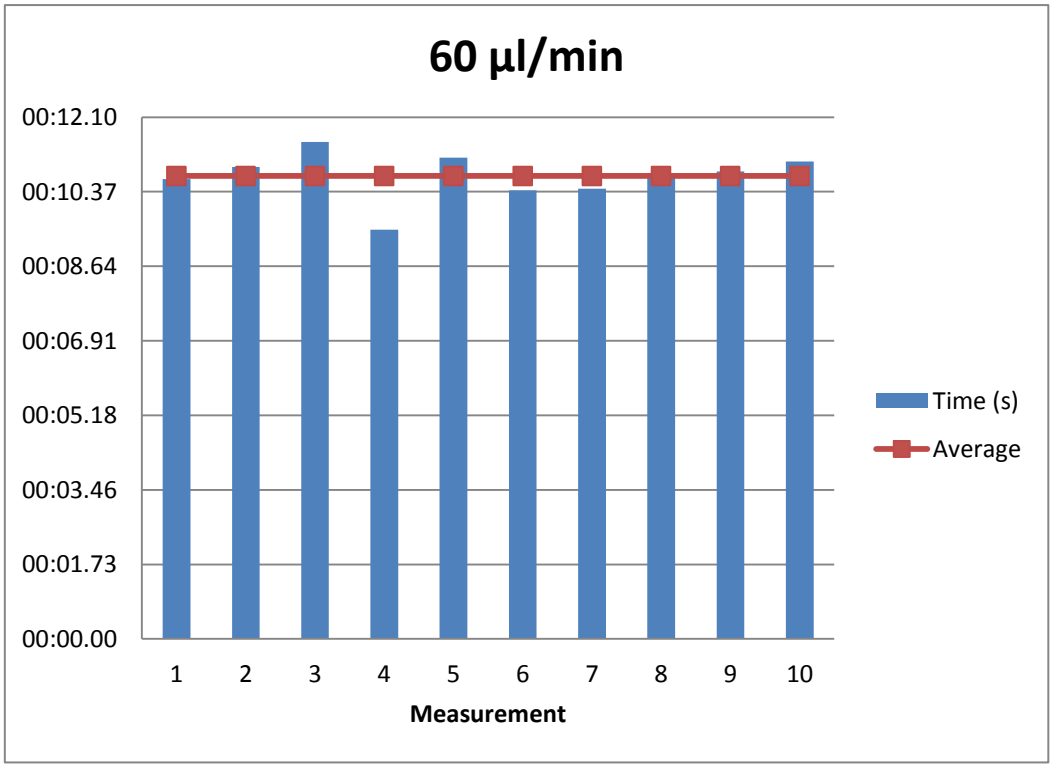

- ***Volume: 90 µl/min***

Measurement	Time (mm:ss,00)	Time between drops
1	**00:07,74**	00:07,74
2	**00:15,66**	00:07,92
3	**00:23,13**	00:07,47
4	**00:30,91**	00:07,78
5	**00:38,52**	00:07,61
6	**00:46,03**	00:07,51
7	**00:53,08**	00:07,05
8	**01:00,88**	00:07,80
9	**01:08,31**	00:07,43
10	**01:15,46**	00:07,15

Average time: 7,55 s

Droplet Volume: 11,33 µl

Droplet Diameter: 2,786 mm

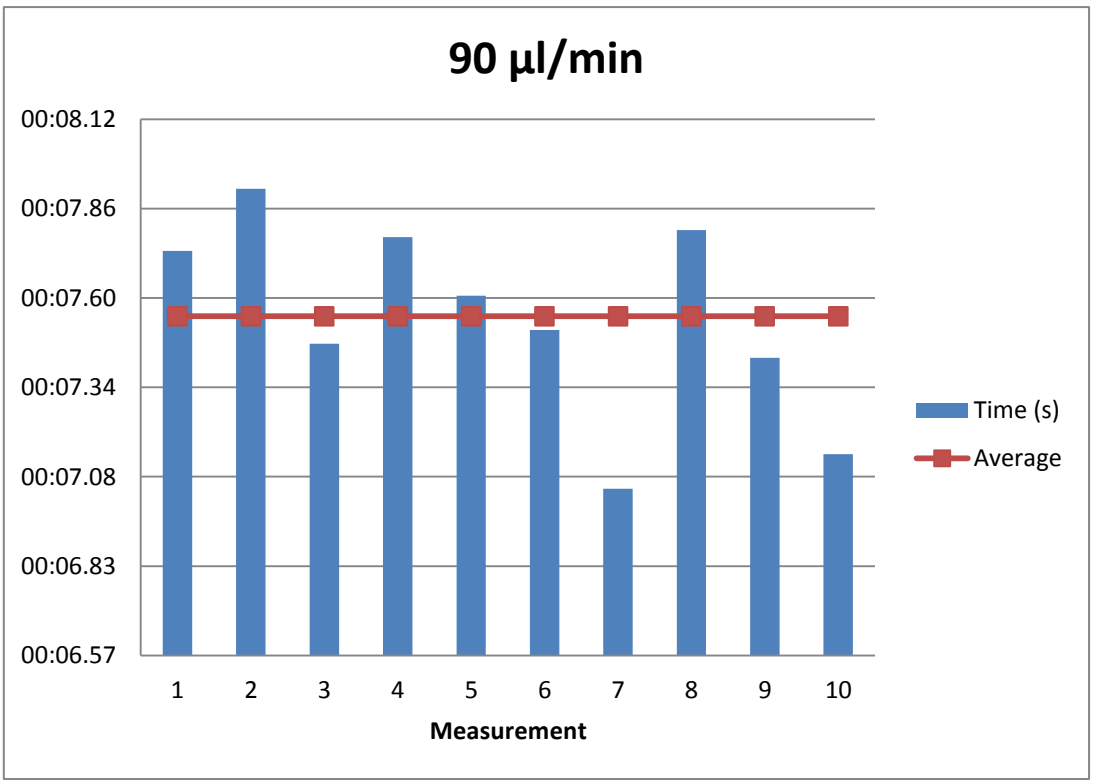

- ***Volume: 120 µl/min***

Measurement	Time (mm:ss,00)	Time between drops
1	**00:05,62**	00:05,62
2	**00:11,25**	00:05,63
3	**00:16,92**	00:05,67
4	**00:22,59**	00:05,67
5	**00:28,30**	00:05,71
6	**00:33,93**	00:05,63
7	**00:39,64**	00:05,71
8	**00:45,36**	00:05,72
9	**00:51,25**	00:05,89
10	**00:57,06**	00:05,81

Average time: 5,71 s

Droplet Volume: 11,42 µl

Droplet Diameter: 2,794 mm

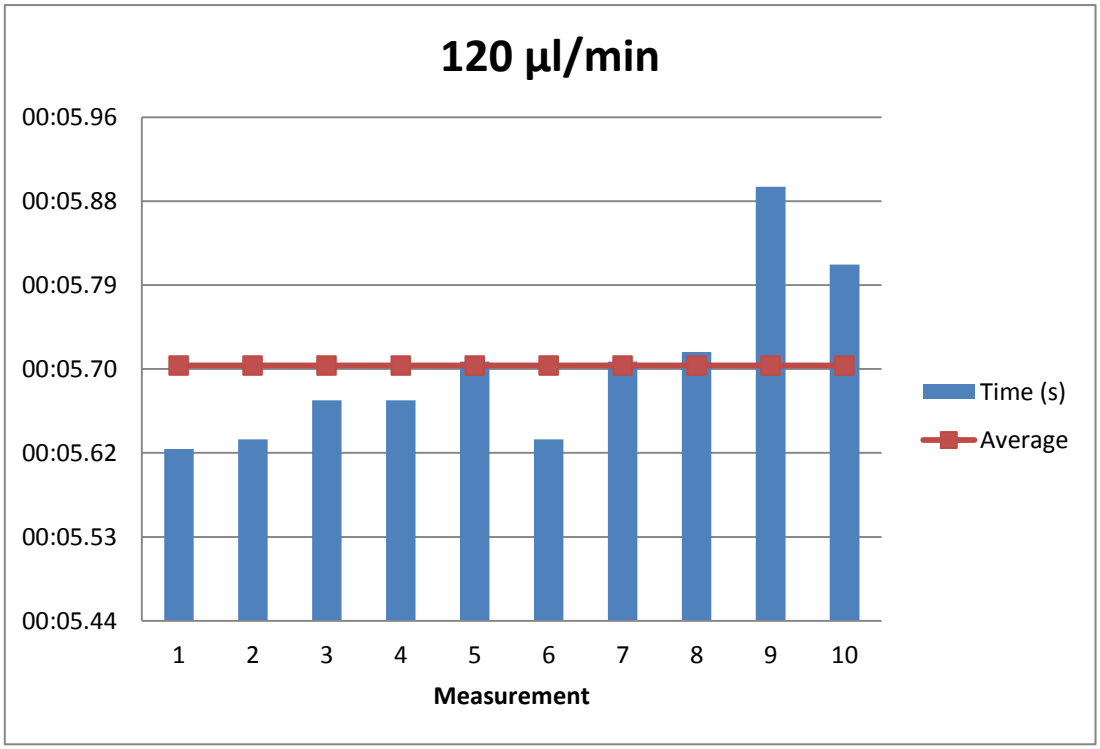

- ***Relationship between water flow and droplet size***

Volume (µl/min)	Average time (s)	D (mm)
7,5	76,66	2,635
15	39,7	2,666
30	21,51	2,739
60	10,73	2,737
90	7,55	2,786
120	5,71	2,794

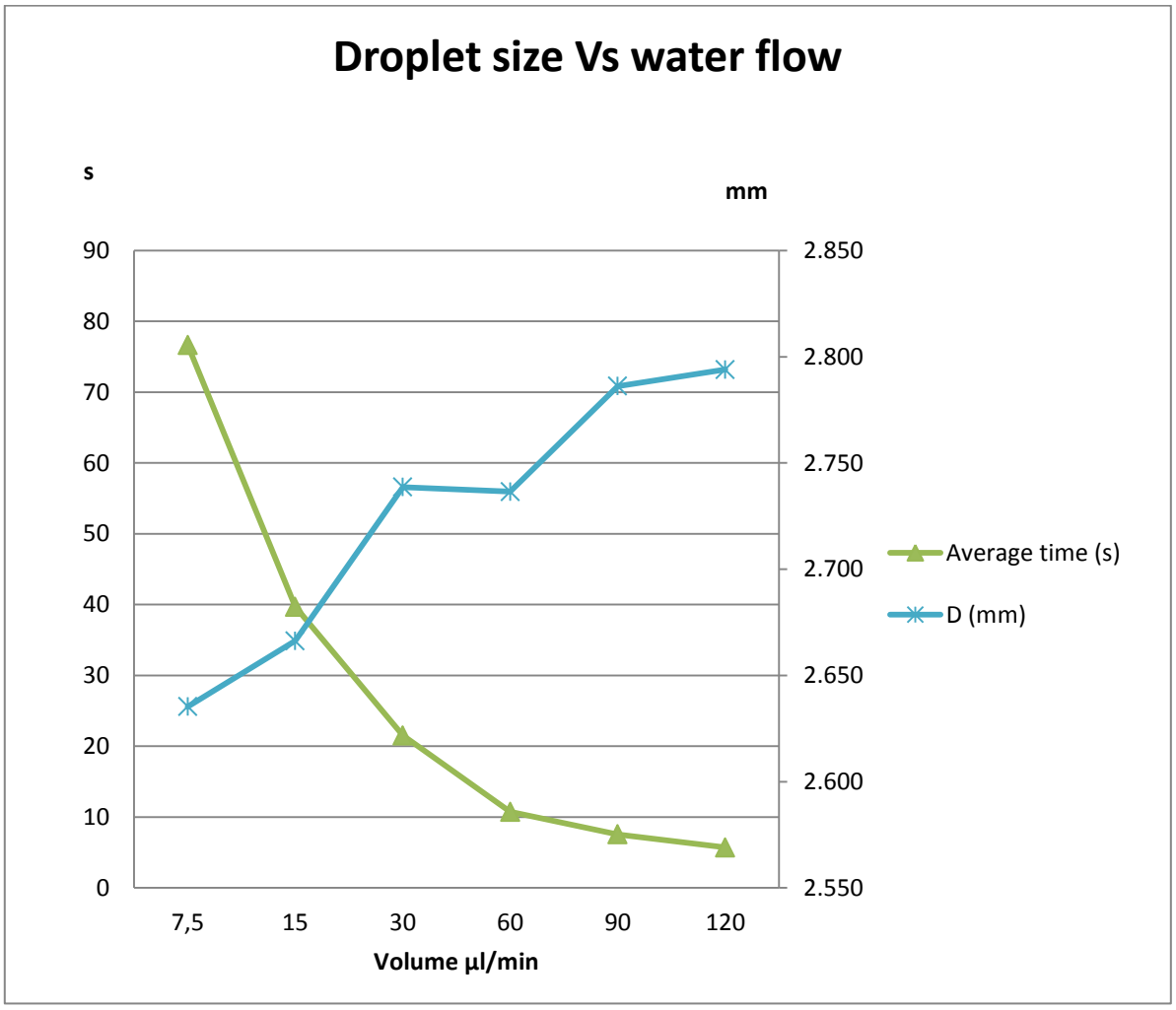

Case B. No voltage. Diameter needle = 400 µm with bevel tip

- ***Volume: 7,5 µl/min***

Measurement	Time (mm:ss,00)	Time between drops
1	**01:14,70**	01:14,70
2	**02:29,44**	01:14,74
3	**03:45,27**	01:15,83
4	**05:00,46**	01:15,19
5	**06:17,32**	01:16,86
6	**07:33,91**	01:16,59
7	**08:52,80**	01:18,89
8	**10:12,99**	01:20,19
9	**11:30,93**	01:17,94
10	**12:50,22**	01:19,29

Average time: 77,02 s

Droplet Volume: 9,63 µl

Droplet Diameter: 2,639 mm

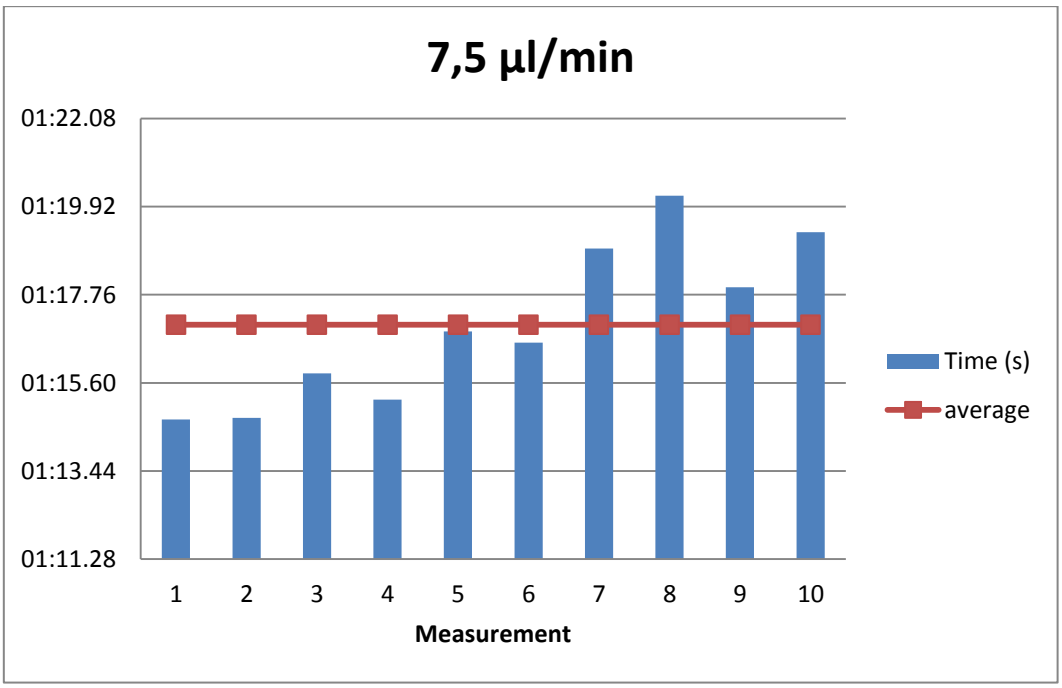

- ***Volume: 15 µl/min***

Measurement	Time (mm:ss,00)	Time between drops
1	**00:41,13**	00:41,13
2	**01:20,82**	00:39,69
3	**02:00,96**	00:40,14
4	**02:41,82**	00:40,86
5	**03:21,96**	00:40,14
6	**04:02,10**	00:40,14
7	**04:42,55**	00:40,45
8	**05:22,65**	00:40,10
9	**06:02,52**	00:39,87
10	**06:42,97**	00:40,45

Average time: 40,30 s

Droplet Volume: 10,08 µl

Droplet Diameter: 2,680 mm

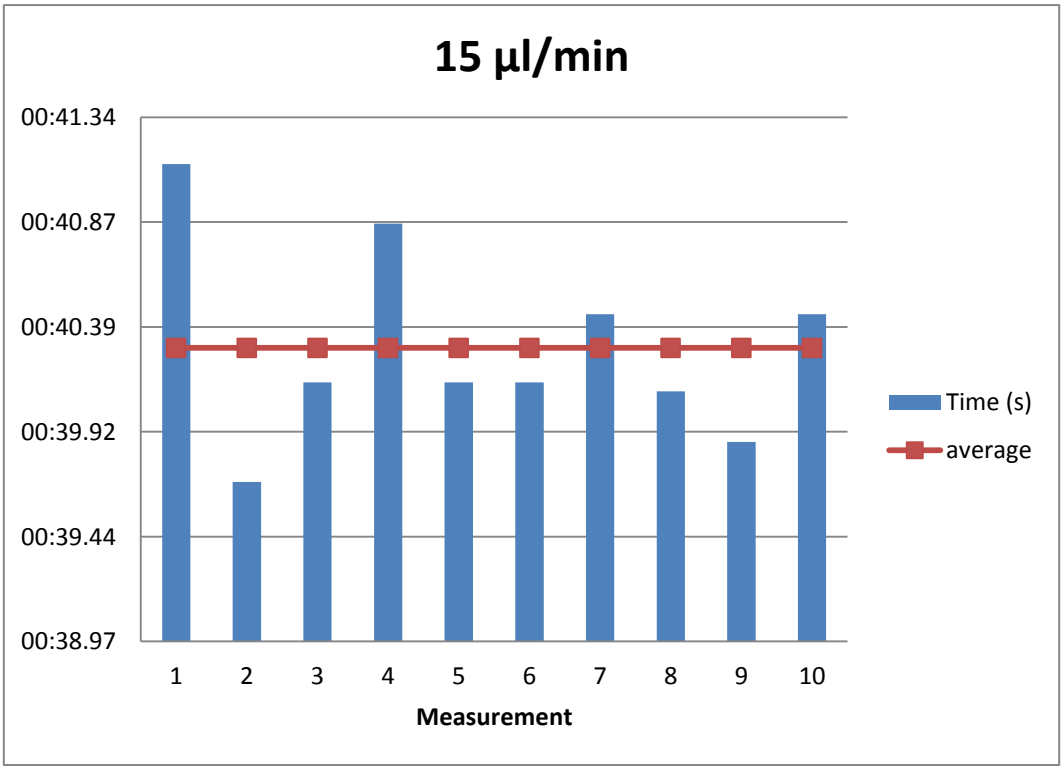

- ***Volume: 30 µl/min***

Measurement	Time (mm:ss,00)	Time between drops
1	**00:21,06**	00:21,06
2	**00:42,34**	00:21,28
3	**01:03,40**	00:21,06
4	**01:25,00**	00:21,60
5	**01:46,38**	00:21,38
6	**02:08,25**	00:21,87
7	**02:30,30**	00:22,05
8	**02:52,62**	00:22,32
9	**03:15,34**	00:22,72
10	**03:37,26**	00:21,92

Average time: 21,73 s

Droplet Volume: 10,87 µl

Droplet Diameter: 2,750 mm

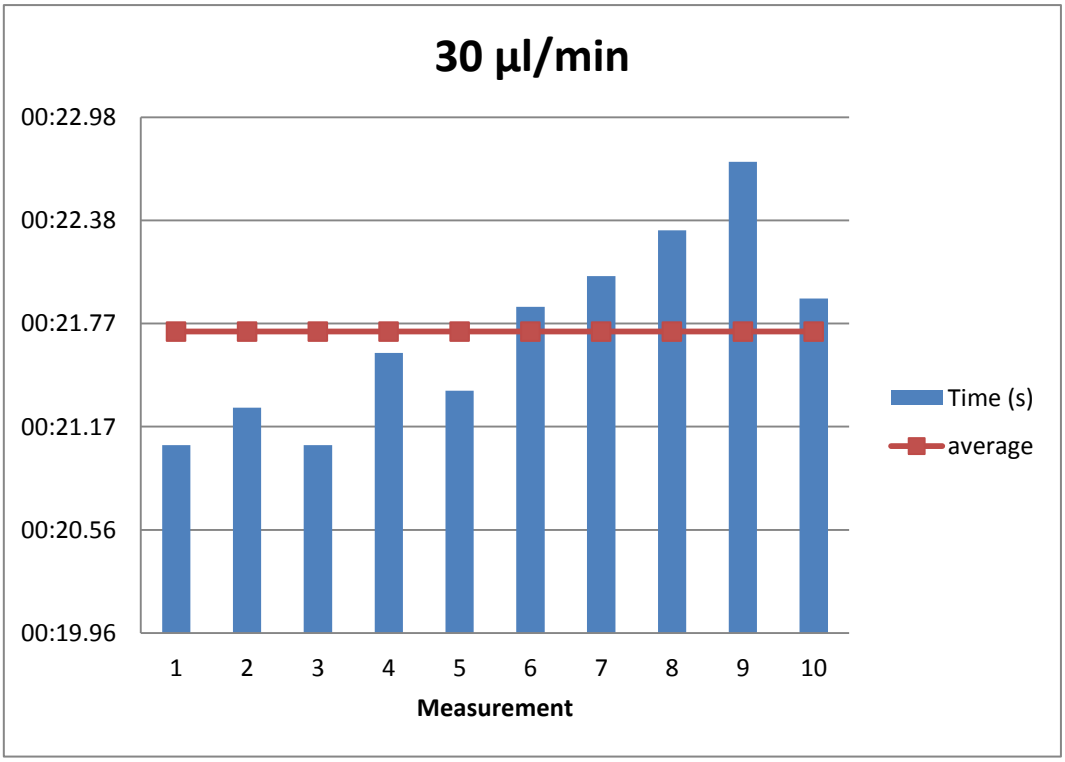

- ***Volume: 60 µl/min***

Measurement	Time (mm:ss,00)	Time between drops
1	**00:11,65**	00:11,65
2	**00:22,63**	00:10,98
3	**00:33,52**	00:10,89
4	**00:44,32**	00:10,80
5	**00:55,30**	00:10,98
6	**01:05,65**	00:10,35
7	**01:16,72**	00:11,07
8	**01:27,52**	00:10,80
9	**01:38,05**	00:10,53
10	**01:48,72**	00:10,67

Average time: 10,87 s

Droplet Volume: 10,87 µl

Droplet Diameter: 2,748 mm

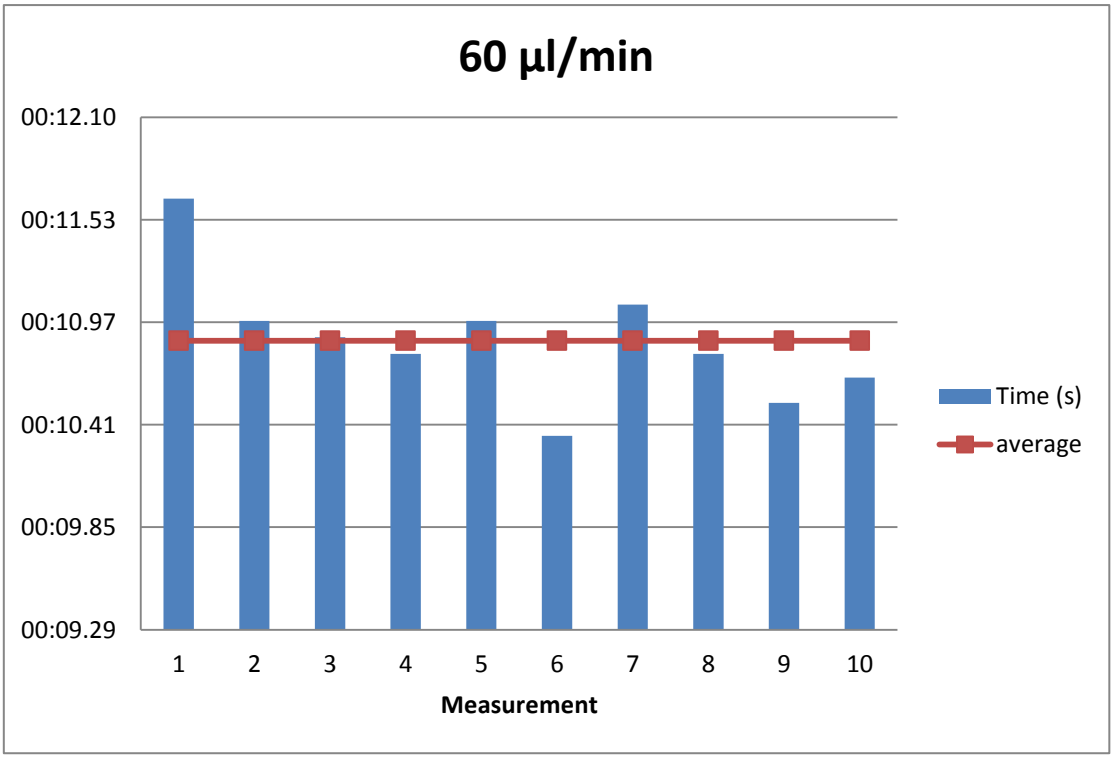

- ***Volume: 90 µl/min***

Measurement	Time (mm:ss,00)	Time between drops
1	**00:07,42**	00:07,42
2	**00:14,62**	00:07,20
3	**00:22,09**	00:07,47
4	**00:29,25**	00:07,16
5	**00:36,67**	00:07,42
6	**00:43,92**	00:07,25
7	**00:51,12**	00:07,20
8	**00:58,36**	00:07,24
9	**01:05,61**	00:07,25
10	**01:12,85**	00:07,24

Average time: 7,29 s

Droplet Volume: 10,94 µl

Droplet Diameter: 2,754 mm

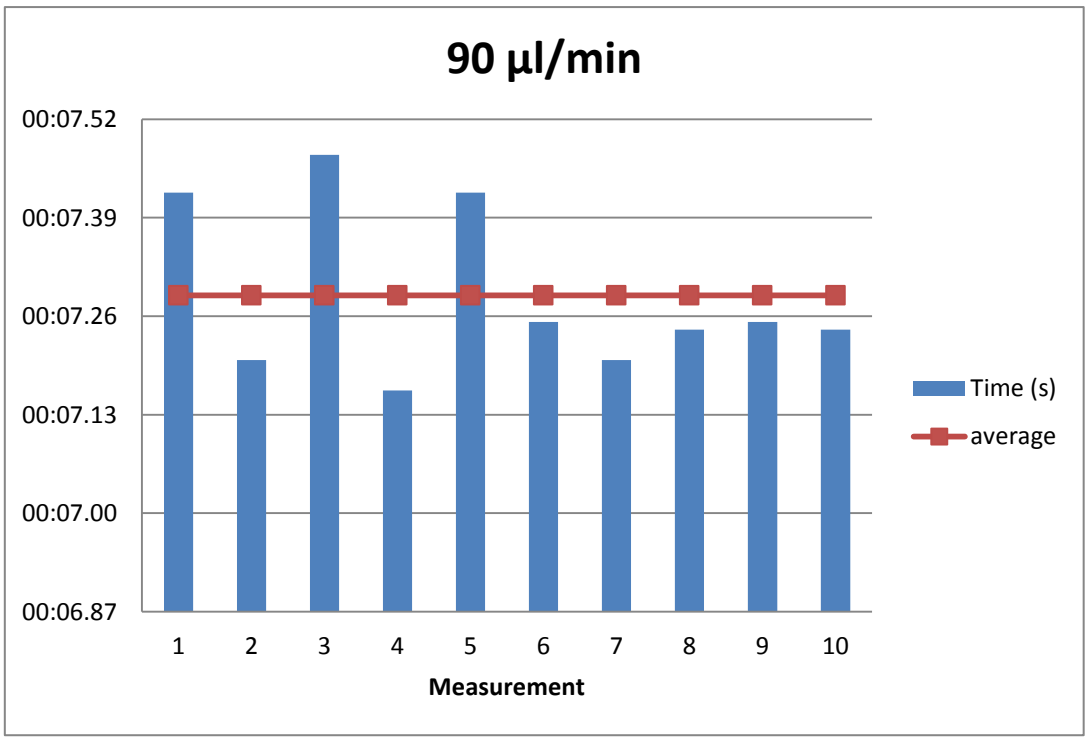

- ***Volume: 120 µl/min***

Measurement	Time (mm:ss,00)	Time between drops
1	**00:05,71**	00:05,71
2	**00:11,38**	00:05,67
3	**00:17,23**	00:05,85
4	**00:23,04**	00:05,81
5	**00:28,80**	00:05,76
6	**00:34,69**	00:05,89
7	**00:40,23**	00:05,54
8	**00:45,90**	00:05,67
9	**00:51,48**	00:05,58
10	**00:57,24**	00:05,76

Average time: 5,72 s

Droplet Volume: 11,44 µl

Droplet Diameter: 2,796 mm

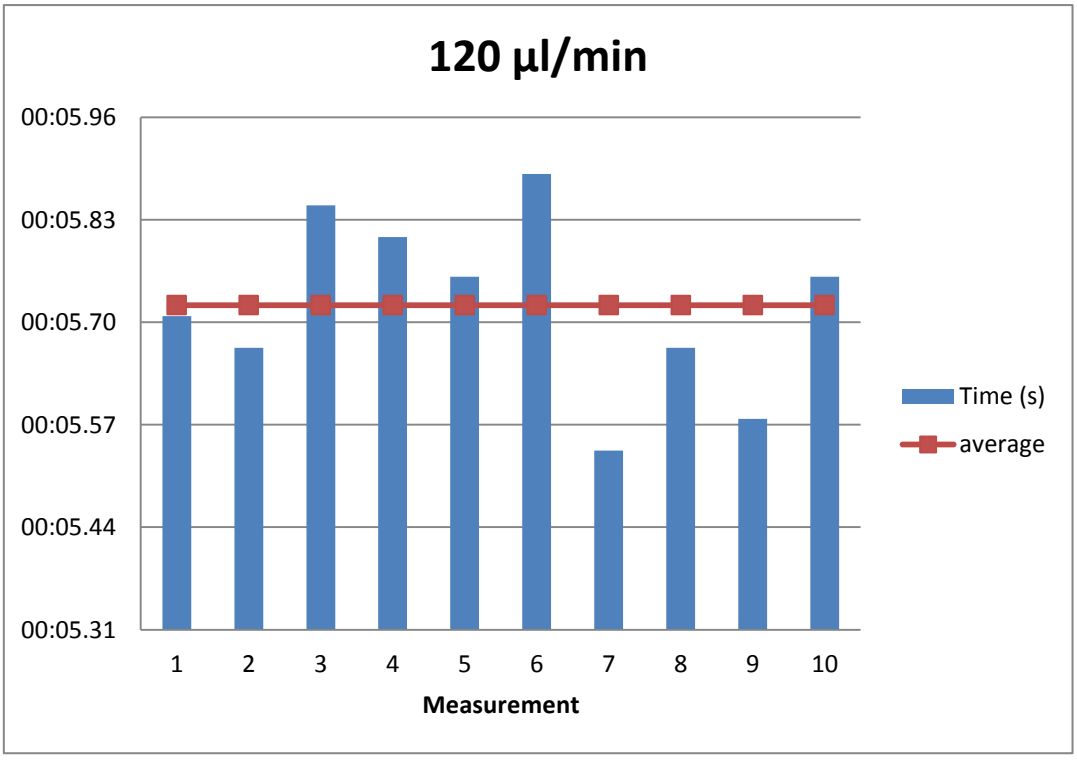

- ***Relation between water flow and droplet size***

Volume (µl/min)	Average time (s)	D (mm)
7,5	77,02	2,639
15	40,30	2,680
30	21,73	2,748
60	10,87	2,748
90	7,29	2,754
120	5,72	2,796

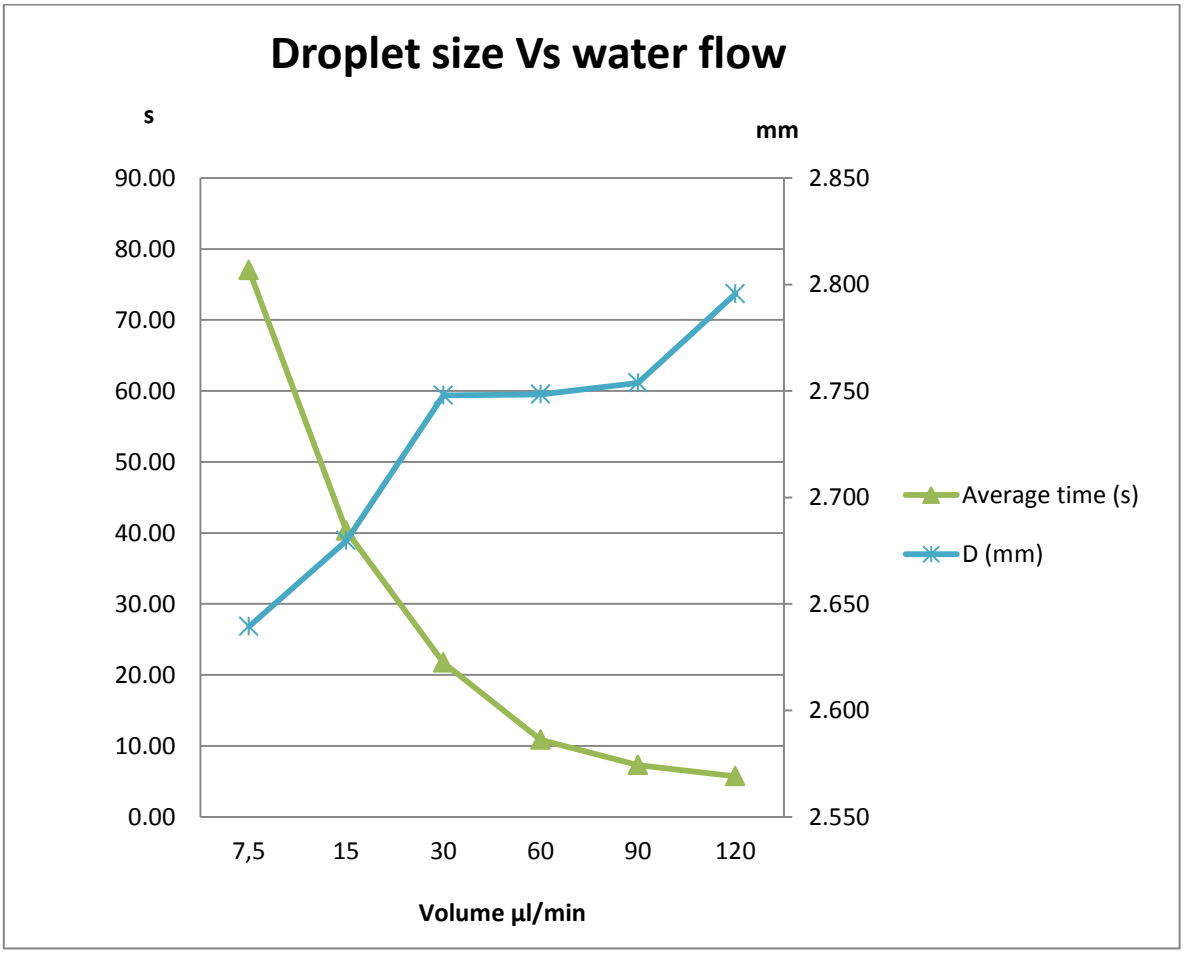

Case C. No voltage. Diameter needle = 800 µm

- ***Volume: 7,5 µl/min***

Measurement	Time (mm:ss,00)	Time between drops
1	**02:50,82**	02:50,82
2	**05:43,44**	02:52,62
3	**08:39,30**	02:55,86
4	**11:31,92**	02:52,62
5	**14:25,98**	02:54,06
6	**17:14,73**	02:48,75
7	**20:03,70**	02:48,97
8	**22:48,94**	02:45,24
9	**25:34,95**	02:46,01
10	**28:25,54**	02:50,59

Average time: 170,55 s

Droplet Volume: 21,32 µl

Droplet Diameter: 3,440 mm

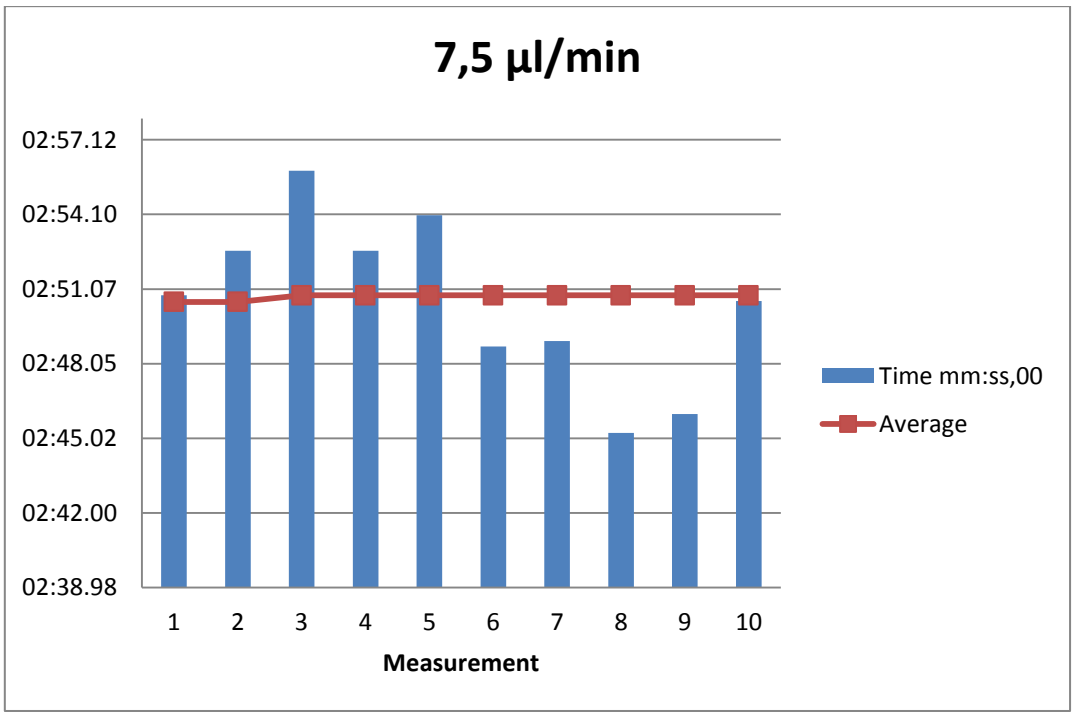

- ***Volume 15 µl/min***

Measurement	Time (mm:ss,00)	Time between drops
1	**01:33,82**	01:33,82
2	**03:09,45**	01:35,63
3	**04:46,06**	01:36,61
4	**06:21,73**	01:35,67
5	**07:56,10**	01:34,37
6	**09:28,44**	01:32,34
7	**10:59,65**	01:31,21
8	**12:30,87**	01:31,22
9	**14:01,90**	01:31,03
10	**15:33,84**	01:31,94

Average time: 93,38 s

Droplet Volume: 23,35 µl

Droplet Diameter: 3,546 mm

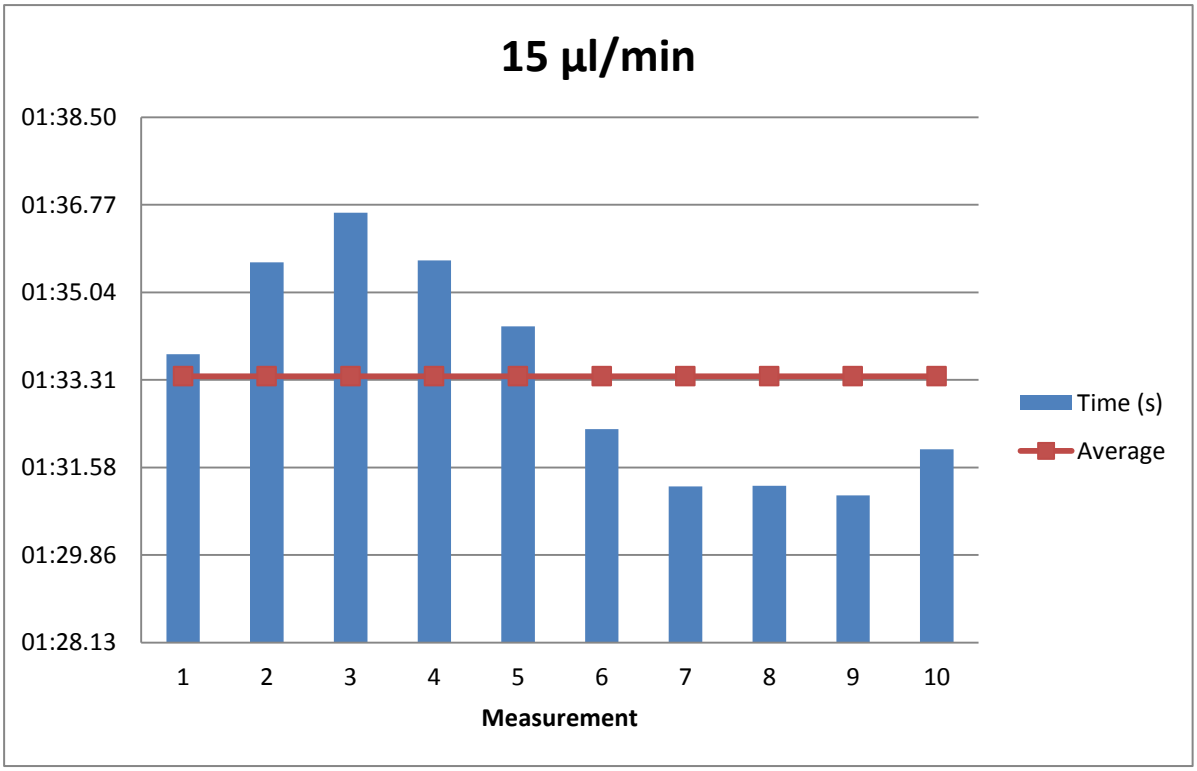

- ***Volume 30 µl/min***

Measurement	Time (mm:ss,00)	Time between drops
1	**00:48,96**	00:48,96
2	**01:37,69**	00:48,73
3	**02:27,06**	00:49,37
4	**03:16,69**	00:49,63
5	**04:07,41**	00:50,72
6	**04:58,80**	00:51,39
7	**05:50,46**	00:51,66
8	**06:42,16**	00:51,70
9	**07:32,97**	00:50,81
10	**08:23,14**	00:50,17

Average time: 50,31 s

Droplet Volume: 25,16 µl

Droplet Diameter: 2,635 mm

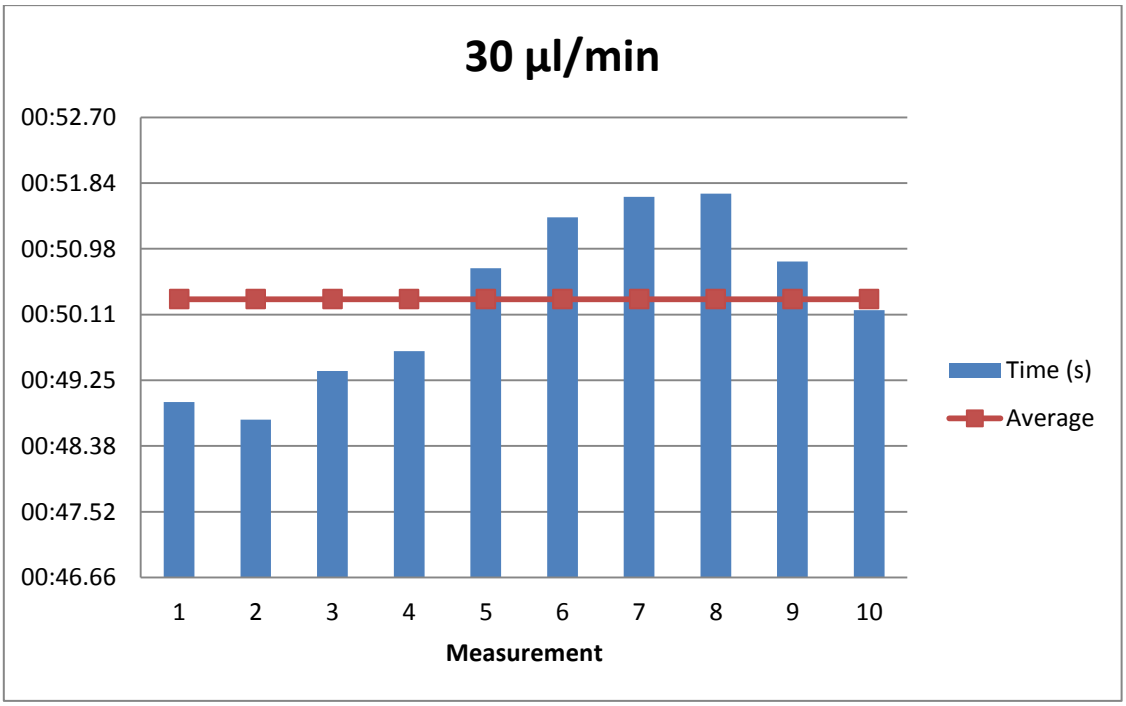

- ***Volume 60 µl/min***

Measurement	Time (mm:ss,00)	Time between drops
1	**00:25,38**	00:25,38
2	**00:51,43**	00:26,05
3	**01:17,17**	00:25,74
4	**01:43,27**	00:26,10
5	**02:09,96**	00:26,69
6	**02:36,91**	00:26,95
7	**03:04,27**	00:27,36
8	**03:30,64**	00:26,37
9	**03:57,15**	00:26,51
10	**04:23,52**	00:26,37

Average time: 26,35 s

Droplet Volume: 26,35 µl

Droplet Diameter: 3,692 mm

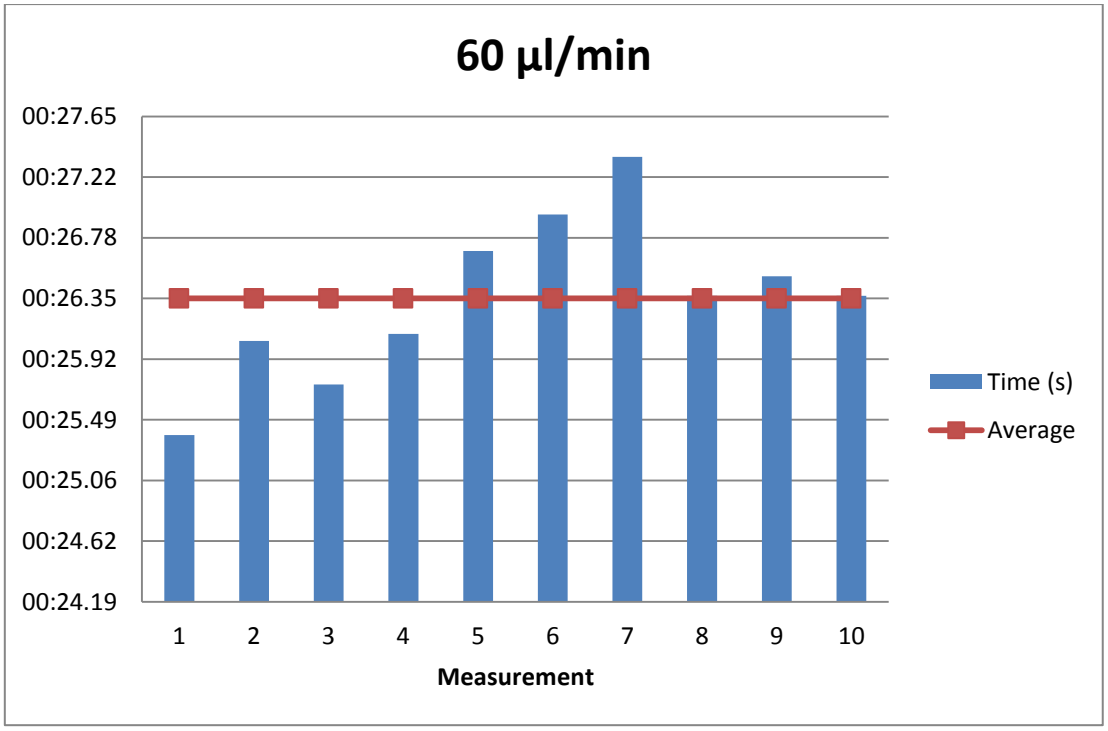

- ***Volume 90 µl/min***

Measurement	Time (mm:ss,00)	Time between drops
1	**00:18,00**	00:18,00
2	**00:36,27**	00:18,27
3	**00:54,81**	00:18,54
4	**01:13,57**	00:18,76
5	**01:31,80**	00:18,23
6	**01:49,93**	00:18,13
7	**02:08,02**	00:18,09
8	**02:25,75**	00:17,73
9	**02:43,48**	00:17,73
10	**03:01,03**	00:17,55

Average time: 18,10 s

Droplet Volume: 27,15 µl

Droplet Diameter: 3,729 mm

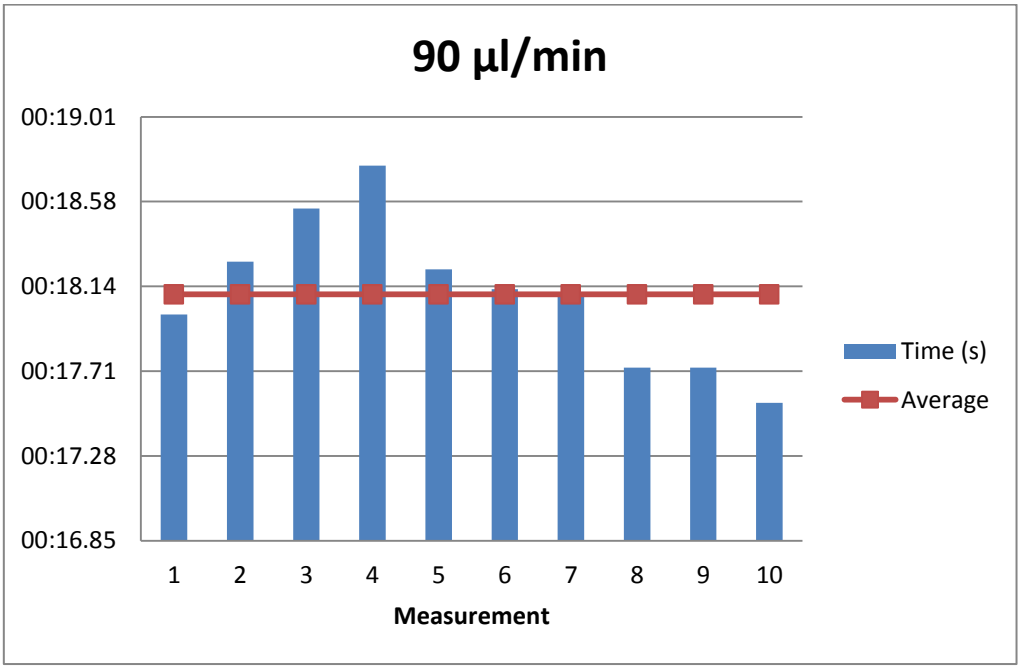

- ***Volume 120 µl/min***

Measurement	Time (mm:ss,00)	Time between drops
1	**00:13,05**	00:13,05
2	**00:26,37**	00:13,32
3	**00:39,82**	00:13,45
4	**00:53,05**	00:13,23
5	**01:06,69**	00:13,64
6	**01:20,37**	00:13,68
7	**01:34,77**	00:14,40
8	**01:48,72**	00:13,95
9	**02:02,31**	00:13,59
10	**02:15,76**	00:13,45

Average time: 13,58 s

Droplet Volume: 27,16µl

Droplet Diameter: 3,729 mm

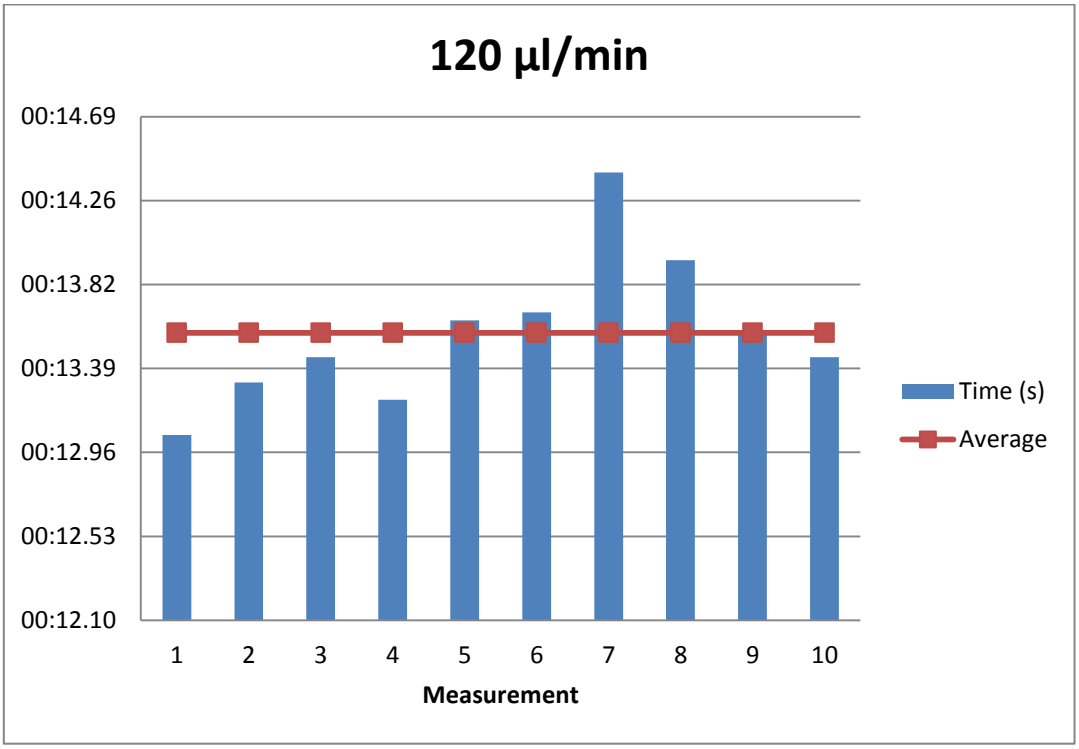

- ***Relation between water flow and droplet size***

Volume (µl/min)	Average time (s)	D (mm)
7,5	170,55	3,440
15	93,38	3,546
30	50,31	3,635
60	26,35	3,692
90	18,10	3,729
120	13,58	3,729

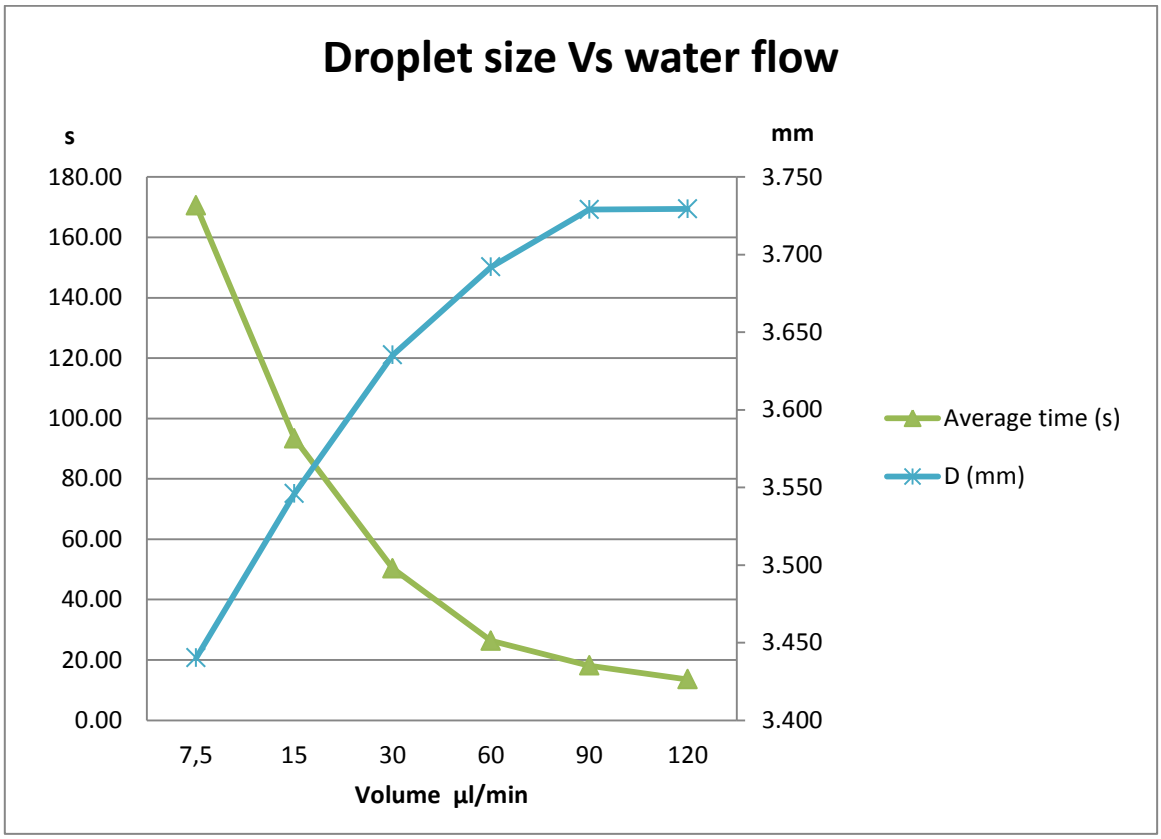

Case D. No voltage. Diameter needle = 800 µm with <u>chamfer</u>

- ***Volume: 7,5 µl/min***

Measurement	Time (mm:ss,00)	Time between drops
1	**02:49,69**	02:49,69
2	**05:22,82**	02:33,13
3	**07:55,47**	02:32,65
4	**10:28,96**	02:33,49
5	**12:59,22**	02:30,26
6	**15:33,70**	02:34,48
7	**18:07,38**	02:33,68
8	**20:40,87**	02:33,49
9	**23:14,77**	02:33,90
10	**25:48,58**	02:33,81

Average time: 154,86 s

Droplet Volume: 19,36 µl

Droplet Diameter: 3,331 mm

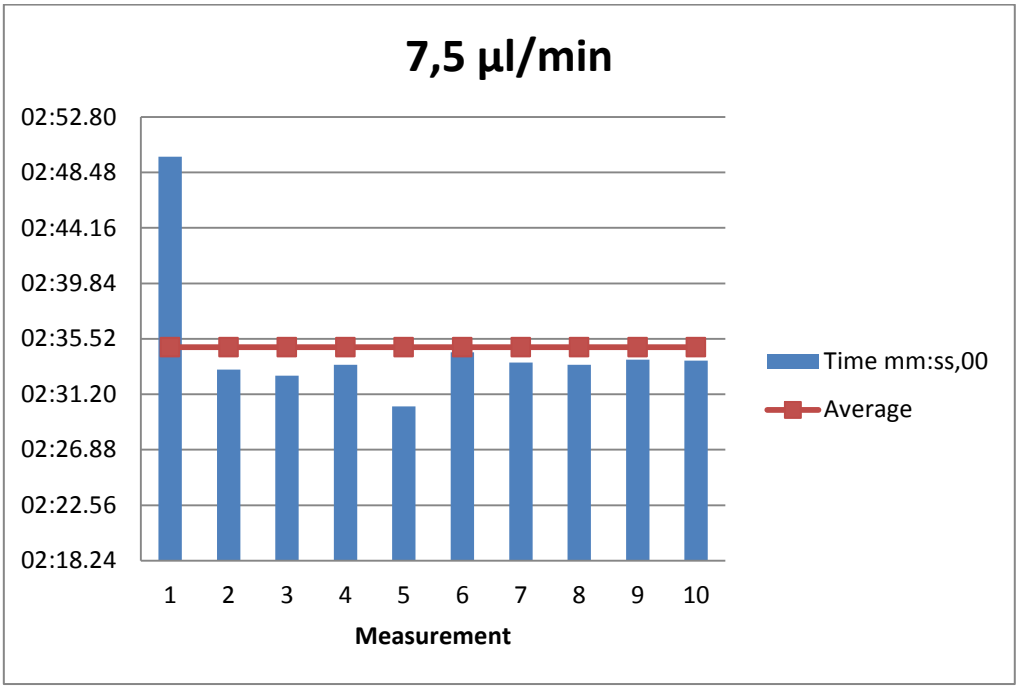

- ***Volume 15 µl/min***

Measurement	Time (mm:ss,00)	Time between drops
1	**01:24,78**	01:24,78
2	**02:49,06**	01:24,28
3	**04:13,35**	01:24,29
4	**05:35,07**	01:21,72
5	**06:57,55**	01:22,48
6	**08:19,36**	01:21,81
7	**09:42,12**	01:22,76
8	**11:04,87**	01:22,75
9	**12:27,63**	01:22,76
10	**13:51,55**	01:23,92

Average time: 83,16 s

Droplet Volume: 20,79 µl

Droplet Diameter: 3,412 mm

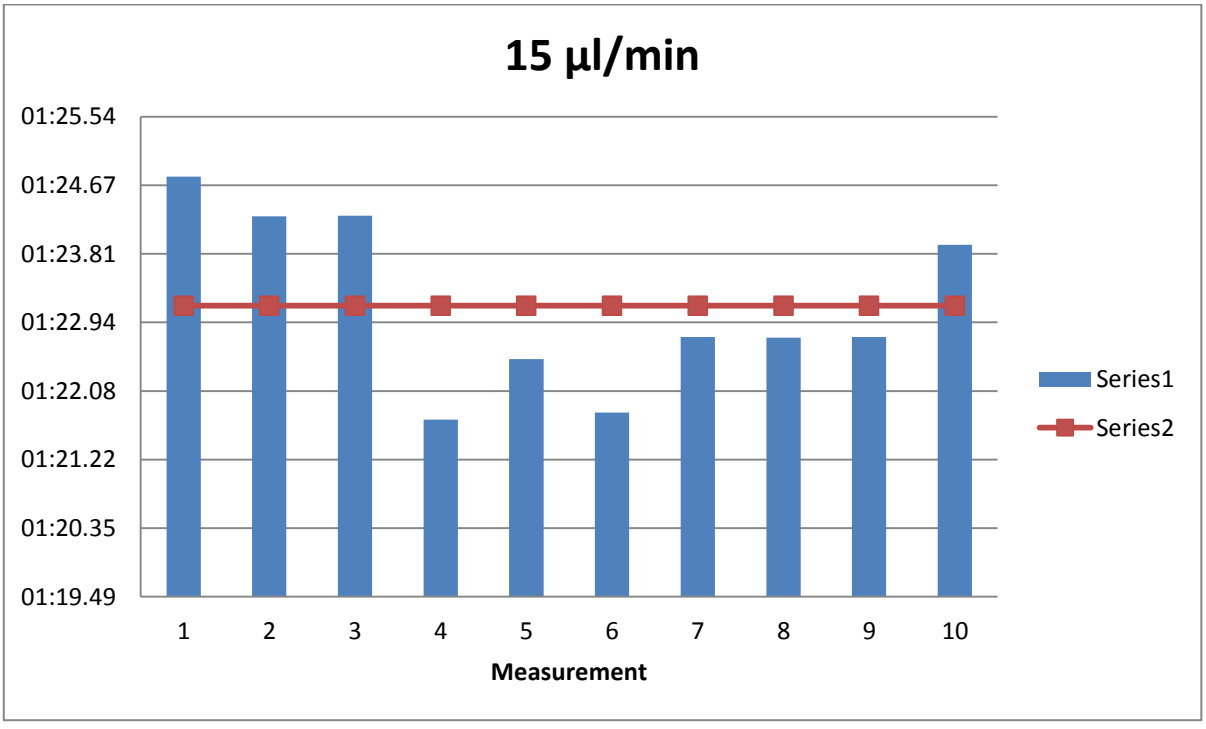

- ***Volume 30 µl/min***

Measurement	Time (mm:ss,00)	Time between drops
1	**00:42,57**	00:42,57
2	**01:25,05**	00:42,48
3	**02:07,98**	00:42,93
4	**02:51,45**	00:43,47
5	**03:33,52**	00:42,07
6	**04:15,15**	00:41,63
7	**04:56,28**	00:41,13
8	**05:37,72**	00:41,44
9	**06:19,48**	00:41,76
10	**07:01,74**	00:42,26

Average time: 42,17 s

Droplet Volume: 21,09 µl

Droplet Diameter: 3,428 mm

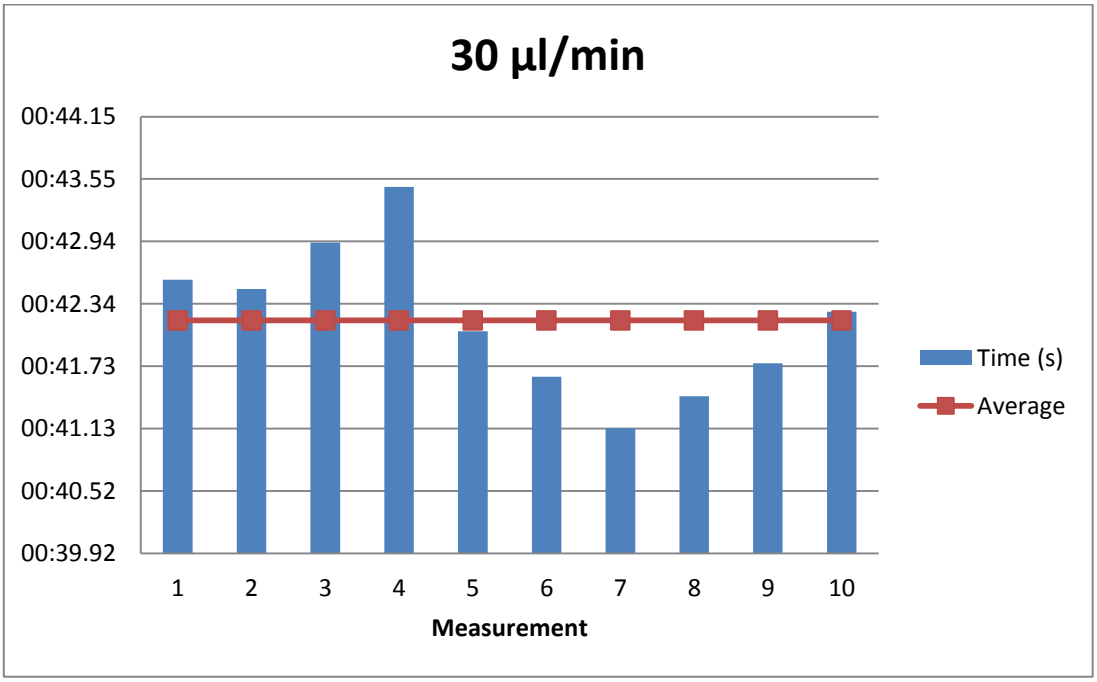

- ***Volume 60 µl/min***

Measurement	Time (mm:ss,00)	Time between drops
1	**00:21,42**	00:21,42
2	**00:42,88**	00:21,46
3	**01:03,94**	00:21,06
4	**01:25,81**	00:21,87
5	**01:47,00**	00:21,19
6	**02:09,24**	00:22,24
7	**02:31,02**	00:21,78
8	**02:53,02**	00:22,00
9	**03:15,21**	00:22,19
10	**03:37,44**	00:22,23

Average time: 21,74 s

Droplet Volume: 21,74 µl

Droplet Diameter: 3,463 mm

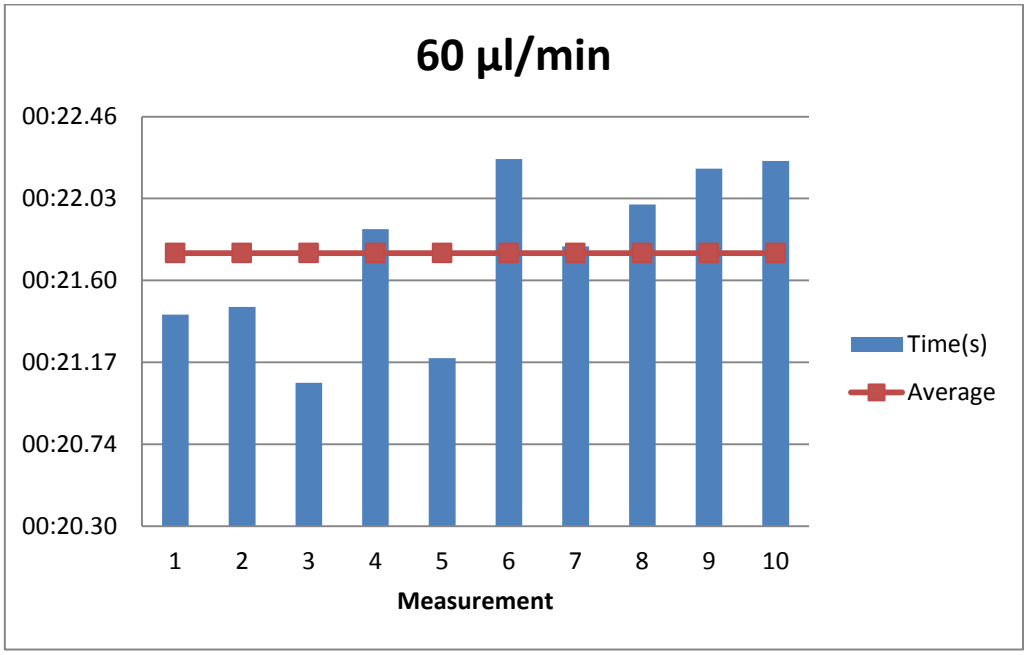

- ***Volume 90 µl/min***

Measurement	Time (mm:ss,00)	Time between drops
1	**00:14,71**	00:14,71
2	**00:29,47**	00:14,76
3	**00:44,10**	00:14,63
4	**00:58,50**	00:14,40
5	**01:13,39**	00:14,89
6	**01:27,97**	00:14,58
7	**01:42,24**	00:14,27
8	**01:57,04**	00:14,80
9	**02:11,49**	00:14,45
10	**02:25,48**	00:13,99

Average time: 14,55 s

Droplet Volume: 21,83 µl

Droplet Diameter: 3,467 mm

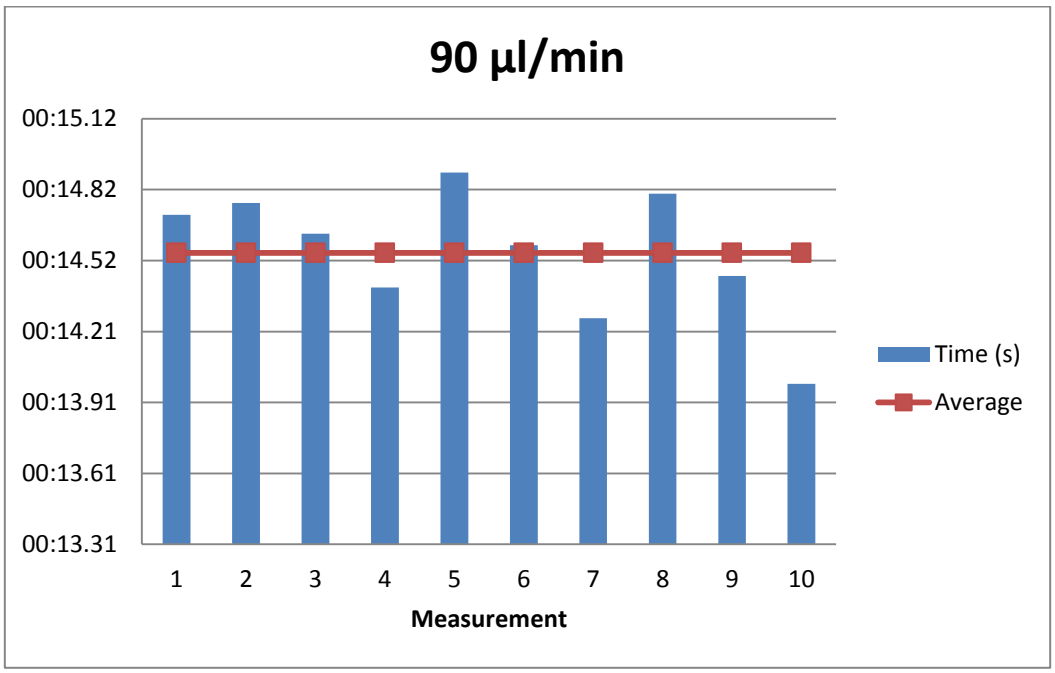

- ***Volume 120 µl/min***

Measurement	Time (mm:ss,00)	Time between drops
1	**00:11,34**	00:11,34
2	**00:22,63**	00:11,29
3	**00:34,15**	00:11,52
4	**00:45,45**	00:11,30
5	**00:57,01**	00:11,56
6	**01:08,26**	00:11,25
7	**01:19,47**	00:11,21
8	**01:30,72**	00:11,25
9	**01:42,60**	00:11,88
10	**01:53,58**	00:10,98

Average time: 11,36 s

Droplet Volume: 22,72 µl

Droplet Diameter: 3,514 mm

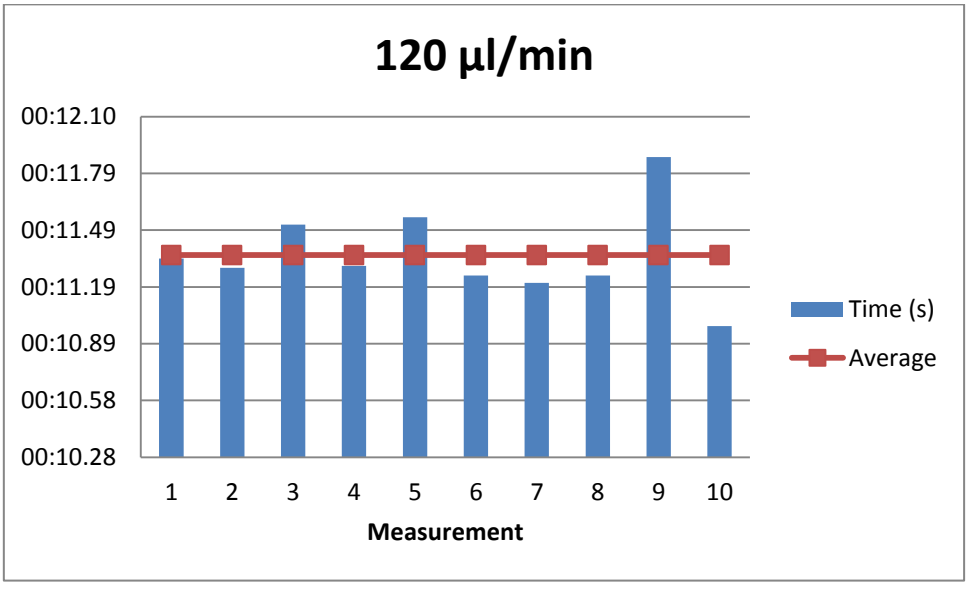

- ***Relation between water flow and droplet size***

Volume (µl/min)	Average time (s)	D (mm)
7,5	170,55	3,440
15	93,38	3,546
30	50,31	3,635
60	26,35	3,692
90	18,10	3,729
120	13,58	3,729

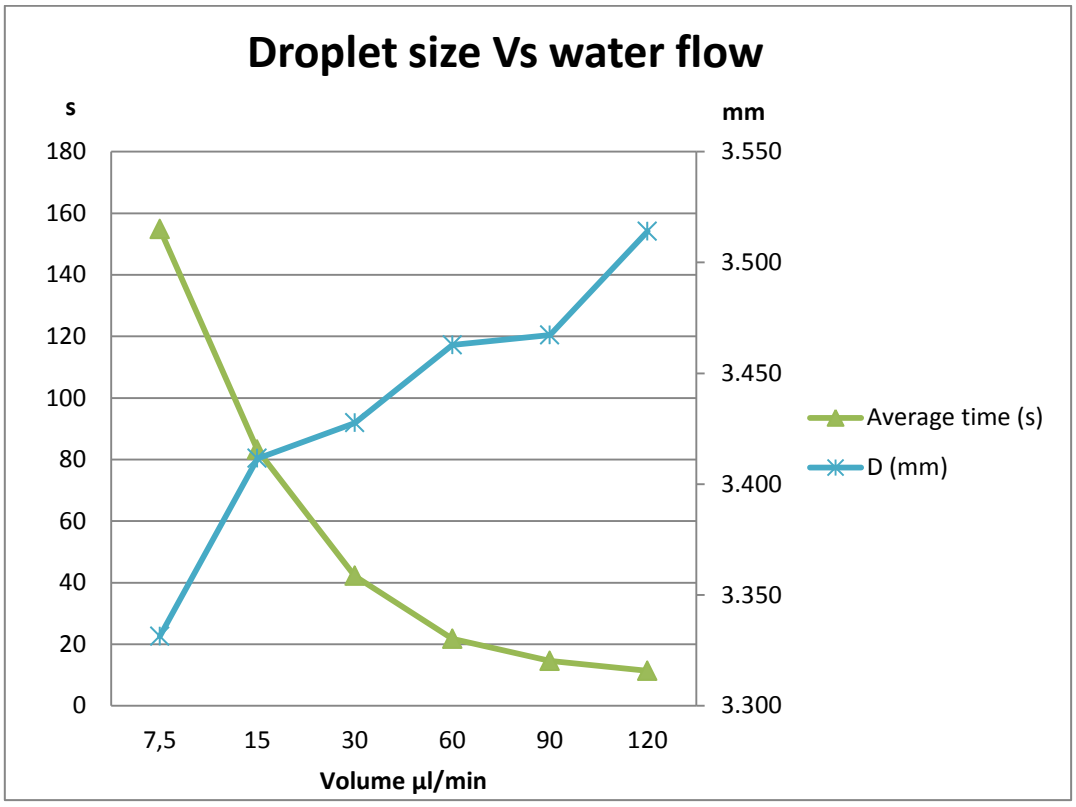

Comparison of average values of different needle sizes

- **Water flow and diameter.**

	Diameter (mm)			
Volume (µl/min)	**0.4**	**0.4 chamfer**	**0.8**	**0.8 chamfer**
7,5	2,635	2,639	3,440	3,331
15	2,666	2,680	3,546	3,412
30	2,739	2,748	3,635	3,428
60	2,737	2,748	3,692	3,463
90	2,786	2,754	3,729	3,467
120	2,794	2,796	3,729	3,514

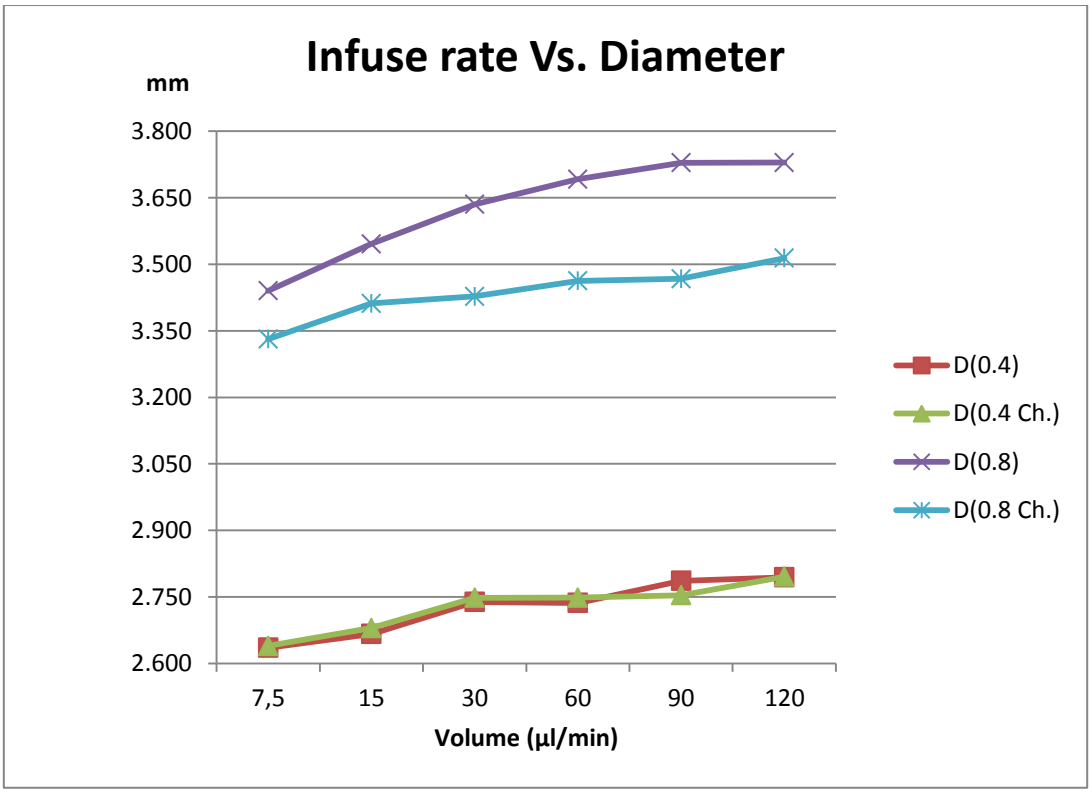

- **Water flow and time between drops.**

	Time (s)			
Volume (µl/min)	**0.4**	**0.4 chamfer**	**0.8**	**0.8 chamfer**
7,5	76,66	77,02	170,55	154,86
15	39,70	40,30	93,38	83,16
30	21,51	21,73	50,31	42,17
60	10,73	10,87	26,35	21,74
90	7,55	7,29	18,10	14,55
120	5,71	5,72	13,58	11,36

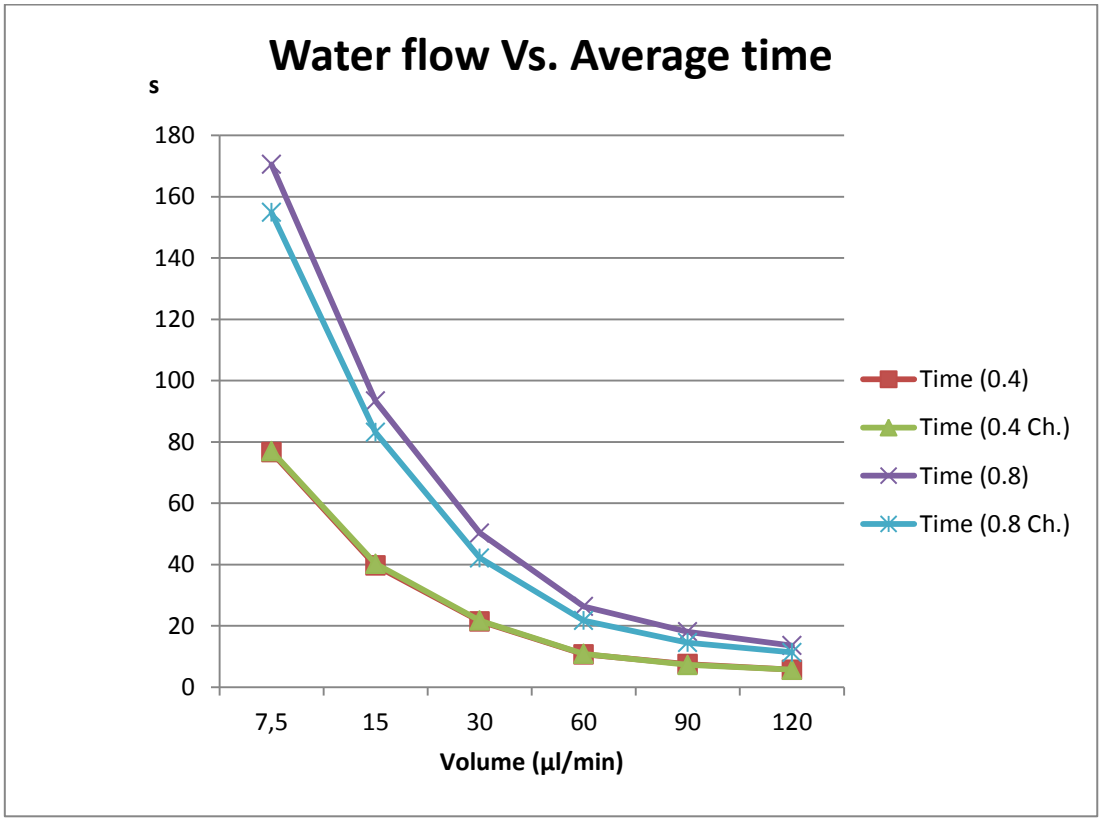

Appendix 2

Matlab scripts

Avi to bmp script “avi2bmp”

```
function FPS=avi2bmp()
% example: avifile('video_01')
% rootfile= 'video_01';

%vid=VideoReader([name '.avi']);
filename=dir('*.avi');
name=filename(1).name;
vid=VideoReader(name);

vidFrames = read(vid);
numFrames = get(vid, 'NumberOfFrames');
FPS=vid.FrameRate

for i=1:numFrames
    frame=i;
    img=vidFrames(:,:,:,frame);
    %figure(frame);
    %imshow(img);
    filename=[name '_' num2str(i,'%.3d') '.bmp'];
    imwrite(img,filename);
end
clear all
close all
```

«Diameter» Script

```
%% Sencond part -> Diameter
function [d1,d2]= Diameter(frame, drop)
filename=dir('*.bmp');
n=size(filename);

p2um= 400/78;

dif = imread(filename(frame).name);
Ev=1.0;
dif=(2^Ev)*dif;
figure (1); imshow(dif); hold on

    bw = im2bw(dif,0.60);
    %figure; imshow(bw)
    bw2 = bwareaopen(bw, 100000);
    %figure; imshow(bw2)
    reversedImage = bw2 < max(bw2(:));
    %figure; imshow(reversedImage)
    reversedImage2 = bwareaopen(reversedImage, 10);
    %figure; imshow(reversedImage2)
    dif=reversedImage2;
    %figure; imshow(dif); hold on;

[B,L] = bwboundaries(dif);
% calculates object properties like diameters and surface area
dropdata = regionprops(L,'all','Centroid');

size_B=[];
for j = 1:length(B)
    size_B(j)=length(B{j});
end
[list_B, IB]=sort(size_B, 'descend' );

y=IB(drop);
boundary=B{y};
plot(boundary(:,2), boundary(:,1), 'r', 'LineWidth', 2);
maxi=max(boundary,[],1);
mini=min(boundary,[],1);
d1 = (maxi(1)-mini(1))*p2um% [mm]
d2 = (maxi(2)-mini(2))*p2um% [mm]
```